

Wildfire impacts on stream water quality in the Pacific Coastal Temperate Rainforest

by

Jeremie Nicholas Mahaux

A thesis submitted in partial fulfillment of the requirements for the degree of

Master of Science

in

Ecology

Department of Biological Sciences
University of Alberta

© Jeremie Nicholas Mahaux, 2024

Abstract

Forests generally provide the highest-quality water among all land cover types, but they are highly susceptible to disturbances like wildfire. Climate change is driving a trend toward hotter, drier conditions that have been intensifying fire regimes worldwide. The Pacific Coastal Temperate Rainforest (PCTR), where severe fire has previously been rare, is the biome projected to experience the greatest proportional increase in area burned relative to past levels. Wildfires can alter dissolved organic carbon (DOC) concentration, dissolved organic matter (DOM) composition and nutrient concentrations in streams, affecting in-stream ecosystem function and aspects of drinking water quality. The extent of these effects varies with landscape making it crucial to understand localized impacts, but research has been focused heavily on historically fire-prone regions. To evaluate how burn-affected catchments in the PCTR propagate their impacts to low order streams and how those impacts differ between baseflow and stormflow, I sampled streams and soils within nine recent (2015-2022) wildfire and paired reference sites. Samples were assessed for DOC concentration and composition, nitrogen (N), phosphorus (P), suspended sediments, and a suite of cations and anions. At baseflow, I found lower concentrations of DOC ($\text{DOC}_{\text{ref}} = 2.5 \pm 0.2 \text{ mg L}^{-1}$, $\text{DOC}_{\text{burn}} = 1.8 \pm 0.2 \text{ mg L}^{-1}$, $p = 0.085$) and N ($\text{TDN}_{\text{ref}} = 187 \pm 30 \mu\text{g L}^{-1}$, $\text{TDN}_{\text{burn}} = 86 \pm 14 \mu\text{g L}^{-1}$, $p = 0.002$) in burned relative to reference sites, but greater concentrations of P ($\text{TDP}_{\text{ref}} = 3.7 \pm 0.3 \mu\text{g L}^{-1}$, $\text{TDP}_{\text{burn}} = 4.5 \pm 0.4 \mu\text{g L}^{-1}$, $p = 0.024$). Throughout storm events, constituents exhibited similar responses between burned and unburned catchments suggesting that the storms I sampled did not produce direct hydrologic connectivity between surficial soils and streams, perhaps due to high soil storage capacities enhanced by the historically dry sampling period. Finally, the effect of burn status was most pronounced in soil leachate samples, implying that the clear, direct impact of fire on terrestrial landscapes was poorly reflected in streams during my sampling period. The changes in nutrient concentrations I

found may have implications for stream food web assemblages and drinking water treatability.

Wildfire prevalence and severity is predicted to increase in this traditionally wet region; as a result, the results discussed here may be modest, compared to possible future effects.

Preface

This thesis is an original work by Jeremie Mahaux and is divided into three distinct chapters. The first chapter is an introductory chapter that provides background information on the field of research and study region, outlines the project objectives, and provides study rationale and significance. The second chapter is written in manuscript format and is intended for publication. The final chapter is a general conclusion that provides a summary and recommendations for future work. Supervisory authors were Drs. Suzanne Tank and William Floyd with further support from Dr. David Olefeldt.

This research was a collaborative effort between multiple individuals. Given these collaborations, this thesis is written in the plural. Jeremie Mahaux wrote the introductory and concluding chapters, and was responsible for study design development, sample collection, data analysis, and manuscript composition for Chapter 2. Drs. Tank and Floyd oversaw this research, providing revisions on all thesis chapters and advice on storyline ideas, study design, and data analysis for Chapters 2. Dr. Olefeldt offered study design and data analysis suggestions for Chapter 2.

Chapter 2

Mahaux, J.N., Floyd, W.C., Olefeldt, D., and Tank, S.E. Wildfire impacts on stream water quality in the Pacific Coastal Temperate Rainforest. In preparation for publication.

Acknowledgments

I would like to express my gratitude to everyone who supported me throughout this journey and without whom this thesis would not have been possible.

First, to Dr. Suzanne Tank, my supervisor, who has consistently shown care and true mentorship throughout my program. Her continuous support and encouragement, invaluable expertise, and gentle guidance have not only improved this work immensely but have helped me grow as both a scholar and person. I am truly grateful. My thanks also to Dr. Bill Floyd, my co-supervisor, for lots of great advice through the various iterations of this project and for reminding me that it's okay not to know everything yet and to enjoy the time spent learning. Thank you for making me feel welcome during my field seasons and for showing confidence in my abilities. And for the e-bikes, which turned several potentially tedious days into very enjoyable ones.

I would also like to extend my gratitude to the third member of my committee, Dr. David Olefeldt, whose thoughtful and insightful suggestions were instrumental in shaping my work. Thank you to Anna Kaveney for your good cheer, excellent suggestions, and great music choices through many long sampling days, and to Katie Schulze, for bearing with me through my first ever field season.

My immense gratitude to all the members of my lab group, Marina Taskovic, Gabrielle Hatten, Alyssa Deurwaarder, Nora Alsafi, and Jaedyn Smith for your friendship and support. You have all made my time here so much better.

Thank you also to everyone in the *forWater* network, and to all the members of the Coastal Research Hydrology Lab, and to everyone else who took the time to offer their thoughts, knowledge, wisdom, and friendship – I appreciate each of you.

Finally, I would like to thank my wife Jen, for her unending love, support, and patience as I pursued this project. Thank you for always believing in me, and for reminding me to go outside every now and then. You have been and continue to be a source of joy and light, and I couldn't have done it without you.

Table of Contents

Abstract.....	ii
Preface	iv
Acknowledgments.....	v
List of Tables.....	viii
Chapter 1. General Introduction.....	1
1.1 Importance of forested watersheds to freshwater supplies	1
1.2 Changing climate and wildfire patterns	4
1.3 Wildfire impacts on aquatic ecosystems	5
1.4 Study Region.....	7
1.5 Research rationale, objectives, and hypotheses	8
1.6 Significance.....	10
Chapter 2. Wildfire impacts on stream water quality in the Pacific Coastal Temperate Rainforest	11
2.1 Introduction.....	11
2.1.1 Study Objectives	14
2.2 Methods.....	15
2.2.1 Study Region.....	15
2.2.2 Sampling Campaigns	16
2.2.3 Surface Water Synoptic Samples	17
2.2.4 Soil Leaching Experiment.....	18
2.2.5 Storm sampling	19
2.2.6 Environmental and Catchment Characteristics	20
2.2.7 Statistical analyses	21
2.3 Results.....	22
2.3.1 DOC concentration and DOM composition.....	23
2.3.2 Nutrients and ions	24
2.3.3 Storm response.....	25
2.3.4 Cowichan Trail (CT) Storm Data.....	25
2.3.5 Mixed-Effect Random Forest.....	26
2.4 Discussion	27
2.4.1 Response to wildfire varies between regions	27
2.4.2 Water chemistry changes during baseflow conditions	28
2.4.3 DOM Compositional Changes	29
2.4.4 A comparison of soil leachates and baseflow conditions	30

2.4.5 Storms influence catchment exports	31
2.4.6 Ecological and water quality implications	33
2.4.7 Water treatment perspective	34
2.5 Conclusion	35
2.6 Tables	37
2.7 Figures	38
Chapter 3. General Conclusion	49
3.1 Summary of findings.....	49
3.2 Limitations and improvements.....	50
3.3 Future directions	52
References.....	54
Appendix 1 – Supporting Information for Chapter 2.....	71
Sample Collection.....	71
Water Quality Analyses.....	71
Soil Leachates	72
Statistical Analyses	73
Tables	75
Figures	80

List of Tables

Table 1. Fire and catchment characteristics. Ranges show the minimum and maximum values of catchments associated with each fire, separated by burn status (reference or burn). Streams were dry during every sampling attempt at the Mayo Lake fire site. Data for fire size and year, and dominant BEC zones were obtained from the BC government's *iMap* service (Government of British Columbia, 2022). Catchments were delineated using the watershed tool in ArcGIS Pro and based on the Canadian Digital Elevation Model (Government of Canada, 2023). All physical characteristics (area, aspect, elevation, slope) were calculated using ArcGIS Pro. Mean annual precipitation data was obtained from ClimateBC (T. Wang et al., 2016). Catchment burn severity was calculated by multiplying the average burn severity (0-4) by percent catchment burned. 37

Table A1. Weather stations used for precipitation data and associated fire sites. Maximum 24h rolling sum precipitation (mm) values are reported for each station for the three storm events captured in this study. Storm 1 occurred between October 27-November 01, 2022, storm 2 occurred between December 24-27, 2022, and storm 3 occurred between January 11-14, 2023. San Juan, Salt Spring, and Nanaimo stations collect hourly data and are operated by the Ministry of Forests, Lands and Natural Resource Operations - Wildfire Management Branch (FNLRO-WMB), Sheringham Point station collects daily data and is operated by Environment Canada (EC). All data were retrieved from the Pacific Climate Impacts Consortium (PCIC) (Pacific Climate Impacts Consortium, 2024). Storms 1 and 2 were captured by passive siphon "rack" samplers sites HC, NL, HO, or CT; storm 3 was captured by ISCO autosamplers at the CT fire site. 75

Table A2. Outputs from one-sample ($\mu = 0$), two-tailed t-tests comparing whether reference and burn samples are different from each other. $P < 0.05$ indicates that the mean Z-score difference ($Z_{\text{burn}} - Z_{\text{ref}}$) is significantly different from zero and the reference and burn sites are statistically different. These t-tests were conducted for each water quality metric and sample type using the same input data that was used to calculate Z-scores (one average value for each combination of site and burn status) for baseflow, soil 0-5cm, and soil 6-10cm which are associated with Figures 3 & 4, and storm burn and storm reference, which are associated with Figures 5 & 6. $P < 0.05$ shown in bold. 76

Table A3. Properties of the five fluorescent DOM components identified using PARAFAC analysis, including excitation (Ex.) and emission (Em.) peak values, mean percent composition, similarity scores, potential component characteristics, and related references for similar components. The OpenFluor database was used to obtain information on similarity scores and component characteristics (Murphy et al., 2014). 78

Table A4. Outputs for stormflow two sample, two-tailed t-tests. The "Storm & Base" group compare all stormflow data to all associated baseflow data regardless of burn status to investigate the presence of an overall storm response. The "Storm Ref & Storm Burn" group compare the stormflow reference and burn samples to investigate if burn status impacts storm response. The data are associated with Figures 5 & 6. $P < 0.05$ shown in bold. 79

List of Figures

- Figure 1. Map showing southern Vancouver Island biogeoclimatic ecosystem classification (BEC) zones, sampled catchments labelled with associated fire site and burn year, and weather stations used. BEC labels are split into zones, subzones, and variants. BEC zones are coastal western hemlock (CWH), coastal douglas-fir (CDF), mountain hemlock (MH), and coastal mountain-heater alpine (CMA). Subzones are moist maritime (mm), very dry maritime (xm), very wet maritime (vm), very wet hypermaritime (vh), and undifferentiated and parkland (unp). Variants, which depend on zone and subzone, are submontane (CWHmm1, CWHvm1), montane (CWHmm2, CWHvm2), southern (CWHvh1), eastern (CWHxm1), western (CWHxm2), and windward (MHmm1). Above the map are rolling 24-hour precipitation data recorded at the Salt Spring (SS; PCIC ID 1637) weather station, and stage data from the Bings Creek near Mouth hydrometric station (Water Survey of Canada; ID 08HA016) located in Duncan, BC. Dashed lines represent the active sampling period (May 01 – May 17, 2022 & October 25, 2022 – January 17, 2023). Ticks on the bottom of the precipitation and stage plots represent sample collection dates..... 39
- Figure 2. Detailed maps of the Harris Creek (HC; left) and Cowichan Trail (CT; right) historic fire sites and sampled catchments. The year next to the site name represents the burn year. The inset maps show southern Vancouver Island – the red star represents the location of the fire site, and the pin shows the associated weather station. Maps of the remaining seven fire sites are available in the appendix (Figure A1)..... 40
- Figure 3. Z-score change of LOI, DOC (mg L^{-1}), DOM composition (SUVA_{254} , nm cm^{-1} ; $S_{275-295}$, nm^{-1} ; BIX, HIX), and EEM components (C1-C5) for baseflow samples and soil leachates. All data are centered and scaled by source (blue = baseflow, green = soil 0-5cm, yellow = soil 6-10cm). The y-axis shows the normalized (Z-score) difference between burn and reference sites expressed in standard deviations. The numbers show the mean and standard deviation (mean (SD)) of each metric, colour-coded according to data source and calculated using non-normalized data. Error bars represent 95% confidence intervals. Raw data can be found in Figures A5-A7; associated t-test outputs can be found in Table A2. 41
- Figure 4. Z-score change of total suspended sediments (TSS, mg L^{-1}), nutrients (TP, $\mu\text{g L}^{-1}$; TDP, $\mu\text{g L}^{-1}$; SRP, $\mu\text{g L}^{-1}$; TN, $\mu\text{g L}^{-1}$; TDN, $\mu\text{g L}^{-1}$; NO_2+NO_3 , $\mu\text{g L}^{-1}$) and specific conductance ($\mu\text{S cm}^{-1}$) and major ions (mg L^{-1}) for baseflow samples and soil leachates, when available. All data are centered and scaled by source (blue = baseflow, green = soil 0-5cm, yellow = soil 6-10cm). The y-axis shows the normalized (Z-score) difference between burn and reference sites expressed in standard deviations. The numbers show the mean and standard deviation (mean (SD)) of each metric, colour-coded according to data source and calculated using non-normalized data. Error bars represent 95% confidence intervals. Raw data can be found in Figures A5-A7; associated t-test outputs can be found in Table A2. 42
- Figure 5. Z-score change of DOC (mg L^{-1}), DOM composition (SUVA_{254} , nm cm^{-1} ; $S_{275-295}$, nm^{-1}), and EEM components (C1-C5) for reference and burn samples. The y-axis shows the normalized (Z-score) difference between stormflow and baseflow samples expressed in standard deviations. Data are from the four sites with stormflow data (HC, NL, HO, and CT), centered and scaled. The numbers show the overall (combined baseflow and stormflow) mean and standard deviation (mean (SD)) of each metric calculated using the pre-normalized dataset. Error

bars represent 95% confidence intervals. Raw data can be found in Figure A9; associated t-test outputs can be found in Table A2 & A4..... 43

Figure 6. Z-score change of total suspended sediments (TSS, mg L^{-1}), nutrients (TP, $\mu\text{g L}^{-1}$; TDP, $\mu\text{g L}^{-1}$; TN, $\mu\text{g L}^{-1}$; TDN, $\mu\text{g L}^{-1}$) and pH, specific conductance ($\mu\text{S cm}^{-1}$), and major ions (mg L^{-1}) for reference and burn samples. The y-axis shows the normalized (Z-score) difference between stormflow and baseflow samples expressed in standard deviations. Data are from the four sites with stormflow data (HC, NL, HO, and CT), centered and scaled. The numbers show the overall (combined baseflow and stormflow) mean and standard deviation (mean (SD)) of each metric calculated using the pre-normalized dataset. Error bars represent 95% confidence intervals. Raw data can be found in Figure A9; associated t-test outputs can be found in Table A2 & A4..... 44

Figure 7. Rainfall (mm), stage (mm, normalized to zero), and water quality (DOC (mg L^{-1}), $S_{275-295}$ (10^3 nm^{-1}), TDN ($\mu\text{g L}^{-1}$), and TDP ($\mu\text{g L}^{-1}$), TSS (mg L^{-1})) responses during a storm event (January 11-14, 2023). Samples were collected every 3h using ISCO autosamplers. The hyetographs show the 24-hour rolling sum of precipitation from the Salt Spring weather station – data were unavailable for January 14-15. All other plots show the change in stage on the left axis and concentration on the right axis. Figure 2 shows site locations: Downstream (burned) and upstream (reference) are paired upstream/downstream sites on the same stream. The upstream site catchment (0.36km^2) represents 72% of the downstream catchment (0.5km^2). A tributary (0.06km^2) joins the stream between the upstream and downstream sites. Adjacent (reference) is a nearby small (0.06km^2) reference stream 45

Figure 8. Surface water baseflow mixed-effect random forest outputs for DOC, $S_{275-295}$, TDN, and TDP. Plots show variable importance metrics (VIMs). The x-axis represents the percent increase in the mean squared error (MSE) of the model when that variable is removed; more important variables introduce more error when not considered. VIMs are coloured according to predictor characteristics: green = biotic, grey = abiotic, blue = climatic, red = fire. R^2 and mean squared error (MSE) calculated using out-of-bag (OOB) data. Associated partial dependence plots (PDPs) for the six most important predictors can be found in the appendix (Figure A10).. 46

Figure 9. Soil leachate mixed-effect random forest outputs for DOC, $S_{275-295}$, TDN, and TDP. Plots show variable importance metrics (VIMs). The x-axis represents the percent increase in the mean squared error (MSE) of the model when that variable is removed; more important variables introduce more error when not considered. VIMs are coloured according to predictor characteristics: green = biotic, grey = abiotic, blue = climatic, red = fire. R^2 and mean squared error (MSE) were calculated using out-of-bag (OOB) data. Associated partial dependence plots (PDPs) for the six most important predictors can be found in the appendix (Figure A11). 47

Figure 10. Surface water stormflow data mixed-effect random forest outputs for DOC, $S_{275-295}$, TDN, and TDP. Plots show variable importance metrics (VIMs). The x-axis represents the percent increase in the mean squared error (MSE) of the model when that variable is removed; more important variables introduce more error when not considered. VIMs are coloured according to predictor characteristics: green = biotic, grey = abiotic, blue = climatic, red = fire. R^2 and mean squared error (MSE) were calculated using out-of-bag (OOB) data. Associated partial dependence plots (PDPs) for the six most important predictors can be found in the appendix (Figure A12). 48

Figure A1. Detailed maps of historic fire sites and sampled catchments. The year next to the site name represents the burn year. The inset maps show southern Vancouver Island – the red star represents the location of the fire site, and the pin shows the associated weather station. Maps of the other the fire sites are shown in Figure 2.	80
Figure A2. Field pictures of passive siphon “rack” samplers set up at the Harris Creek (HC, 2015) fire site in a burn-affected (HCBrn1 - left) and reference stream (HCTRef1 - right). Rack samplers were typically installed during periods of low flow.	81
Figure A3. Hyetograph spanning March 2022 to January 2023 and stage hydrographs for two storm events captured by at least one rack sampler (Figure A2). Points on the hydrographs show where a sample was collected. Orange represents a storm event from October 27 – November 01, 2022, red represents a storm event from December 24 – 28, 2022. Precipitation data was acquired from the San Juan weather station.	82
Figure A4. Precipitation data from the four weather stations used in associated with wildfire sites. All data were retrieved from the Pacific Climate Impacts Consortium (PCIC) (Pacific Climate Impacts Consortium, 2024). The San Juan, Salt Spring, and Nanaimo weather stations collect hourly data which are shown here as a 24-hour rolling sum and are operated by the Ministry of Forests, Lands and Natural Resource Operations - Wildfire Management Branch (FNLRO-WMB). Sheringham Point station collects daily data which is shown here a 24-hour total precipitation and is operated by Environment Canada. San Juan was associated with site HC, Salt Spring was associated with sites ML, MM, HO, and CT, Nanaimo was associated with sites NL and MH, and Sheringham Point was associated with sites JC and TC. The rug ticks show when a sample was collected at one of the associated sites.	83
Figure A5. Boxplots comparing water quality metrics (TSS, DOC, $S_{275-295}$, $SUVA_{254}$, TDN, TDP, TN, TP) from reference and burn-affected streams at eight sites (HC, JC, TC, MM, NL, HO, MH, CT) during baseflow. Sites are ordered chronologically by date of wildfire, from oldest to newest (2015 – 2022).	84
Figure A6. Boxplots showing loss-on-ignition (LOI) and water quality metrics (DOC, $S_{275-295}$, $SUVA_{254}$, TDN, TDP) for 0-5cm soil leachates. Sites are ordered chronologically, by date of wildfire, from oldest to newest (2015 – 2022) and colour coded according to burn status (reference or burn). CT_F and CT_W represent samples from the Cowichan Trail (2022) fire site, collected prior to wet-up in the fall (CT_F) or during the winter wet season (CT_W).	85
Figure A7. Boxplots showing loss-on-ignition (LOI) and water quality metrics (DOC, $S_{275-295}$, $SUVA_{254}$, TDN, TDP) for 6-10cm soil leachates. Sites are ordered chronologically, by date of wildfire, from oldest to newest (2015 – 2022) and colour coded according to burn status (reference or burn). CT_F and CT_W represent samples from the Cowichan Trail (2022) fire site, collected prior to wet-up in the fall (CT_F) or during the winter wet season (CT_W).	86
Figure A8. PARAFAC components of excitation-emission matrices (EEMs) measured in samples collected across southern Vancouver Island. Five fluorescence peaks (C1-C5) were identified and displayed in optical space. The colour gradient indicates fluorescence intensity in Raman units.	87
Figure A9. Boxplots comparing water quality metrics (TSS, DOC, $S_{275-295}$, $SUVA_{254}$, TDN, TDP, TN, TP) from reference and burn-affected stream samples at four sites (HC, NL, HO, CT) during baseflow and stormflow. Sites are ordered chronologically, by date of wildfire, from oldest to	

newest (2015 – 2022). No samples were available at NL and HO for TN and TP because the passive siphon collection method did not capture enough volume for all analyses. 88

Figure A10. Partial dependence plots (PDPs) for the six most important predictors in the baseflow MERFs. PDPs show the interaction between a subset of variables while accounting for the average effect of the other predictors in the model. Here, each subset of six shows the predicted response of one of variables of interest (DOC, $S_{275-295}$, TDN, TDP) across different values of each predictor. The y-axis represents the change in concentration (DOC mg L^{-1} , TDN $\mu\text{g L}^{-1}$, TDP $\mu\text{g L}^{-1}$) or slope ($S_{275-295} 10^3 \text{ nm}^{-1}$). 89

Figure A11. Partial dependence plots (PDPs) for the six most important predictors in the soil leachate MERFs. PDPs show the interaction between a subset of variables while accounting for the average effect of the other predictors in the model. Here, each subset of six shows the predicted response of one of variables of interest (DOC, $S_{275-295}$, TDN, TDP) across different values of each predictor. The y-axis represents the change in concentration (DOC mg L^{-1} , TDN $\mu\text{g L}^{-1}$, TDP $\mu\text{g L}^{-1}$) or slope ($S_{275-295} 10^3 \text{ nm}^{-1}$). 90

Figure A12. Partial dependence plots (PDPs) for the six most important predictors in the for stormflow MERFs. PDPs show the interaction between a subset of variables while accounting for the average effect of the other predictors in the model. Here, each subset of six shows the predicted response of one of variables of interest (DOC, $S_{275-295}$, TDN, TDP) across different values of each predictor. The y-axis represents the change in concentration (DOC mg L^{-1} , TDN $\mu\text{g L}^{-1}$, TDP $\mu\text{g L}^{-1}$) or slope ($S_{275-295} 10^3 \text{ nm}^{-1}$). 91

Figure A13. DOC (mg L^{-1}), $S_{275-295}$ (10^3 nm^{-1}), TDN ($\mu\text{g L}^{-1}$), and TDP ($\mu\text{g L}^{-1}$) versus change in stream water level (mm) at the upstream and downstream sampling sites of the Cowichan Trail fire (CT, 2022) during the Jan. 11–14, 2023 storm event. The arrows represent the temporal direction of the storm from the rising to falling limb. Stream water level data were normalized to zero. 92

Chapter 1. General Introduction

1.1 Importance of forested watersheds to freshwater supplies

Forested ecosystems provide high quality and sustainable surface freshwater sources (Caldwell et al., 2023; Neary et al., 2009). The invaluable water filtration and storage services they offer are driven by the interaction of several biological, chemical, and physical characteristics (Barten and Ernst, 2004; Caldwell et al., 2023; Neary et al., 2009). Interception and evapotranspiration reduce the intensity and amount of precipitation reaching the forest floor thereby helping to reduce soil erosion and limiting sediment transport into waterways (Baillie and Neary, 2015). Forested soils tend to be porous because of extensive root networks, animal burrowing, subsurface erosion, and other natural processes that all increase soil porosity and infiltration rates (Caldwell et al., 2023). High infiltration rates mean water is often carried to streams by subsurface flow pathways where nutrient uptake and cycling processes are rapid (Neary et al., 2009). The structure of forest floors is fairly resistant to erosion – leaf litter and debris dissipate raindrop energy, and soils are anchored by root stabilization and organic aggregates (Gartner et al., 2014; Neary et al., 2009). Forested soils tend to have large storage and infiltration capacities, which can help limit overland flow and minimize direct inputs of sediment or nutrients from landscapes to streams – this acts as a buffer and helps regulate stream water inputs during periods of intense precipitation (Dunne and Black, 1970). The diverse and abundant forest biota play an important role in controlling nutrient fluxes (e.g., nitrogen and phosphorus) by facilitating the storage of these nutrients through plant uptake or their transformation via microbial processes (e.g., denitrification) (Pike et al., 2010). Soil material can capture contaminants by sorption, thereby reducing nutrient and pollutant delivery to streams (de la Cretaz and Barten, 2007). Riparian zones are also important for biogeochemical processing. They contribute to filtration, nutrient recycling, and pathogen removal (Bladon et al., 2014) and can exert a strong control on landscape inputs of organic matter and nutrients to aquatic ecosystems (Gregory et al., 1991). These services help maintain healthy aquatic ecosystems and reduce the costs of drinking water treatment for the communities that rely on them by reducing the demands on treatment infrastructure and chemical materials (Gartner et al., 2014; Levine et al., 2016; Robinne et al., 2019), with the global value of natural forest water storage and filtration estimated at \$4.1 trillion US (2013) annually (Bladon et al., 2014). The specifics of

these patterns in forest-modulated water quality are dependent on catchment characteristics like parent material, slope gradient, soil depth, and vegetation type and cover, and therefore vary from region to region (Cool et al., 2014). Though the specifics may vary, intact forests generally produce the highest quality water of any ecosystem type (Caldwell et al., 2023).

Small streams often account for more than seventy percent of stream-channel length in river networks (Leopold et al., 2020). They can be intimately connected with the surrounding terrestrial ecosystems and have a strong influence on downstream water quality, with a role and importance similar to the smallest branches of the human respiratory system (Lowe and Likens, 2005). Headwater forested streams play a critical role in the regulation of aquatic ecosystem services and are important processing and retention sites for elements like carbon (C), nitrogen (N), and phosphorus (P) (Ferreira et al., 2023; Mulholland, 2004). Nutrient processing and delivery are directly influenced by hydrologic processes that control the level of connectivity between landscapes and streams and therefore regulate terrestrial subsidies to aquatic networks (Nadeau and Rains, 2007). The four principal transport pathways between catchments and streams are groundwater flow (subsurface flow below the water table), throughflow (subsurface flow above the water table), infiltration excess overland flow (overland flow when the rainfall rate exceeds soil infiltration rates), and saturated overland flow (overland flow that occurs when the water table rises to the surface) (Knighton, 1998). Water moving through deeper flow paths tends to be poorly connected to current surface soil conditions because of long transport times and processes that can modify dissolved constituents such as adsorption to sediments or uptake by vegetation and microorganisms (Nadeau and Rains, 2007). Surface (i.e., overland) flows, by contrast, permit rapid transport of water into channels and can directly carry surface sediments and nutrients and thus represent a tighter coupling of landscape and stream (Dunne and Black, 1970). The processes that control hydrologic response are complex and depend on the interaction between climate (e.g., precipitation amount and intensity) and landscape dynamics (e.g., soil type, vegetation, slope) (Nadeau and Rains, 2007). However, headwater streams often lack extensive surface and subsurface storage zones that may be present in river valleys and have shorter flow paths connecting channels to their upland sources (Gomi et al., 2002; McGlynn et al., 2004). Therefore, they are generally regarded as source regions for terrestrial inputs (Wohl, 2017). Given this close connection, small streams can be especially sensitive to disturbances like wildfire within their catchments (Meyer et al., 2007; Wampler et al., 2024).

Dissolved organic matter (DOM) plays several critical roles in aquatic ecosystems. It fuels stream metabolism, helps regulate biogeochemical cycles (e.g., nitrogen transformation), and impacts trace metal and contaminant transport (Aiken, 2014). Dissolved organic carbon (DOC) is a component of the DOM pool and is often the dominant form of organic C in streams. While they are often used interchangeably, here, DOC refers to the concentration of dissolved carbon, whereas DOM refers to the complex material that is predominantly carbon but also includes nitrogen, oxygen, hydrogen, and various other elements (Moody and Worrall, 2017). DOM molecules can have varying chemical structures that affect their molecular weight (i.e., size) and aromaticity (i.e., complexity) and are largely regulated by where they originate (i.e., terrestrial or aquatic sources) (Cory et al., 2011). Chemical structure influences DOM bioavailability and lability (i.e., reactivity), which in turn impacts downstream water quality, ecosystem functions, and carbon cycling as DOM is consumed through various microbial metabolic pathways (Battin et al., 2008). DOM generated through in-stream processes (i.e., autochthonous DOM) is associated with autotrophic organisms and tends to be relatively labile (Kellerman et al., 2018). Terrestrially-sourced DOM (i.e., allochthonous DOM) comes from vegetation or soil matter (Aitkenhead-Peterson et al., 2003), and often includes humic and fulvic acids and a variety of other compounds (e.g., lignins, proteins, carbohydrates) which tend to be more recalcitrant (Ruhala and Zarnetske, 2017). Further differences in DOM composition can be driven by processing (e.g., microbial or photochemical degradation) and flow paths (overland or subsurface) (Judd et al., 2006; Stubbins et al., 2014). The concentration and composition of DOM are therefore strongly influenced by surrounding landscape characteristics, hydrologic regimes, and watershed disturbances.

Headwater streams provide habitat for many sensitive species that rely on the unique physical or biological conditions to survive (Richardson, 2019). Cool, shaded forest streams have been associated with reductions of in-stream primary producer biomass due to limitations in both light and nutrients (Baillie and Neary, 2015). The biota of forested streams tend to be composed of species that are more sensitive to disturbance and often rely on allochthonous (i.e., terrestrial) organic matter inputs (e.g., shredders), rather than those that rely primarily on algal food sources (Baillie and Neary, 2015; Goss et al., 2014). Given the high terrestrial inputs, most have detrital-based (i.e., heterotrophic) food webs (Mulholland, 2004). The basal elements of the food web (autotrophic or heterotrophic) can influence the biomass and composition of organisms at higher

trophic levels. While exact information about the number and diversity of species that rely on forested headwater streams does not exist, it would likely include hundreds to thousands of species (Wohl, 2017). Disruption of the conditions in which they exist could lead to significant shifts in aquatic ecosystem structure and function (Wall et al., 2024).

In Canada, seventy to eighty percent of accessible freshwater originates in forested watersheds (Webb, 2021). Forty percent of the potable water derived from these sources undergoes limited treatment – meaning that it is either disinfected or filtered only, rather than applying the conventional treatment processes of coagulation, flocculation, sedimentation and granular media filtration (Statistics Canada, 2011). Several municipalities with limited treatment facilities instead rely on high quality source waters and are therefore vulnerable to source water degradation (Moghaddam-Ghadimi et al., 2023). Given the high cost and potential complications of water treatment, managing and protecting forested watersheds to maintain source water quality is a well-recognized part of the multi-barrier approach, which integrates policy and processes from source-to-tap to collectively prevent or reduce the contamination of drinking water (Health Canada, 2004). The multi-barrier approach has been established as an effective approach for reducing costs and providing reliable access to clean water (Aguilar et al., 2018; Barten and Ernst, 2004; Caldwell et al., 2023; Chowdhury, 2018; Gartner et al., 2014; Majidzadeh et al., 2019; Price and Heberling, 2018); however, both climate change and wildfire are set to add additional stressors to these systems that may reduce the effectiveness of current treatment infrastructure and technology.

1.2 Changing climate and wildfire patterns

Anthropogenic climate change is a well-established concept that impacts nearly every aspect of the natural world (IPCC, 2023). Temperatures are increasing worldwide (Hansen et al., 2010; Valipour et al., 2021) and precipitation patterns are being disrupted (Trenberth, 2011). This has led to a substantial increase in the frequency of hot and dry weather conditions (and compound hot-dry extremes) in recent decades (Alizadeh et al., 2020). Precipitation, streamflow, and soil moisture indices all show an increasing trend of aridity in many regions worldwide (Dai, 2013). This can have potentially devastating repercussions for forested areas by increasing the length of fire seasons, drying out fuels, and causing tree mortality thus leading to increases in wildfire frequency and severity (Flannigan et al., 2013). Fire is a natural part of many ecosystems and

several require periodic disturbance to maintain their structure and function (Harris et al., 2016), but when fires exceed their historical patterns of intensity, extent, severity, seasonality, and frequency, they can harm ecosystem functions, biodiversity, and human societies (Kelly et al., 2020; Sayedi et al., 2024). Fire regimes are largely driven by the interaction between climate and vegetation (Harris et al., 2016), although climate (e.g., precipitation and temperature) is perhaps the more important of these as it also exerts strong control on plant community composition (Sayedi et al., 2024).

Fires are projected to increase in frequency, area burned, and intensity both worldwide (Robinne et al., 2018) and specifically in Canada (Coogan et al., 2019; Wang et al., 2017). Ecosystems that have not historically been fire prone, like the highly productive Pacific Coastal Temperate Rainforest (PCTR) found on the coast of British Columbia, are especially vulnerable to changing fire regimes (Abatzoglou and Williams, 2016; Holden et al., 2018; Littell et al., 2018). The PCTR has been predicted to experience the largest increase in area burned (relative to past area burned) compared to any other ecozone due to warming temperatures, decreased precipitation, and high fuel loads (Halofsky et al., 2020; Rupp et al., 2017; Wimberly and Liu, 2014), with a high possibility of more frequent, large fires (especially >40,000 ha), and shifts in fire seasonality (Dye et al., 2024).

1.3 Wildfire impacts on aquatic ecosystems

Wildfires can have highly variable impacts on aquatic ecosystems. Studies from around the world have often reported conflicting outcomes for a variety of water quality constituents (Gomez Isaza et al., 2022; Morales Parrado et al., 2023; Paul et al., 2022). High variability has also been recorded in the duration of impacts, with short-term event-driven pulses spanning hours or days (Emmerton et al., 2020) and long-term changes in nutrient export that can reflect the changing conditions of recovering catchments up to fourteen years post-fire (Rhoades et al., 2019a). This variability can be broadly attributed to differences in regional characteristics and fire behaviour. Regional characteristics – which include soil type and depth, parent material, vegetation type and density, topography (e.g., slope), and climate (e.g., temperature and precipitation) – influence the type and amount of constituents exported to aquatic systems because different soils and plant matter produce different outputs when burned (Paul et al., 2022; Smith et al., 2011). Slope, soil type, and climate also play a major role in hydrologic

connectivity, which controls how these post-fire products can be delivered into streams; the timing and amount of precipitation after a fire can substantially influence the strength of in-stream responses (Hallema et al., 2017). Fire has been reported to produce a hydrophobic layer in soil, which can potentially limit forest soil infiltration and retention capacities (Agbeshie et al., 2022; Beatty and Smith, 2013). This can modify hydrologic response and lead to higher overland flow (and sediment/nutrient inputs) as well as increased risk of flood (Delpla et al., 2009; Doerr et al., 2006). Fire behaviour – which refers to the manner in which fuels ignite and fire spreads, and includes area burned, intensity (i.e., fire temperature), patchiness, and type (i.e., crown, surface, ground) – controls how much of the catchment is impacted, how much vegetation is consumed, and how constituents are modified (McLauchlan et al., 2020). For example, post-fire DOM composition (Wang et al., 2015a) and C and N volatilization (Hohner et al., 2019) all depend on burn temperature.

The indirect effects of fire (e.g., erosion, increased runoff, channel alteration, nutrient enrichment) can impact food web and community dynamics (Minshall, 2003). As with water quality, these aquatic ecosystem impacts are highly variable and heavily influenced by burn severity and vegetation composition, as well as post-fire precipitation regimes (Carvalho et al., 2019; Gomez Isaza et al., 2022; Judd et al., 2006; Pinto et al., 2009; Pradhan et al., 2020; Verkaik et al., 2015). Changes in nutrient stoichiometry (i.e., nutrient balance) can impact food webs by altering community composition and overall biomass. Terrestrial nutrients can be mobilized by fire and lead to altered nutrient loading in streams (Bixby et al., 2015). Nutrient enrichment can promote increases in algal biomass and changes in invertebrate community structures, with possible changes impacting the food web all the way up to the highest trophic levels (Koetsier et al., 2007; Silins et al., 2014). Wildfire can also alter decomposition regimes and disrupt detrital food webs by reducing the activity of bacterial decomposers and modifying bacterial species assemblages (Butler et al., 2019; Carvalho et al., 2019). Shifts between autotrophic (i.e., algal) and heterotrophic (i.e., bacterial/detrital) based food webs have implications for trophic energy transfer and aquatic community composition. Heavy rainfall can be a triggering factor for ecosystem changes by promoting inputs of soil and burned material via overland flow (Carvalho et al., 2019). Heavy flow or debris pulses can modify channel morphology and have strong short-term impacts that may not be reflected in the long-term changes (e.g., high OM inputs stimulating decomposition and creating low dissolved oxygen conditions) (Jager et al., 2021).

Wildfire can also make aquatic communities less resilient to other disturbances like flood, drought, or logging (Jager et al., 2021; Leonard et al., 2017; Robson et al., 2018), though intact riparian areas can go a long way towards moderating impacts on aquatic communities by intercepting nutrients and sediment and limiting increases in light exposure (Carvalho et al., 2019; Minshall, 2003; Verkaik et al., 2015).

From a drinking water treatability perspective, increases in DOM, nutrients, and suspended sediments are all potentially problematic. High DOC and suspended sediments reduce the effectiveness of chlorination and ultraviolet radiation, both of which are common elements of treatment processes (Emelko et al., 2011; MWH, 2012). Disinfection processes (e.g., chlorination) can interact with DOM to form a variety of disinfection by-products (DBPs), several of which are carcinogenic or may cause reproductive complications (Chowdhury, 2018; Emelko et al., 2011; Richardson and Postigo, 2012). While many of these DBPs are regulated (Government of Canada, 2015), more than 600 DBPs have been reported in the scientific literature, with only a fraction having been addressed in toxicity studies (Richardson and Postigo, 2012). DOM composition affects the type of DBPs formed – for instance, humic and fulvic acids are the primary precursors for a suite of regulated DBPs (Richardson and Postigo, 2012) – so maintaining a stable and predictable source of high quality source water can help reduce risks. Wildfires can influence both the quantity and composition of DOM which can impact treatability (Chen et al., 2020) and potentially increase the risk of DBP formation even when catchments are only partially burned (Hohner et al., 2019). Wildfires can also influence the balance of nutrients like N and P which can present challenges by enhancing algal growth. Both eukaryotic algae and cyanobacteria can cause objectionable taste and odor in drinking water, while cyanobacteria, in particular, can develop into harmful algal blooms that generate toxic products (Emelko et al., 2011; Schinck et al., 2020).

1.4 Study Region

Coastal temperate rainforests are found primarily on the Pacific coast of North America and in southern Chile, with small patches occurring in New Zealand, Australia, portions of western Europe, and on islands in eastern Asia (Alaback, 1991). These are characterized by high annual precipitation (>1400mm) and moderate temperatures year-round, with relatively cool summers and mild wet winters. Another key characteristic of coastal temperate rainforests is their highly

productive forests, which accumulate substantial biomass and feature long-lived, massive tree species. In the northern hemisphere, these forests are predominantly composed of coniferous species such as western hemlock (*Tsuga heterophylla*), western redcedar (*Thuja plicata*), Douglas fir (*Pseudotsuga menziesii*), and Sitka spruce (*Picea sitchensis*); the southern hemisphere primarily supports deciduous broadleaf species (Alaback, 1991). An ecological consequence of this unique climate is frequent disturbance by wind, and the lack of fire as an important factor in forest dynamics (Alaback, 1991). The historical occurrence of fire shows infrequent, high severity, stand replacing fires with long return intervals (>200 years) as fuels accumulate and climatic conditions permit ignition (Gavin et al., 2003). Twentieth-century fire suppression policies have further contributed to significant fuel buildup (Haugo et al., 2019). However, climate projections for the PCTR show more periods of hot, dry weather that will increase the size, frequency, and severity of fires, and may contribute to lasting changes in vegetation community assemblages (Halofsky et al., 2020).

1.5 Research rationale, objectives, and hypotheses

This research was carried out in partnership with the *forWater* network, a Canada-wide, interdisciplinary initiative to provide new knowledge for the protection of drinking water from source to tap in a changing climate (forWater, 2024). The various themes involved support the multi-barrier approach, which is “an integrated system of procedures, processes and tools that collectively prevent or reduce the contamination of drinking water from source to tap in order to reduce risks to public health” (Health Canada, 2004). Functionally, this means that watershed integrity and management are incorporated as formal elements of safe drinking water delivery, alongside water treatment and legislative policies. This work fits into the source water protection component of the *forWater* initiative.

Our study takes place on southern Vancouver Island, BC, where 140 water supply systems rely upon surface water sources – 43 of which serve large (more than 500 people) populations (Island Health, 2014). Several of these employ the multi-barrier approach and rely on maintaining source water quality alongside limited treatment infrastructure (Capital Regional District, 2016) that may be overwhelmed by a wildfire in their supply catchments. Fire-driven increases in turbidity (i.e., suspended sediments) or organics (i.e., DOM) could exceed the removal capacities of existing disinfection systems and increase the risk of pathogens entering

the water supply (Capital Regional District, 2022). Increases in nutrient availability could risk harmful algal blooms that may produce toxins and further stress filtration capacities (Hohner et al., 2019). Overall, wildfire impacts could damage infrastructure, increase treatment costs, and disrupt drinking water availability (Robichaud and Padowski, 2024).

In this thesis, I worked across a series of recent (2015-2022) wildfire and paired reference sites within the Coastal Western Hemlock and Coastal Douglas Fir biogeoclimatic ecozones of British Columbia (Pojar et al., 1991), which are part of the PCTR. I sampled streams at baseflow, adjacent soils, and select sites at stormflow to gain a holistic understanding of the effects of wildfire, which is traditionally uncommon in this region. The research objectives were to: (1) quantify the magnitude, duration, and key drivers of water quality responses in burn-affected streams; (2) investigate the extent to which directly burned soil impacts are reflected in surface waters; and (3) investigate how water quality responses differ during baseflow and stormflow in burned and reference catchments. I chose to collect three sample types (baseflow, soil leachates, stormflow) that represented different levels of landscape connectivity. Baseflow samples represented the predominant flow condition – effects measured at baseflow may be indicative of fundamental changes in stream dynamics that persist during periods of low connectivity between terrestrial and aquatic systems. The soil leachates were selected to investigate how water-extractable constituents can be altered by fire and the extent to which those changes are reflected in actual stream conditions. From these, I also aimed to quantify potential stream inputs should a significant precipitation event prompt direct connectivity between surficial soils and streams. Finally, the purpose of the stormflow samples was to investigate whether natural storm inputs overwhelmed stream responses to wildfire and describe the types of conditions water managers may encounter during periods of increased flow. I considered each of these sample types alongside several environmental characteristics, including vegetation and soil types, slope, aspect, mean annual precipitation, and catchment burn severity to identify the most important controlling variables of each constituent of interest.

The thesis is formatted as one manuscript-style chapter (Chapter 2) with appendices, and a general introduction and conclusion. The general introduction (Chapter 1) provides context and background information relating to forested watersheds and wildfire while the conclusion (Chapter 3) provides a summary of findings and suggestions for future improvements and research.

1.6 Significance

This study aims to be among the first to describe the effects of wildfire on water quality in the PCTR and uncover the main drivers controlling the response of key elements like C, N, and P. This region has been understudied due to a historical lack of fire, but climate change projections suggest that there will be a significant increase in the frequency and size of fires that may engender increases in the severity of water quality impacts. The outcomes of this research will contribute to the global understanding of wildfire-watershed drivers and add an important perspective of impacts from historically non-fire-prone ecosystems. Finally, it will help water managers in coastal temperate rainforests by providing information about how their landscapes can respond to wildfire and which catchment or climatic characteristics are most likely to impact water quality. This will enable them to take a more proactive approach to wildfire risk governance by planning where to concentrate mitigation efforts in order to maintain water security in a changing climate.

Chapter 2. Wildfire impacts on stream water quality in the Pacific Coastal Temperate Rainforest

2.1 Introduction

Wildfires have a major influence on forested watersheds, altering ecosystem processes that can directly impact freshwater quality and ecosystem function (Bixby et al., 2015; Bladon et al., 2014; Pinto et al., 2009; Smith et al., 2011). Climate change is intensifying fire regimes worldwide, lengthening fire seasons and increasing the size, frequency, and severity of wildfires (Jones et al., 2022; Sayedi et al., 2024). This increase has been correlated with drier conditions, earlier snowmelt, and severe droughts (Paul et al., 2022). Additionally, fire ranges are being altered, with noted expansions into coastal temperate rainforests and other wet ecozones where fire has historically been uncommon (Abatzoglou et al., 2018; Bedia et al., 2015; Littell et al., 2018). This intensification of fire regimes is projected to continue and become more pronounced over the next century (Flannigan et al., 2013; Robinne et al., 2021; Wotton et al., 2017).

Wildfires can have strong impacts on forested catchments. They can destroy vegetation, change soil and organic matter chemistry, and increase erosion (Moody et al., 2013; Rhoades et al., 2019b; Shakesby and Doerr, 2006). Subsequent precipitation events can transport the products of wildfire into streams, causing altered loads of suspended solids, nutrients, dissolved organic matter (DOM), and various metals and ions (Bladon et al., 2014; Emelko et al., 2011; Hohner et al., 2019; Rhoades et al., 2019b; Robinne et al., 2020; Shakesby and Doerr, 2006; Smith et al., 2011; Stednick, 2010; Wang et al., 2015a). Changes in key nutrient balances (e.g., nitrogen and phosphorus) can alter food web dynamics and may lead to degraded ecosystem health or harmful algal blooms (Butler et al., 2019; Jager et al., 2021; Leonard et al., 2017; Writer et al., 2012). Heat can alter organic matter within soils, which may then be leached and transported into streams. This process results in DOM with modified reactivity and bioavailability, potentially influencing the composition of food webs (Thuile Bistarelli et al., 2021). Wildfire induced changes can also be problematic from a water treatment perspective: increasing concentrations of DOC can increase coagulant demand, reduce disinfection efficiency, and result in increased production of potentially carcinogenic disinfection by-products (DBPs) (Emelko et al., 2011; Parr et al., 2019; Uzun et al., 2020). Changes in DOM composition (e.g.,

increased aromaticity, altered N content) can further influence both the likelihood of DBP formation and the type of DBP created, which include regulated (e.g., carbonaceous) and unregulated (e.g., nitrogenous) variants (Emelko et al., 2011; Smith et al., 2011; Wang et al., 2015a; Yang et al., 2015). Understanding the possible outputs of wildfire is therefore important for forest and water managers, especially in small, rural or remote communities that may not have access to large-scale water treatment facilities (Moghaddam-Ghadimi et al., 2023).

High-severity wildfires tend to have the largest impacts. They cause high vegetation and soil microbe mortality, combust surface soil organic horizons, and create hydrophobic soils that can alter the hydrologic functioning of hillslopes and influence landscape-stream connectivity (Shakesby and Doerr, 2006). Organic matter combustion at the soil surface affects the molecular composition of DOM and causes the volatilization of elements with a gaseous phase (C, N) (Agbeshie et al., 2022; Hohner et al., 2019; Neary et al., 2005), alongside the transformation of N to inorganic forms (NO_2^- , NO_3^- , NH_4^+) (Sharma et al., 2017). Phosphorus, which does not have a gaseous phase, can be released from complex organic matrices and form bioavailable orthophosphate (PO_4^{3-}) (Neary et al., 2005; Zhang and Biswas, 2017). However, the loss of the biotic community means fewer of these newly available nutrients are intercepted (Leonard et al., 2017), while changes to soil porosity can drive an increase in surface runoff that can carry ash and sediments directly into streams (Doerr et al., 2006). Increases in several water quality constituents (e.g., DOC, dissolved inorganic nitrogen [DIN] and total dissolved and particulate phosphorus) have been frequently reported in the literature following large-scale or high severity fires (Chow et al., 2019; Emmerton et al., 2020; Gustine et al., 2022; Tecle and Neary, 2015; Uzun et al., 2020). While the low to moderate combustion temperatures ($\sim 200\text{-}300^\circ\text{C}$) of low-severity fires can engender greater changes to DOM concentration and composition when compared to higher-temperature burns (Chow et al., 2019; Hohner et al., 2017), the intact soils and plants that are more likely present after a low-severity burn can help mitigate in-stream impacts (Richardson et al., 2024).

Climatic variability further adds to the difficulty of accurately predicting water quality responses to fire. Undisturbed watersheds can see drastic changes in flow and water quality with seasonal cycles and in response to rainfall events (Chhetri et al., 2019; Parr et al., 2019; Rust et al., 2018). Storms in the Pacific Coastal Temperate Rainforest (PCTR) of North America drive increases in DOC concentrations and DOM molecular diversity derived from terrestrial soil

sources that become hydrologically connected to streams during precipitation events (Fellman et al., 2020), alongside increased delivery of terrestrial sediments and nutrients (Rhoades et al., 2019a; Rust et al., 2018). These storm-associated changes can present a challenge for drinking water treatment even when forests are intact (Delpla and Rodriguez, 2017). Wildfire can intensify these effects by increasing surface runoff that carries pyrogenic sediments, nutrients, and DOM (Murphy et al., 2015) – these effects may be especially pronounced in regions with high annual precipitation like the PCTR. Wildfire also affects flood regimes, with increased risks of larger and more frequent floods due to reduced vegetation interception and soil infiltration rates, though these effects depend on the size and severity of the burn (Atchley et al., 2018; Havel et al., 2018; Robinne et al., 2021).

The PCTR of North America has historically been a cool and wet region with a low frequency high severity fire regime, characterised by long return-intervals (200-500 years) between stand-replacing fires (Haugo et al., 2019). However, changing climate patterns are predicted to cause a breakdown in past fire patterns and these highly productive coastal temperate rainforests are likely to see the greatest proportional increase in area burned of all biomes compared to their historic conditions (Abatzoglou et al., 2021; Dye et al., 2024; Littell et al., 2018; Rogers et al., 2011; Wimberly and Liu, 2014). The PCTR has already begun to see increases in fire activity, with nearly 11% of the Oregon Cascades (USA) burning in 2020 (Abatzoglou et al., 2021; Reilly et al., 2022). However, the water quality consequences of fires in this region are poorly defined (but see Coble et al., 2023; Wampler et al., 2024). Instead, much of the research on wildfire and water quality has been centred in fire-prone ecosystems like the mixed forests of Australia and southwestern Europe (Carvalho et al., 2019; Cawson et al., 2013; Santín et al., 2015; Serpa et al., 2020), dry temperate forests and chaparral shrub lands of California and the Western U.S. (Goodridge et al., 2018; Oliver et al., 2012; Revchuk and Suffet, 2014; Santos et al., 2019), and the boreal forests of Canada (Bladon et al., 2008; Emmerton et al., 2020; Hutchins et al., 2023; Silins et al., 2014). There has been great variability reported in the magnitude, directionality, and duration of responses across multiple constituents of interest across the globe (Morales Parrado et al., 2023; Paul et al., 2022; Robinne et al., 2020; Smith et al., 2011), further highlighting the need for studies focusing on underrepresented biomes (Roces-Díaz et al., 2022). This is particularly true given that the variability of water quality response to fire can be attributed to differences in landscape characteristics (watershed hydrology, vegetation

and soil type), climate (precipitation and temperature), and fire behaviour (intensity, area burned, patchiness) (Cawson et al., 2013; Hohner et al., 2019, 2016; Nunes et al., 2018; Richardson et al., 2024; Wampler et al., 2024), making it difficult to predict outcomes based on data from other regions. In-situ observations are therefore necessary to gain a sense of what may be expected.

2.1.1 Study Objectives

In this study, we sampled streams and soils within nine recent (2015-2022) wildfire and paired reference sites within the Coastal Western Hemlock and Coastal Douglas Fir biogeoclimatic ecozones of British Columbia (Pojar et al., 1991), which are part of the PCTR. Specifically, our objectives were to: (1) quantify the magnitude, duration, and key drivers of water quality responses in burn-affected streams; (2) investigate the extent to which directly burned soil impacts are reflected in surface waters; and (3) investigate how water quality responses differ during baseflow and stormflow in burned and reference catchments. We predicted that: (1) water quality will be most impaired in severely burned catchments, with impacts diminishing with time since fire; (2) changes observed within soil extracts will be poorly connected to baseflow samples but share some characteristics with stormflow samples; and (3) burned catchments will have different response to storm events than reference catchments.

We undertake this work in a region where eighty-six percent of the population relies on forested source waters for their drinking water supplies (Statistics Canada, 2023), with the majority relying on small or medium-sized streams (Government of British Columbia, 1996). The existing treatment infrastructure is targeted to meet past and present risks, with several communities employing a multi-barrier approach that relies partially on forested areas to deliver high quality source water (Island Health, 2014). Wildfire, which constitutes a historically rare event in the PCTR, may therefore seriously alter ecosystem function and impede the delivery of safe drinking water if managers are not prepared (Robichaud and Padowski, 2024). This research will help shed light on the water quality responses that may be expected as fire regimes intensify and more watersheds are impacted by fire in coastal temperate rainforests.

2.2 Methods

2.2.1 Study Region

All study sites were located on southern Vancouver Island, which is dominated by the Coastal Western Hemlock (CWH) biogeoclimatic ecosystem classification (BEC) zone, with the Coastal Douglas Fir (CDF) BEC zone present along the eastern coast, at lower elevations in the rain shadow of the Island mountain ranges (MacKenzie and Meidinger, 2017) (Figure 1). The CWH zone occurs from sea level to 900m and is one of the wettest zones of British Columbia's BEC classification system, and occurs on both the west coast and east coast of Vancouver Island and the mainland coast of BC, with mean annual precipitation ranging from 1000-4400mm (Pojar et al., 1991). July is typically the driest month, with a mean precipitation of ~65mm, whereas the wettest month, December, has a mean precipitation of ~330mm (total precipitation, 1951-1980; Meidinger and Pojar, 1991). A cool mesothermal climate is characteristic of the CWH zone, with cool summers, periodic hot dry spells, and mild winters – the mean annual temperature is 8°C but can range from 5.2 to 10.5°C among the CWH subzones (Pojar et al., 1991). The hydroclimatic regime of Vancouver Island varies longitudinally and by elevation. The low lying areas of the east and west coast have a rain-dominated regime with high mean annual precipitation, but the rain-shadow caused by the central mountains gives the east side a generally lower monthly and annual mean precipitation as compared to the west (Eaton and Moore, 2010). In watersheds with significant areas of high elevation, seasonal snow can accumulate and a mixed hydrologic regime with elevated flows in the fall and spring (due to snowmelt) can occur (Bidlack et al., 2021). Stream flows generally follow seasonal patterns, with many smaller streams declining or becoming ephemeral during the warmer months. Peak flows generally occur from September through January and are often driven by atmospheric rivers (Sharma and Déry, 2020). Data averages derived for our study sites (mean annual temperature = 8.6°C, mean annual precipitation = 2101mm; 1991-2020) (T. Wang et al., 2016) were representative of the CWH zone. Across our sites, most precipitation (~90%) occurs between September 1 and April 30 (1991-2020), with July as the driest month (normal₁₉₉₁₋₂₀₂₀ = 29mm) and November the wettest (normal₁₉₉₁₋₂₀₂₀ = 346mm) (T. Wang et al., 2016).

The dominant vegetation is composed of western hemlock (*Tsuga heterophylla*), Douglas-fir (*Pseudotsuga menziesii*), and western redcedar (*Thuja plicata*), with a well-

developed shrub layer dominated by salal (*Gaultheria shallon*) (Government of British Columbia, 2024a; Pojar et al., 1991). Steep terrain and shallow soils are common, making the area generally unsuitable for agriculture (Pojar et al., 1991; Valentine et al., 1978). Logging is the main commercial land use on southern Vancouver Island and the majority of forests are second growth, with harvesting occurring since the early twentieth century (Government of British Columbia, 2000). Soils are predominantly humo-ferric podzols and dystic brunisols with frequent exposed bedrock (Government of British Columbia, 2018; Jungen, 1985). Parent materials are mainly of glacial origin and consist of tills, colluvium, and marine and glaciofluvial deposits (Jungen, 1985; Keser and St. Pierre, 1973).

The fire regime on southern Vancouver Island has varied over time, with a mixed-severity, lower frequency fire regime developing as climate moistened about 6,000 years ago and the CWH zone assumed its modern-day temperature and precipitation range (Brown et al., 2022). However, recent climate trends indicate warming and drying conditions, which are contributing to an increase in climate-driven emergencies (Wan et al., 2019). The typical moist, mild climates of the CWH and CDF zones favour forest growth and high fuel loads that are prone to ignition during prolonged dry periods (Brown et al., 2022). Given these conditions and the recognized challenges that can be presented by a post-fire landscapes, including altered DOM and nutrient loading and changes to hydrologic patterns like higher direct runoff and less vegetative interception and soil infiltration (Bladon et al., 2014; Hallema et al., 2018; Smith et al., 2011), the government of British Columbia has invested \$235 million (between 2004-2018) to define high risk areas and create detailed response protocols including post-fire environmental assessments in an effort to minimize the risks to public health, safety, and infrastructure (BC Flood and Wildfire Review Team, 2018; Hope et al., 2015). Fire management and mitigation has proved necessary in British Columbia with recent record-setting fire seasons (area burned or damage caused) in 2017, 2018, 2021 (Government of British Columbia, 2023a), and the 2023 season called “the most destructive in British Columbia’s recorded history” (Government of British Columbia, 2023b).

2.2.2 Sampling Campaigns

Nine historic wildfire sites were selected on southern Vancouver Island, across a range of sizes (5.7ha to 402ha), burn years (2015 to 2022), and burn severities (see below) (Figure 1, Table 1).

Fires were selected based on size (minimum 5ha), proximity to streams, and accessibility. Given our interest in the short- to mid- term impacts of fire, 2015 was selected as a natural break point amongst fires that met size and accessibility criteria. Eight of the nine sites were in the CWH zone, though they expressed a gradient of soil, vegetation, and topographic characteristics, as well as differing wildfire severities (Table 1). To assess how fires affected stream water quality on southern Vancouver Island, we undertook a synoptic surface water sampling campaign during baseflow conditions, collected soil samples adjacent to the synoptic sampling sites, and collected stormflow samples at select locations. We further undertook a geospatial assessment of catchment characteristics to explore the importance of wildfire relative to other catchment-specific and climactic drivers for determining water chemistry across sites.

2.2.3 Surface Water Synoptic Samples

Grab samples were collected at thirty-seven streams across eight of the nine fire sites during two sampling campaigns that captured the end and onset of the wet period: April-May 2022 and October 2022-January 2023 (Figure 1). Streams were visited two to five times, targeting baseflow conditions to allow for cross-site comparison under similar hydrologic conditions – though some visits did not yield any samples due to a lack of streamflow in ephemeral streams. The Mayo Lake (ML) fire site was dry during every sampling attempt and was therefore only sampled for soils. At each wildfire site, sampling locations were established to capture as many burn-affected streams as possible (one to seven, depending on the fire site), in addition to two to three adjacent reference streams (Figure 2, Figure A1). When a stream intersected with a path or roadway, samples were collected approximately 10 meters upstream to minimize road impacts. Of the thirty-seven streams sampled, nineteen were burn-affected and eighteen were considered reference sites. Reference sites were selected to be as comparable to the burn streams as possible – they were physically near, with similar channel size and comparable slope, vegetation, and disturbance histories (assessed prior to sampling using GIS data when possible, or visually at the time of sample collection).

We analyzed synoptic stream water samples for total suspended solids (TSS), nutrients (total dissolved nitrogen [TDN], total dissolved phosphorus [TDP], total nitrogen [TN], total phosphorus [TP], soluble reactive phosphorus [SRP], nitrite + nitrate [$\text{NO}_2^- + \text{NO}_3^-$] and ammonium [NH_4^+]), dissolved organic carbon (DOC) concentration, and dissolved organic

matter (DOM) absorbance and fluorescence, as well as specific conductance, cations (Ca^{2+} , K^{+} , Mg^{2+} , Na^{+} , Al^{3+} , dissolved Fe [dFe]), and anions (SO_4^{2-} , Cl^{-}). Samples were collected and analyzed as described in the appendix (Appendix A1). For each sample, specific conductance was measured in situ with a YSI multiparameter probe (YSI Professional Plus). DOM absorbance and fluorescence were used to calculate the spectral slope coefficient from 275-295 nm ($S_{275-295}$; inversely related to molecular weight), specific ultraviolet absorbance at 254 nm (SUVA_{254} ; positively related to aromaticity), and conduct a PARAFAC analysis (Helms et al., 2008; Murphy et al., 2013; Weishaar et al., 2003) (Appendix A1).

2.2.4 Soil Leaching Experiment

To consider the potential propagation of wildfire effects from soil to stream, soil samples were measured for water-extractable organic matter and nutrients. Eight soil samples were collected for each fire site – four from the burned area and four from surrounding reference areas (Figure 2, Figure A1). Each sample consisted of a composite of three soil cores (subsamples) collected within a 2m radius to account for spatial heterogeneity (Revchuk and Suffet, 2014; Wang et al., 2015b). Each soil core was split into 0-5cm and 6-10cm segments to separate the more organic upper soils from the deeper, more mineral soils (Fernández et al., 1997; Valentine et al., 1978). The upper 5cm also tends to be the most impacted by fire (Son et al., 2015). Samples taken from within burn scars were targeted to different burn intensities when possible. Cores were collected using a 1-inch diameter soil probe, separated by depth, put in plastic “Ziploc” bags, and frozen until analysis. Samples were collected at all sites except Jacob Creek (JC; Figure A1), which was omitted due to safety concerns. Repeat soil samples were also collected from the CT fire site before (Oct 2022) and after (Jan 2023) the start of the wet season to capture changes following the first post-fire precipitation event, with the January samples collected at the same global positioning system (GPS) location, using a GPS unit (Garmin GPSMAP 64st) with a resolution of ~3.5m (Figure 2). Samples were processed as described in the appendix text (Appendix A1) and assessed for Loss on Ignition (LOI) and water-extracted DOC concentration, DOM composition, TDN, and TDP. All composite soil samples were combined, screened (pore size 2mm), and homogenized before being split and leached in triplicate; reported values represent the mean of each sample triplicate (DOC and DOM), or measures from composite samples (TDN and TDP).

2.2.5 Storm sampling

In addition to baseflow sampling, low-resolution storm samples were collected using a paired design (reference/burn) at four sites (HC, NL, HO, CT; Table 1) using passive rack samplers, and high-resolution storm samples were additionally collected from site CT using automatic pump samplers (see below). For the lower resolution passive rack samples, each rack consisted of several 250mL HDPE bottles equipped with siphoning lids mounted at staggered heights, with a central stilling well made of PVC pipe (1.5 inch) with holes (0.5 inch) along its length and a measuring tape affixed to it (Figure A2) (Graczyk et al., 2000; McSorley, 2020). Inside the stilling well, an Odyssey Capacitance Water Level Logger (Dataflow Systems Ltd., New Zealand) measured stage every 10 minutes. Stage measurements were used to determine when the bottles filled, and the shape of the hydrograph. Due to the passive nature of siphon filling, bottles only collected water on the rising limb and were designed to ensure discrete sample collection (McSorley, 2020). Two storm events were captured; the first was a 101mm (max sum 24h precipitation, San Juan weather station, Figure 1, Table A1) event between October 27 - November 01, 2022 that mostly impacted the west side of Vancouver Island and was therefore only captured at site HC. The second was a 131mm event captured across three of the four sites on December 24-26, 2022, with 1-2 bottles filled on each sampler (Figure A3, Table A1). Samples were retrieved as quickly as possible (two to three weeks post-event) and analyzed for DOC concentration, DOM composition, TDN, and TDP following the same methods as surface baseflow samples (Appendix A1).

In addition, we installed ISCO 6712 samplers at the most recent fire site (CT, 2022) with the aim of capturing relatively high-resolution data in the first post-fire wet-up period. This fire was declared out at the end of October 2022, and the site was instrumented on November 12, 2022. Two ISCOs were installed on the main burn-affected stream, with one autosampler upstream of the burn and one downstream, and a third autosampler at one of the adjacent reference streams (Figure 2). This installation allowed us to capture the second regionally significant post-burn storm event (48mm max 24h precipitation, January 11-14, 2023, Salt Spring meteorological station, PCIC ID 1637; Figure 1, Table A1), with samples collected every three hours. Precipitation centroid lag-to-peak was calculated to help compare stream responses (Dingman and Dingman, 2015).

2.2.6 Environmental and Catchment Characteristics

Rain data were obtained from the Pacific Climate Impacts Consortium (PCIC) for four weather stations on or near Vancouver Island (Pacific Climate Impacts Consortium, 2024) (Figure 1). Several weather stations were assessed, and those that had sufficiently complete data for the study period were paired with the nearest fire sites – three of the selected stations are operated by the British Columbia Ministry of Forests, Lands and Natural Resource Operations - Wildfire Management Branch (FNLRO-WMB), one by Environment Canada (EC) (Table A1). Recorded precipitation sometimes varied greatly between weather stations, with those on the west side of Vancouver Island (San Juan, Sheringham Point) typically recording higher precipitation than those on the east (Salt Spring, Nanaimo) (Table A1, Figure A4).

Catchment and climate characteristics were derived from geographic information systems (GIS) data using ESRI ArcGIS Pro 3.2.1. The Canadian Digital Elevation Model (CDEM) (32m x 32m) was obtained from GeoGratis (Government of Canada, 2023) and pre-processed to “burn in” stream networks in ArcGIS Pro (Fill Sinks, Flow Direction, Flow Accumulation). Catchments were then delineated using the “Watershed” tool, with the surface water sample collection locations used as pour points. Wildfire and BEC zone data were obtained from *iMapBC*, using the “Wildfire Fire Perimeters – Historical” and the “BEC Analysis” datasets (Government of British Columbia, 2022). Mean annual temperatures and precipitation were obtained from ClimateBC (Wang et al., 2023), using data from 1991-2020. Soil composition data were collected using the Soil Information Finder Tool (SIFT) (Government of British Columbia, 2018), a digital compilation and repository of the data initially collected during the British Columbia soil surveys of the 1980s (Jungen, 1985). Vegetation and harvest history data were derived from the British Columbia Vegetation Resource Inventory (Government of British Columbia, 2024a), a comprehensive data repository maintained by the Forest Analysis and Inventory Branch of the BC government. For each of the vegetation and soil data classes (e.g., soil texture, soil drainage, vegetation type), the percent-coverage within each watershed was calculated and used for analysis. Burn severity maps were developed using Sentinel-2 and Landsat 8-9 satellite imagery (Modified Copernicus Sentinel data, 2023) following the same-year burn area reflectance classification (BARC) protocol employed by the BC government (Government of British Columbia, 2023c). Average burn severity for each fire was obtained by calculating the proportional area impacted by each burn severity class, multiplying that by their

associated numeric ratings (Reference = 0, Unburned = 1, low = 2, moderate = 3, high = 4), then summing the resultant values to assign an overall burn severity. Catchment burn severity was defined as the average burn severity multiplied by the proportion of the catchment burned.

2.2.7 Statistical analyses

All statistical analyses were performed in R (4.3.2) (R Core Team, 2023), including frequently used packages *data.table*, *lubridate*, *ggplot2*, and *dplyr* (Barrett et al., 2023; Grolemund and Wickham, 2011; Wickham, 2016; Wickham et al., 2023). Data were tested for normality and heteroscedasticity prior to analysis and were generally assessed in three separate groups based on their source: baseflow surface waters, stormflow surface waters, and soil leachates ($n_{\text{base}} = 74$, $n_{\text{storm}} = 44$, $n_{\text{soil}} = 144$), except when constructing our PARAFAC analysis, which used the combined dataset (Appendix A1). The excitation emission matrices (EEMs) were used to identify individual fluorescence components and calculate the biological index (BIX) and the humification index (HIX) – common fluorescence indices that broadly characterize DOM composition and help identify organic matter sources as autochthonous or allochthonous (Huguet et al., 2009; Ohno, 2002). Molar N:P ratios were calculated for surface baseflow samples using the molar ratio of dissolved inorganic nitrogen (DIN; $\text{NH}_4^+ + \text{NO}_2^- + \text{NO}_3^-$ as N) to total phosphorus (TP as P), which is a better indicator than the TN:TP ratio for N and P limitation of phytoplankton in oligotrophic freshwater systems (Bergström, 2010; Keck and Lepori, 2012). Systems may be N-limited when DIN:TP is lower than 1.5 and P-limited when DIN:TP is greater than 3.4, with co-limitation occurring in between (Bergström, 2010).

To better visualize how water quality changed between reference and burn sites, individual water chemistry parameters were normalized by source (surface baseflow, soil_{0-5cm}, soil_{6-10cm}), to create a pool of Z-scores that had a mean of zero and standard deviation of 1 within each source type. Mean Z-scores were then calculated for each site and burn status (e.g., HC_{ref} and HC_{burn}), and the difference between reference and burn were obtained for each site to describe the change in burn-affected streams ($Z_{\text{burn}} - Z_{\text{ref}}$). The average difference for all sites was then calculated and used to express the overall average change in DOC, DOM composition, nutrients, and ions. One-sample, two-tailed t-tests ($\mu = 0$) were used to identify significant changes between reference and burn sites in each data type. We also used the Z-score approach to assess stormflow response and the differences between reference and burned sites. Within

each water chemistry parameter, a pool of Z-scores was calculated for stormflow data and paired baseflow data ($n_{\text{storm}} = 44$, $n_{\text{base}} = 36$). Paired t-tests were used to compare baseflow and stormflow, and two-sample t-tests were used to compare the responses of burned and reference catchments to one another.

We used mixed-effects random forest (MERF) models to assess the influence of landscape characteristics on DOC, $S_{275-295}$, TDN and TDP (*LongituRF*; Capitaine, 2020; Capitaine et al., 2021). MERF was selected for its ability to deal with longitudinal data (i.e., repeated measures), handle high dimensional data and calculate variable importance metrics (VIMs), and its robustness to outliers and departures from normality (Biau and Scornet, 2016; Tyralis et al., 2019) (see Appendix A1 for more detail). Three MERFs were constructed using data from different sources, as described above. Sample site was included as a random effect for all data sources, with seasonality added for the surface waters and sample depth added for the soil leachates.

2.3 Results

Relative to the 1991-2020 climate normal (2101 mm yr⁻¹), southern Vancouver Island was drier in 2022 (1763 mm yr⁻¹) (T. Wang et al., 2016). Seasonal patterns were also reversed; although the 2022 mean annual temperature was similar to the long term normal (normal₁₉₉₁₋₂₀₂₀ = 8.6°C, 2022 = 8.7°C), spring 2022 (March-May) was cooler (normal₁₉₉₁₋₂₀₂₀ = 7.5°C, 2022 = 6.5°C) and experienced 25% more precipitation than normal (normal₁₉₉₁₋₂₀₂₀ = 421mm, 2022 = 526mm), whereas fall (Sept-Nov) was warmer (normal₁₉₉₁₋₂₀₂₀ = 9.0°C, 2022 = 9.9°C) and experienced 46% less precipitation (normal₁₉₉₁₋₂₀₂₀ = 633mm, 2022 = 342mm) (T. Wang et al., 2016). This dry period represented a historic seasonal drought that reached B.C.'s highest drought warning level by October 2022 (Government of British Columbia, 2024b) and impacted stream, river, and reservoir levels.

Given these prevalent dry conditions during the fall sampling period – when most sampling was conducted (Figure 1) – and that most of the streams were perennial or of very low Strahler order, it was common for baseflow samples to be collected with relatively little streamflow. Streams also had a muted rainfall response, possibly due to a larger than usual amount of soil storage to overcome; several sample streams returned to dry conditions following the first few precipitation events of the fall season (Figure 1).

2.3.1 DOC concentration and DOM composition

Surface water DOC concentrations ranged from 0.5 mg L⁻¹, measured in one of the largest burn-affected streams at baseflow (site HC_{burn-6}), to 10.2 mg L⁻¹, measured on the rising limb of one of the first precipitation events following an extended dry period at a reference site (HC_{ref-1}). In baseflow samples, burned sites tended to have lower DOC concentrations than reference sites (DOC_{ref} = 2.5±0.2 mg L⁻¹, DOC_{burn} = 1.8±0.2 mg L⁻¹; mean ± se; p=0.085) (Figure 3, Figure A5, Table A2). The soil leachates followed the same trend but had a more pronounced response: water extracted DOC was lower for burn sites at both soil depths, with reductions of 55% at depth 0-5cm (DOC_{ref} = 14.2±2.0 mg L⁻¹, DOC_{burn} = 6.4±0.6 mg L⁻¹, p=0.016) and 47% at 6-10cm (DOC_{ref} = 10.8±1.4 mg L⁻¹, DOC_{burn} = 5.7±0.6 mg L⁻¹, p=0.027) (Figure 3, Figure A6, Figure A7, Table A2). This aligns with differences in LOI, for which reference samples had twice as much organic matter as burn samples (LOI_{ref} = 12.3±1.6%, LOI_{burn} = 6.3±0.4%; p=0.022) (Figure 3).

Surface water DOM tended to be humic-like, with HIX values (HIX_{mean} = 0.9±0.01) indicative of high fulvic acid content (Ohno, 2002), and BIX values well within the range associated with low autochthonous productivity (BIX_{mean} = 0.55±0.01; high autochthonous productivity BIX > 1) (Huguet et al., 2009) (Figure 3). Baseflow samples had higher SUVA₂₅₄ (i.e., aromaticity) than the soil leachates (SUVA₂₅₄ baseflow_{mean} = 3.6±0.1, soil 0-5cm_{mean} = 2.1±0.1, soil 6-10cm_{mean} = 2.0±0.1) and likewise had higher molecular weight (S₂₇₅₋₂₉₅ baseflow_{mean} = 13.2±0.1 • 10⁻³ nm⁻¹; soil 0-5cm_{mean} = 14.2±0.2 • 10⁻³ nm⁻¹, soil 6-10cm_{mean} = 14.5±0.3 • 10⁻³ nm⁻¹) (Figure 3, Figure A5, Figure A6, Figure A7). A PARAFAC analysis resulted in a validated five-component model (Figure A8). Using the OpenFluor database (Murphy et al., 2014), PARAFAC components 1, 2, and 4 (C1, C2, C4) were identified as humic-like, component 3 (C3) was identified as microbial-humic like, and component 5 (C5) was identified as tryptophan-like (protein-like) (Table A3). Overall, composition was dominated by the humic-like components (C1+C2+C4 = 69±1%), with the microbial-humic and protein-like components roughly evenly dividing the remainder (C3 = 17±1%, C5 = 14±0.3%) (Figure 3).

DOM composition was similar between the burn and reference streams in baseflow samples, though BIX was statistically lower in reference samples, despite only slight differences between site types (BIX_{ref} = 0.55±0.007, BIX_{burn} = 0.56±0.005, p=0.040). S₂₇₅₋₂₉₅ was also

marginally lower in burn sites ($p=0.107$). The soil leachates had a stronger response, especially in the surficial (0-5cm) layer. Of the five PARAFAC components, the relative contribution of C5 (protein-like) was half that of reference sites in burn-affected soil extracts ($C5_{\text{ref}} = 23\pm2\%$, $C5_{\text{burn}} = 13\pm1\%$, $p=0.003$) while C3 (microbial-humic) was doubled ($C3_{\text{ref}} = 6\pm1\%$, $C3_{\text{burn}} = 13\pm1\%$, $p=0.01$). HIX was lower in burned soil_{0-5cm} ($HIX_{\text{ref}} = 0.87\pm0.01$, $HIX_{\text{burn}} = 0.80\pm0.01$, $p=0.008$) but showed no difference in soil_{6-10cm} ($p=0.571$). Similarly, $S_{275-295}$ was lower in burned soil_{0-5cm} (i.e., suggesting greater molecular weight; $p=0.003$) but not in soil_{6-10cm} ($p=0.696$) (Figure 3, Figure A6, Figure A7, Table A2).

2.3.2 Nutrients and ions

All baseflow samples displayed overall low TSS ($\text{TSS} = 0.7\pm0.2 \text{ mg L}^{-1}$; Figure A5), with little difference between burned and reference sites ($p=0.808$) (Figure 4, Table A2). Nutrient response for streams at baseflow varied – TP did not show a statistical difference between burned and unburned sites ($\text{TP}_{\text{ref}} = 9.1\pm1.2 \text{ } \mu\text{g L}^{-1}$; $\text{TP}_{\text{burn}} = 8.4\pm0.9 \text{ } \mu\text{g L}^{-1}$; $p=0.360$), but burned sites had 22% greater concentrations of TDP ($\text{TDP}_{\text{ref}} = 3.7\pm0.35 \text{ } \mu\text{g L}^{-1}$; $\text{TDP}_{\text{burn}} = 4.5\pm0.37 \text{ } \mu\text{g L}^{-1}$; $p=0.024$) and 52% and 54% lower concentrations of TN ($\text{TN}_{\text{ref}} = 170.1\pm28.8 \text{ } \mu\text{g L}^{-1}$; $\text{TN}_{\text{burn}} = 82.6\pm13.1 \text{ } \mu\text{g L}^{-1}$; $p=0.007$) and TDN ($\text{TDN}_{\text{ref}} = 186.7\pm29.7 \text{ } \mu\text{g L}^{-1}$; $\text{TDN}_{\text{burn}} = 85.7\pm13.6 \text{ } \mu\text{g L}^{-1}$; $p=0.002$), respectively (Figure 4, Figure A5, Table A2). Surface soil (0-5cm) leachates from burned sites had 51% less nitrogen than reference ($\text{TDN}_{\text{ref}} = 733\pm115 \text{ } \mu\text{g L}^{-1}$; $\text{TDN}_{\text{burn}} = 358\pm47 \text{ } \mu\text{g L}^{-1}$; $p=0.031$), following the trend of baseflow samples (Figure 4, Figure A6, Figure A7, Table A2). Burned soil leachates also suggested a loss of TDP ($\text{TDP}_{\text{ref}} = 258\pm67 \text{ } \mu\text{g L}^{-1}$; $\text{TDP}_{\text{burn}} = 99\pm14 \text{ } \mu\text{g L}^{-1}$; $p=0.078$), in contrast to the TDP increase observed in burned surface water samples. The DIN:TP ratio (Bergström, 2010) of surface waters dropped from 29.5 for reference streams to 11.9 for burned streams, primarily driven by a 63% decrease in $\text{NO}_2^- + \text{NO}_3^-$ ($\text{NO}_2^- + \text{NO}_3^-_{\text{ref}} = 117.4\pm32.3 \text{ } \mu\text{g L}^{-1}$, $\text{NO}_2^- + \text{NO}_3^-_{\text{burn}} = 42.6\pm15.1 \text{ } \mu\text{g L}^{-1}$; $p < 0.002$); NH_4^+ was low in the majority of samples and therefore exerted little control over DIN (72% BDL, $<3 \text{ } \mu\text{g L}^{-1}$; $\text{NH}_4^+_{\text{ref}} = 4.1\pm2.0 \text{ } \mu\text{g L}^{-1}$, $\text{NH}_4^+_{\text{burn}} = 2.8\pm1.0 \text{ } \mu\text{g L}^{-1}$). Dissolved organic nitrogen ($\text{DON} = \text{TDN} - \text{DIN}$) was also lower in burned, when compared to reference, streams ($\text{DON}_{\text{ref}} = 65.2 \pm 12.5 \text{ } \mu\text{g L}^{-1}$, $\text{DON}_{\text{burn}} = 40.2\pm5.5 \text{ } \mu\text{g L}^{-1}$).

Specific conductance and the overall ionic composition of the baseflow stream samples did not respond strongly in the studied catchments (Figure 4, Table A2).

2.3.3 Storm response

A comparison of the low-resolution (i.e., rack sampler & peak-only pump sampler) storm samples and paired baseflow samples showed that the storm responses of reference and burn-affected catchments were statistically equivalent to one another at this level of sampling resolution (Figure 5, Figure 6, Figure A9, Table A4). We detected a storm-driven increase in DOC of 1.3 and 1.2 standard deviations for reference ($p=0.002$) and burned ($p<0.001$) streams, respectively (overall stormflow and baseflow $\text{DOC}_{\text{mean}} = 2.7 \pm 0.2 \text{ mg L}^{-1}$; $\text{SD} = 1.6 \text{ mg L}^{-1}$), alongside an increase in molecular weight (decreased $S_{275-295}$, $p=0.002$) regardless of burn status (Figure 5, Figure A9, Table A2). Overall TSS was also higher during storms when considering all samples ($\text{TSS}_{\text{storm}} = 22.9 \pm 14.4 \text{ mg L}^{-1}$, $\text{TSS}_{\text{base}} = 0.7 \pm 0.2 \text{ mg L}^{-1}$; $p=0.049$), although this pattern became statistically non-significant when isolating either reference or burn streams (Figure 6, Table A2, Table A4). TN, TDN, and TDP also increased during storm events for both catchment types (Figure 6, Figure A9). DOM composition was largely unaffected by storm events, although a modest but consistent decrease of the microbial-humic C3 was observed in reference streams ($p=0.037$, Figure 5, Table A2). Despite the lack of statistical significance, the finer scale storm sampling at the most recently burned site, Cowichan Trail (CT – 2022), visual inspection of the data showed an elevated storm response in the burn-affected samples for DOC, MW, TDN and TSS (see below).

2.3.4 Cowichan Trail (CT) Storm Data

High-resolution event samples were collected every 3h throughout a storm event from January 11 to January 14, 2023, during the first post-fire wet season at site CT (2022). Both the reference and burn-affected sites showed storm-driven changes in all constituents (Figure 7). While we did not capture enough storm events to perform statistical analyses using high-resolution data, the downstream burn-affected site tended to have larger increases in TSS, MW, and TDN when compared to the paired upstream reference site, and DOC was slower to return to pre-event concentrations (Figure 7). An adjacent reference stream highlighted the natural variability of the system with a much stronger TSS response and a different baseline concentration of TDN when compared to the stream with the paired reference and burned samples, but the overall pattern of storm response was similar. An assessment of hysteresis at the upstream (unburned) and downstream (burned) sites indicated that DOC, TDN, and TDP had a flushing response at both

sites, with DOC showing an apparent switch between counterclockwise hysteresis at the downstream (burned) site, and clockwise hysteresis at the upstream (unburned) (Figure A13).

We also explored how soil leachates changed using the repeat soil samples collected both immediately after the fire, but prior to any precipitation (CT-F, October 2022) and after the start of the wet season (CT-W, January 2023) (Figure A6, Figure A7). A decrease in LOI for the burn-affected surface soils (0-5cm) was the only statistically significant change between seasons ($\text{LOI}_{\text{burn-fall}} = 10.2\%$, $\text{LOI}_{\text{burn-winter}} = 6.7\%$, $p=0.021$, Figure A6), although leachable TDN tended to be lower in the burned soils in winter (post wet up) when compared to the fall (prior to wet up) ($p=0.111$). In contrast, reference soils showed no change in LOI ($p=0.792$) or TDN ($p=0.527$) from before, to after, wet up, although TDP tended to be greater after the start of the rainy season ($p=0.070$; Figure A6).

2.3.5 Mixed-Effect Random Forest

Irrespective of the water quality parameter being examined, vegetation type, latitude/longitude, and aspect tended to be important determinants of water quality, with burn severity being an important, but often secondary, driver (Figure 8, Figure 9, Figure 10). For baseflow samples, vegetation composition (% shrub) was the most important factor explaining variation in DOC and DOM composition (i.e., $S_{275-295}$) across sub-catchments, closely followed by catchment burn severity, which encompasses fire size and severity (Figure 8). Partial dependence plots indicated that DOC concentration and DOM molecular weight decreased as catchment burn severity increased (Figure A10). Variation in baseflow concentrations of TDN were largely attributed to differences in geographic setting (i.e., aspect, latitude, and longitude), combined with soil and vegetation composition. Baseflow TDP was most strongly driven by vegetation and soil composition, alongside slope, aspect, and latitude. For both TDN and TDP, time since fire and catchment burn severity were assigned moderate-low importance (Figure 8).

By contrast, burn severity was consistently ranked in the top three most important predictors of soil leachate chemistry (Figure 9). As above, leachate DOC concentrations declined as burn severity increased (Figure A11). Unlike baseflow samples, leachate molecular weight increased with burn severity. Both TDN and TDP decreased as burn severity increased. In all cases except TDN, the soil MERFs had greater explanatory power than those for the baseflow surface waters, and strong explanatory power overall ($r^2 > 0.75$).

The storm event MERFs had the lowest explanatory power but suggested heightened importance of climatic variables (Figure 10, Figure A12). The top two predictors for baseflow DOC, which were shrub percentage and catchment burn severity, were replaced by longitude and percent sand-in-soil in the storm event model. Explanatory variables for $S_{275-295}$ likewise shifted in the storm MERFs, with latitude classified as most important and catchment burn severity dropping from second to third rank. Latitude and longitude were both correlated with mean annual precipitation, due to the central mountain rain shadow (see Figure 1; Pearson's $r = -0.63$, -0.79 , respectively). Catchment burn severity was given moderate-low importance for both TDN and TDP, as was the case for the baseflow models.

2.4 Discussion

2.4.1 Response to wildfire varies between regions

Research considering the impacts of wildfire on water quality has been focused heavily in historically fire-prone areas like California, Australia, and the mountainous region of Canada (Emmerton et al., 2020; Morales Parrado et al., 2023; Robinne et al., 2019; Wagenbrenner et al., 2021). To our knowledge, only two other studies have reported the water quality impacts of wildfire in North American coastal temperate rainforests (Coble et al., 2023; Wampler et al., 2024), though several have examined post-fire vegetation dynamics (Beese et al., 2006; Belillas and Feller, 1998; Curran, 1994; Homann et al., 2011; Jablónczy, 1964) and past or projected fire regimes (Brown et al., 2022; Dye et al., 2024; Haugo et al., 2019; Heyerdahl et al., 2012; Hoffman et al., 2016; Long and Whitlock, 2002; Rogers et al., 2011; Wimberly and Liu, 2014). Wildfire impacts on water quality are highly variable across regions. A recent review of studies published on this topic since 1980 highlighted the variability of observed responses – for example, 48% of studies that recorded post-fire DOC concentration found an increase, 26% found a decrease (as we did), and 26% found no change, while only 7% of the studies reviewed reported a decrease in nitrogen like we found in our study ($n=83$, N-form unspecified) (Paul et al., 2022). Another review noted a decrease in NO_3^- and TN in 3 of 28 (11%) and 4 of 23 (17%) of the studies considered, respectively (Morales Parrado et al., 2023). This disparity of results highlights the importance of site-specific studies to elucidate likely outcomes in different biomes. Notably, the lower DOC and N we measured were in the minority of reported results, though

decreased DOC was consistent with the results of one of the other studies in our region (Wampler et al., 2024).

We also did not find any significant effects of time since fire, which was surprising given that temporal changes in wildfire effects on stream water quality are commonly reported (Francos et al., 2018; Hauer and Spencer, 1998; Leonard et al., 2017; Niemeyer et al., 2020; Nunes et al., 2018; Rust et al., 2018; Santos et al., 2019; J.-J. Wang et al., 2016; Yu et al., 2019), the longest of which lasted fourteen years post-fire (Rhoades et al., 2019a). Our study considered multiple fires spanning a range of burn years, unlike the long-term, repeated sampling approach employed by the above-mentioned works. It is possible that inter-site variation obscured trends that may have been detectable with a multi-year sampling design given that our sites had a range of burn sizes and severities, both of which modulate water quality impacts, and had some variation in catchment and climatic characteristics known to affect surface water quality (for examples, see Figure 8, Figure 9, Figure 10). Time since fire was somewhat correlated with several site characteristics in our study including longitude, slope, northing, and mean annual precipitation (Pearson's $r > 0.73$), further suggesting that the natural site characteristics may have overwhelmed time-driven changes. Temporal changes have sometimes been attributed to terrestrial subsidies gradually flushing through the system (Santos et al., 2019; Yu et al., 2019), which may not have been occurring in our study sites. Revegetation has also often been noted as a key factor in the magnitude and duration of wildfire effects (Francos et al., 2018; Gustine et al., 2022; Rhoades et al., 2019a; Rust et al., 2019). The highly productive nature of the PCTR may therefore help mitigate some of the impacts as vegetation intercepts fire-mobilized nutrients (Curran, 1994) and sediments before they are transported to streams, especially when burns are patchy or less severe (i.e., not stand-replacing). The decrease in soil leachate organic carbon and N we saw pre and post wet-up (CT-F and CT-W, respectively) also point to potential fast flushing that may make it difficult to capture the rapid, pulsed effect.

2.4.2 Water chemistry changes during baseflow conditions

Although burn severity was ranked within the top three most important predictors for baseflow DOC and S₂₇₅₋₂₉₅ MERFs, it was placed after biotic factors (e.g., shrub percentage), reinforcing that it plays an important but secondary role in determining the amount and composition of DOM transported to streams, when compared to the composition of catchment vegetation

(Kothawala et al., 2015; Liu et al., 2021). Bulk landscape C and N are likely to decrease after a fire due to volatilization even at low burn severities – combustive losses have been recorded starting at temperatures as low as 150°C and typically increase with temperature (Hohner et al., 2019). However, fire can also lead to increased mobilization as C is released from sequestration (e.g., burning plant matter), and N is converted to more bioavailable forms. Vegetation and microbe mortality, which are dependent on fire severity, can influence recovery by impacting nutrient uptake and N-fixation in the post-fire landscape. Despite this, baseflow TDN MERFs attributed very low importance to catchment burn severity, potentially indicating a lack of near surface flow paths during the very dry sampling period.

We measured greater surface water TDP in burned catchments, though SRP remained unchanged. The TDP MERF assigned moderate importance to time since fire while catchment burn severity was ranked near the bottom. Unlike C and N, P has a high volatilization temperature (>774°C) and is much more likely to mineralize or be deposited during a fire (Son et al., 2015), which may explain the reduced importance of burn severity. Particulate P in sediments transported to streams following fire can remain elevated for years post-fire and slowly release, especially if stream beds are coarse and able to trap sediment (Emelko et al., 2016), even if the more readily bioavailable SRP can be quickly utilized in-stream (House et al., 1995). While we did not directly measure sediment particulate P, the heightened importance of time since fire in VIM rankings suggests that this type of dynamic may be occurring in our study area, with released SRP possibly being quickly consumed in this P limited environment (see below).

2.4.3 DOM Compositional Changes

The effect of wildfire on DOM composition is modulated by temperature. Partially burned plant matter can generate molecularly complex carbon which has been associated with an increase in aromaticity (i.e., SUVA₂₅₄) (Wang et al., 2015b). At our study sites, molecular complexity showed no significant change between reference and burned catchments despite an increase in molecular weight (MW; from S₂₇₅₋₂₇₅). Fire can reverse the relationship between size and complexity through the formation small, aromatic, soluble compounds that increase SUVA₂₅₄ but decrease MW (Hohner et al., 2019). However, moderate heating (~250°C) can change MW independently of aromaticity via the release of soluble, large-size aliphatic molecules, possibly due to the thermal degradation of cellulose and phospholipids from cell walls (Santos et al., 2016), which

may explain why the post-fire increase in MW we observed was not accompanied by any significant change in aromaticity. Our results reinforce previous observations that SUVA₂₅₄ and MW can become decoupled in wildfire-affected catchments (Hohner et al., 2019; McKay et al., 2020). This may have implications for drinking water disinfection by-products (Hua et al., 2020) – water managers should therefore not rely on correlative relationships but instead be explicit in their measurements of MW and aromaticity.

2.4.4 A comparison of soil leachates and baseflow conditions

The dominance of humic-like components (C1, C2, C4) and low BIX values in our baseflow samples indicate strong terrestrial inputs, as may be expected for low order streams. However, the changes in relative DOM component contributions between the baseflow and soil leachates suggest either poor hydrologic connection between soil collection sites and streams at baseflow, or that there are significant biogeochemical changes occurring between the soil sample collection locations (i.e., the catchment) and the stream. Burn severity was a less important predictor of DOC, TDN, and TDP concentrations in the baseflow samples than the soil leachates and the baseflow MERFs had less explanatory power, which suggests that soils were more directly impacted by fire. Most sampled catchments were only partially burned (Figure 1, Table 1) so this dampening of importance may be partially attributable to dilution. Processing in intact riparian areas can contribute to homogenizing stream inputs (Carvalho et al., 2019; Verkaik et al., 2015), but water in this region travels quickly (Anderson et al., 2009) and the dry conditions of our sampling period may have partially decoupled riparian zones from terrestrial inputs (Luke et al., 2007). Furthermore, during baseflow, terrestrial DOC and nutrient sources can be disconnected from the surface water stream network as a whole and can remain poorly connected even throughout precipitation events, depending on soil infiltration dynamics and storage capacity (Dunne and Black, 1970). Since streams at baseflow are generally sustained by groundwater inputs (Singh, 1969), it may be that the baseflow samples are almost entirely independent from surface soil conditions. Even within our two depths of soils, the 0-5cm layer almost always showed a greater wildfire response than the deeper, 6-10cm layer, which supports that direct exposure to fire (including both heat and charred material) is an important regulator of impacts (Gustine et al., 2022) and suggests that effects are not always readily transmitted to greater soil depths or groundwater tables. However, it should also be noted that the combustion of the soil

organic layer can reduce soil depths in a post-fire landscape (Walker et al., 2018). Our soil sampling did not account for this potential change in depth profiles, so while our samples represent the first 0-5cm and 6-10cm rainwater will flow through, they may correspond to slightly different soil horizons in burned and reference areas. The mirrored decreases in DOC and TDN in both baseflow samples and soil leachates suggest that some changes may persist even when there is little active connectivity between landscape and stream, perhaps arising from overarching landscape changes like a significant reduction of organic material.

While no compositional differences were apparent between burned and reference streams at baseflow, the protein-like component (C5) in burn-affected soil leachates decreased by more than half while the microbial-humic component (C3) nearly doubled compared to reference. Increases in microbial activity can occur in a post-fire landscape since microbes tend to be more resistant to heat than plants and fungi, and recover quickly when released from competition for fire-mobilized nutrients (Bollen, 1969; Deka and Mishra, 1983). Previous studies examining the optical properties of fire-affected DOM have also identified that fire can produce aliphatic, microbial-source-like DOM in a range similar to that of C3 (C3: Ex 240 nm/Em 391 nm; pyrogenic DOM range: Ex 230–250 nm/Em 340–390 nm) and have suggested it might be useful as a “biogeochemical thermometer” (Wang et al., 2015b). This implies that the post-fire increase in C3 we observed may be partially attributable to this pyrogenic source of carbon alongside (or instead of) increased post-fire microbial activity.

2.4.5 Storms influence catchment exports

We expected the effects of wildfire to be more pronounced during periods of increased landscape connectivity (i.e., precipitation events). While we detected storm-driven nutrient pulses, consistent with previous studies in coastal temperate rainforests (Fellman et al., 2009), we found that the magnitude of peak stormflow responses was not statistically different between reference and burned areas based on the low-resolution data from the eight instrumented locations (four reference and burned stream pairs). This was surprising given the fire-driven changes apparent in our soil leachates and the prevalence of altered storm response in other works (Hallema et al., 2017; Hohner et al., 2019; Malmon et al., 2007; Paul et al., 2022; Wilson et al., 2018). However, our storm response data only captured a few points, and the lack of data combined with spatial variability may have masked the true storm response. The higher resolution data from the pump

samplers installed at the CT site, which was instrumented through the start of first post-fire wet season, indicated potential differences between burn and unburned catchments. Specifically, fire-affected samples showed higher increases in MW, TDN, and TSS, as well as a lingering DOC response (Figure 7). This pattern aligns with previous research that suggests changes in hillslope runoff patterns (Hallema et al., 2017) and increases in readily transported material (Malmon et al., 2007) can intensify storm inputs to streams, particularly in recently burned areas – though this effect is strongly influenced by the severity of the burn and the intensity of post-fire precipitation (Wilson et al., 2018). Fire-heightened storm responses can be driven by the formation of a layer of water repellent soils, which can persist for several years after a fire depending on severity (Beatty and Smith, 2013; Doerr et al., 2006; Doerr and Cerdà, 2005), and reduced vegetation interception (Niemeyer et al., 2020). Soil hydrophobicity in particular can lead to reduced infiltration capacity and increased overland flow, which might contribute to higher subsidies of fire-mobilized sediments and nutrients into streams (Doerr et al., 2006). However, soil hydrophobicity is also influenced by several other factors including droughts, soil types, and vegetation (Doerr et al., 2000). Soils in the reference catchments may have had a measure of hydrophobicity following the extended dry period of fall 2022, which could have contributed to the similarity of response noted in the majority of our storm samples. The storm data MERFs had the lowest explanatory power overall and consistently attributed less importance to catchment burn severity than in the baseflow and soil models, which suggests that during storms, characteristics such as slope, aspect, vegetation and soil composition tended to overwhelm fire impacts. Storm pulses can be associated with increased landscape connectivity, but soil infiltration and storage can act as significant buffers when retention capacities exceed precipitation (Dunne and Black, 1970). During a severe seasonal drought, like the one experienced on Vancouver Island during fall 2022, terrestrial sources would be substantially disconnected from streams and require much greater precipitation input than usual to saturate soil storage and reconnect with streams – this may be further contributing to the weak storm response we observed. Furthermore, preferential flow paths, created by plant roots and burrowing animals, can exert a strong influence on the movement of water through the landscape. In this region, large voids in the soil (i.e., soil pipes) and highly conductive zones (e.g., fine gravels) are common and can dominate soil transport pathways (Anderson et al., 2009), thus increasing the speed of soil drainage and limiting soil-water contact when soils

become saturated. Our results suggest that overland flow inputs from the fire scars were limited during the storm events we captured, which may be partially attributable to high soil storage capacity following the unseasonably dry fall, insufficient precipitation intensity to drive surface runoff during the events we captured, or interception by intact vegetation zones.

2.4.6 Ecological and water quality implications

Wildfires can impact aquatic ecosystems by altering the concentration and balance of nutrients (i.e., stoichiometry), or modifying the conditions of the habitats in which communities operate (Pinto et al., 2009). Absolute nutrient concentrations can limit gross productivity (Goldman, 1968; Rizhinashvili, 2022), while stoichiometry can alter the form that productivity takes (Dodds et al., 2004; Glibert, 2012). Post-fire P enrichment in particular has been linked to increases in primary production and invertebrate biomass (Minshall et al., 2001; Silins et al., 2014). Our study streams had a lower DIN:TP ratio in the burn-affected streams (reference = 29.5, burned = 11.9), though they remained on the side of theoretical P-limitation (DIN:TP > 3.5) (Bergström, 2010; Keck and Lepori, 2012). Many coastal streams in the PCTR are at least partially P-limited (Perrin et al., 1987) and have exhibited increases in algal biomass and changes in community compositions when released from this limitation, including more filamentous algae and shifts in dominant diatom species (Stockner and Shortreed, 1978). Co-limitation in freshwater streams is common and N and P together often better explain algal biomass than either alone (Dodds and Smith, 2016). Hence, the decrease in N may temper algal response to P enrichment. However, in addition to the fertilizing effects of P, the decrease in N we observed may trigger an increase in the abundance of N-fixing cyanobacteria (Howarth et al., 1988). Cyanobacteria can be disruptive to aquatic ecosystems as they can become highly abundant when released from nutrient limitation and form colonial mats or filaments that are resistant to grazing, thus disrupting food web dynamics and reducing trophic efficiency (Elser and Goldman, 1991). Further, cyanobacterial blooms can release toxins that are harmful to zooplankton and fish (Moustaka-Gouni and Sommer, 2020). Increases in cyanobacteria can therefore exert a strong control over food web assemblages. Although this study was conducted in a generally low nutrient system that remained in an oligotrophic state (Dodds et al., 1998) and is therefore unlikely to support harmful algal blooms, strongly impacted catchments (e.g., large, severe fires) or more nutrient rich ecosystems could see significant changes. Riparian areas can also have an influence on in-

stream production as they influence light availability and in-stream temperature (Leonard et al., 2017). Our sites exhibited a variety of riparian areas (e.g., forested, herbaceous, burned), but this was not formally quantified beyond visual inspection in this study and would be a worthwhile consideration for future works.

Beyond directly influencing community composition, changing C:N:P ratios can also impact food webs by altering their basal pathways (i.e., autotrophic or heterotrophic) or altering the nutritional quality of primary producers for consumer organisms (higher carbon-to-nutrient ratios = lower quality). In addition to changing N and P, we observed a decrease in DOC, which may impose limits on heterotrophic bacteria (Matveev and Robson, 2014), and thus shift the balance between autotrophic and heterotrophic food webs. This can have implications for carbon trophic transfer and macroinvertebrate community compositions (Demars et al., 2021). Bacterial-based food webs are less efficient in transferring energy to higher trophic levels (Berglund et al., 2007; Kirkwood and Lawton, 1981), so increasing the proportion of autotrophic production could exert bottom-up controls on food web composition (Degerman et al., 2018; Emelko et al., 2016; Silins et al., 2014; Spencer et al., 2003). Post-fire DOM compositional changes can also influence microbial communities as different species preferentially consume labile or aromatic pyrogenic C (Carvalho et al., 2019; Judd et al., 2006; Myers-Pigg et al., 2015; Norwood et al., 2013).

2.4.7 Water treatment perspective

Some of the major water treatment concerns reported in a post-fire landscape include increased DOC, which can impact coagulant demand and efficiency, nutrient enrichment, which may lead to algal blooms, and increased suspended sediments, which can clog systems and carry harmful bacteria (Emelko et al., 2011; Hohner et al., 2016; Smith et al., 2011). Therefore, the decreases in DOC and N reported here may lessen some concerns related to drinking water treatability and wildfire, though with the increase in P there is the possibility of a shift towards N-fixers (e.g., cyanobacteria), which tend to be nuisance species and pose the risk of producing toxins (Emelko et al., 2016; Schinck et al., 2020). It is also important to consider wildfire-induced changes in DOM quality which may challenge treatability, even at reduced concentrations (Chen et al., 2020; Wang et al., 2015b). For example, heat-altered DOM has been shown to be less amenable to coagulation, with reductions in efficiency as much as 1/3 that of unaltered DOM (Hohner et

al., 2019). Nitrogenous-DBP precursors, which are currently unregulated but may be more of a health concern than C-DBPs (Fernández et al., 1997; Hohner et al., 2019), have been shown to increase following heating at moderate temperatures and may be elevated even when carbonaceous DBPs are not, especially during storm events (Cawley et al., 2018; Hohner et al., 2017). The location of a wildfire can also inform its potential risks for drinking water, with threats heightened when fires are situated near intake sources (Neris et al., 2021) or occur on previous disturbed landscapes (e.g., insect outbreaks, droughts, harvesting) (Diemer et al., 2015; Rhoades et al., 2019b).

2.5 Conclusion

We observed apparent declines in stream water and soil extract DOC and N but increases in P as a result of wildfire; these changes can be expected to affect stream ecosystem function and may also have drinking water quality implications. The effect of burning was most pronounced in the soil leachates and dampened in streams at baseflow. Contrary to what we expected, burn status was not a statistically significant control on storm response; however, higher resolution storm sampling suggests that burn-affected areas may generate higher stream inputs than unburned catchments.

Forested watersheds in the Pacific Northwest have been highlighted as especially vulnerable to fire increases due to large fuel buildups (Adams, 2013; Littell et al., 2018) and changing climate conditions (Alizadeh et al., 2020; Rupp et al., 2017). Much of the increase in wildfire frequency and area burned has been correlated with drier conditions and severe droughts (Abatzoglou and Williams, 2016; Holden et al., 2018; Reilly et al., 2017), similar to the conditions observed on southern Vancouver Island during our study period. Accordingly, although the effects of wildfire that we measured were modest, expected increases in fire size and severity may augment the changes in water quality that we observed, with consequent effects on aquatic ecosystem function and drinking water quality (Wall et al., 2024). Furthermore, our study considered wildfires in several different catchments. Although fire was often a secondary driver when compared to natural landscape variation, its significance may increase when evaluating water quality impacts in a single watershed pre- and post-fire. This is a particularly important consideration for water supply areas. Given the overall small size and modest severity of the wildfires we studied, our results may be useful to understand possible effects of prescribed

burns in this region, which similarly tend to be small and of low severity, and are potentially beneficial for water quality by reducing DOC and mitigating severe wildfire risk by reducing fuel loads (Majidzadeh et al., 2019). However, a better understanding of the mechanistic pathways that control post-fire DOM compositional changes and nitrogenous-DBP formation potential is important, especially in drinking water supply watersheds. The interaction of burn severity and seasonality has been highlighted as an important factor in our study region (Wampler et al., 2024) and would be worth future investigation.

2.6 Tables

Table 1. Fire and catchment characteristics. Ranges show the minimum and maximum values of catchments associated with each fire, separated by burn status (reference or burn). Streams were dry during every sampling attempt at the Mayo Lake fire site. Data for fire size and year, and dominant BEC zones were obtained from the BC government's *iMap* service (Government of British Columbia, 2022). Catchments were delineated using the watershed tool in ArcGIS Pro and based on the Canadian Digital Elevation Model (Government of Canada, 2023). All physical characteristics (area, aspect, elevation, slope) were calculated using ArcGIS Pro. Mean annual precipitation data was obtained from ClimateBC (T. Wang et al., 2016). Catchment burn severity was calculated by multiplying the average burn severity (0-4) by percent catchment burned.

Fire Site	Fire Year	Fire Size (km ²)	Percent Catch. Burned	Catch. Area (km ²)*	Catch. Burn Severity	Sampled Streams*	Mean Annual Precip. (mm)	Mean Aspect*	Mean Elevation (m)*	Mean Slope (° Angle)*	Dominant BEC Zone
HC (Harris Creek)	2015	4.02	2 – 100	0.08 – 0.77 0.06 – 2.54	0.07 – 3.90	3 7	3079	SW SW	494 283	31 24	CWH mm 1
ML (Mayo Lake)	2015	0.16	NA	NA	NA	0 0	1613	SW SW	299 299	25 25	CWH xm 1
JC (Jacob Creek)	2017	0.40	16 – 19	0.23 – 0.57 0.32 – 2.52	0.29 – 0.38	2 2	2505	S S	375 522	18 12	CWH xm 2
TC (Tugwell Creek)	2018	0.83	16 – 30	0.82 0.43 – 3.45	0.49 – 0.76	1 2	2115	SW SW	295 338	9 7	CWH xm 2
MM (Maple Mountain)	2018	0.06	3	0.82 2.03	0.07	1 1	1196	W W	252 232	12 12	CDF mm
NL (Nanaimo Lakes)	2018	1.85	22 – 29	1.18 – 8.42 0.36 – 1.65	0.57 – 0.84	3 3	1739	S S	540 377	11 8	CWH xm 1 & xm 2
HO (HolyOak)	2021	0.30	10	0.9 – 1.52 1.06	0.26	2 1	1906	W W	575 506	10 12	CWH xm 1 & xm 2
MH (Mt. Hayes)	2021	0.61	52	0.08 – 0.61 0.12	1.64	2 1	1364	W SE	326 340	9 13	CWH xm 1
CT (Cowichan Trail)	2022	0.06	4 – 20	0.06 – 1.26 0.03 – 0.50	0.12 – 0.21	4 2	1602	N N	188 178	11 12	CWH xm 1

*Reference catchment values on top, burn catchment values below.

2.7 Figures

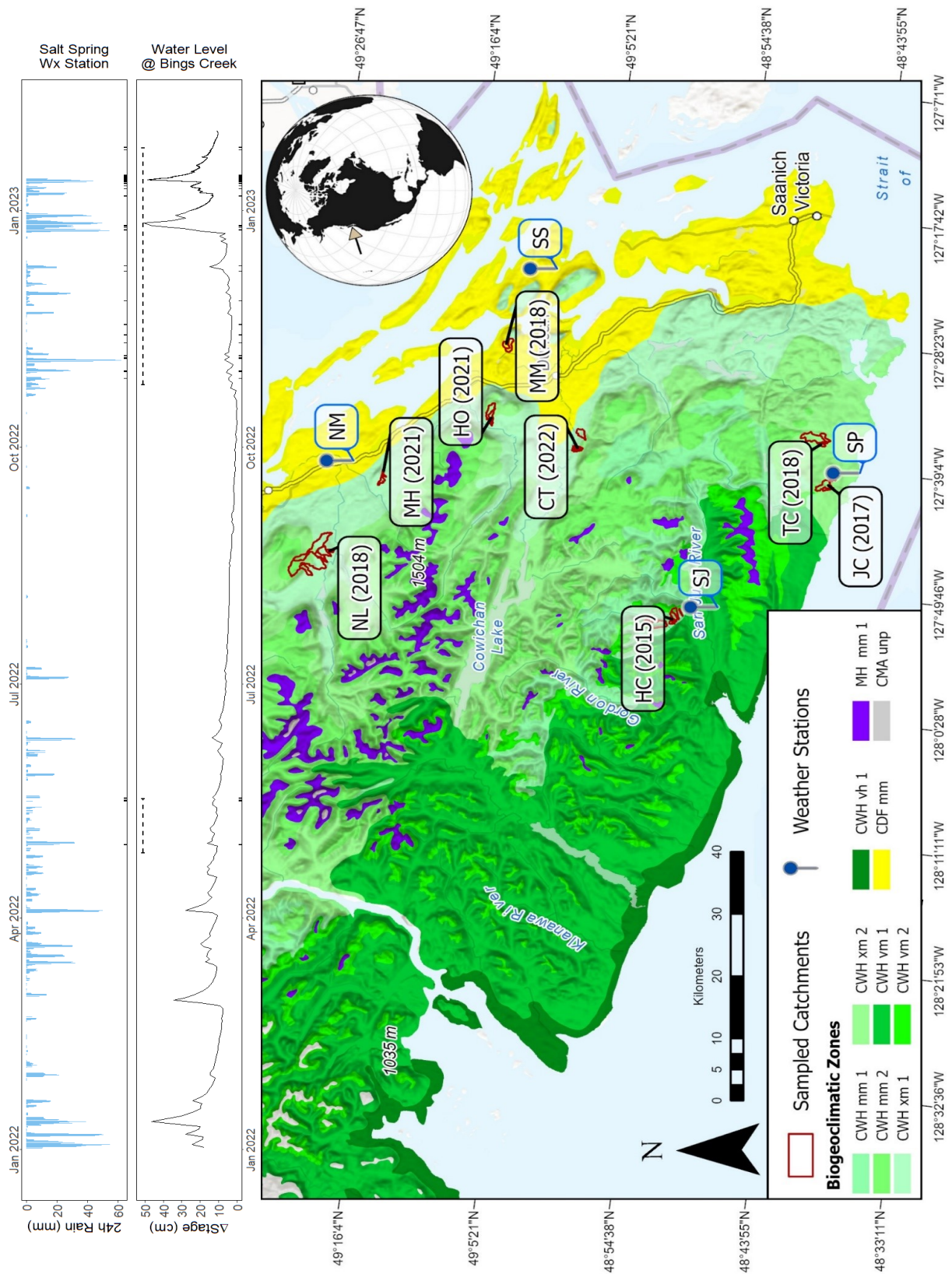


Figure 1. Map showing southern Vancouver Island biogeoclimatic ecosystem classification (BEC) zones, sampled catchments labelled with associated fire site and burn year, and weather stations used. BEC labels are split into zones, subzones, and variants. BEC zones are coastal western hemlock (CWH), coastal douglas-fir (CDF), mountain hemlock (MH), and coastal mountain-heater alpine (CMA). Subzones are moist maritime (mm), very dry maritime (xm), very wet maritime (vm), very wet hypermaritime (vh), and undifferentiated and parkland (unp). Variants, which depend on zone and subzone, are submontane (CWHmm1, CWHvm1), montane (CWHmm2, CWHvm2), southern (CWHvh1), eastern (CWHxm1), western (CWHxm2), and windward (MHmm1). Above the map are rolling 24-hour precipitation data recorded at the Salt Spring (SS; PCIC ID 1637) weather station, and stage data from the Bings Creek near Mouth hydrometric station (Water Survey of Canada; ID 08HA016) located in Duncan, BC. Dashed lines represent the active sampling period (May 01 – May 17, 2022 & October 25, 2022 – January 17, 2023). Ticks on the bottom of the precipitation and stage plots represent sample collection dates.

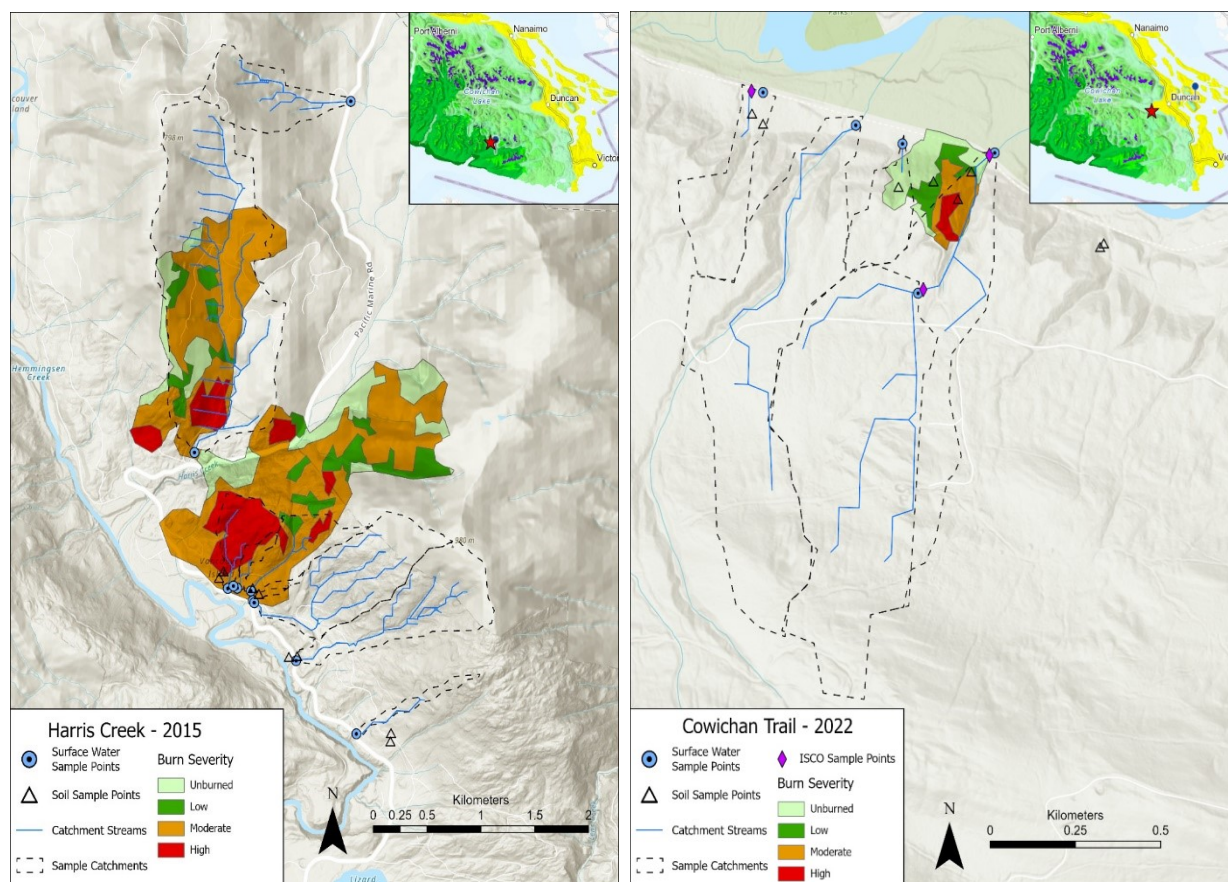


Figure 2. Detailed maps of the Harris Creek (HC; left) and Cowichan Trail (CT; right) historic fire sites and sampled catchments. The year next to the site name represents the burn year. The inset maps show southern Vancouver Island – the red star represents the location of the fire site, and the pin shows the associated weather station. Maps of the remaining seven fire sites are available in the appendix (Figure A1).

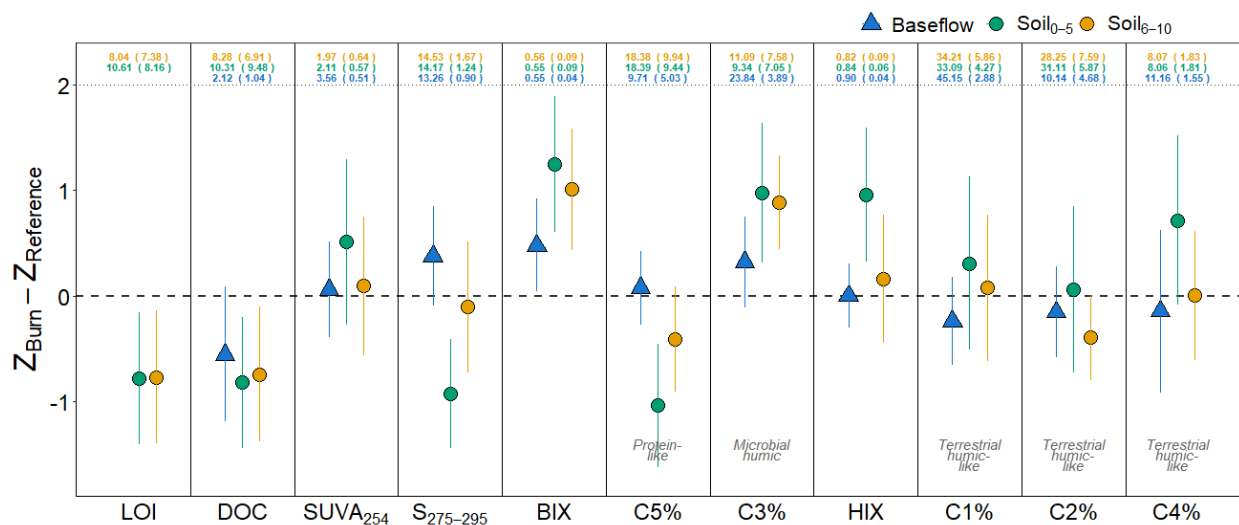


Figure 3. Z-score change of LOI, DOC (mg L^{-1}), DOM composition (SUVA_{254} , nm cm^{-1} ; $\text{S}_{275-295}$, nm^{-1} ; BIX, HIX), and EEM components (C1-C5) for baseflow samples and soil leachates. All data are centered and scaled by source (blue = baseflow, green = soil 0-5cm, yellow = soil 6-10cm). The y-axis shows the normalized (Z-score) difference between burn and reference sites expressed in standard deviations. The numbers show the mean and standard deviation (mean (SD)) of each metric, colour-coded according to data source and calculated using non-normalized data. Error bars represent 95% confidence intervals. Raw data can be found in Figures A5-A7; associated t-test outputs can be found in Table A2.

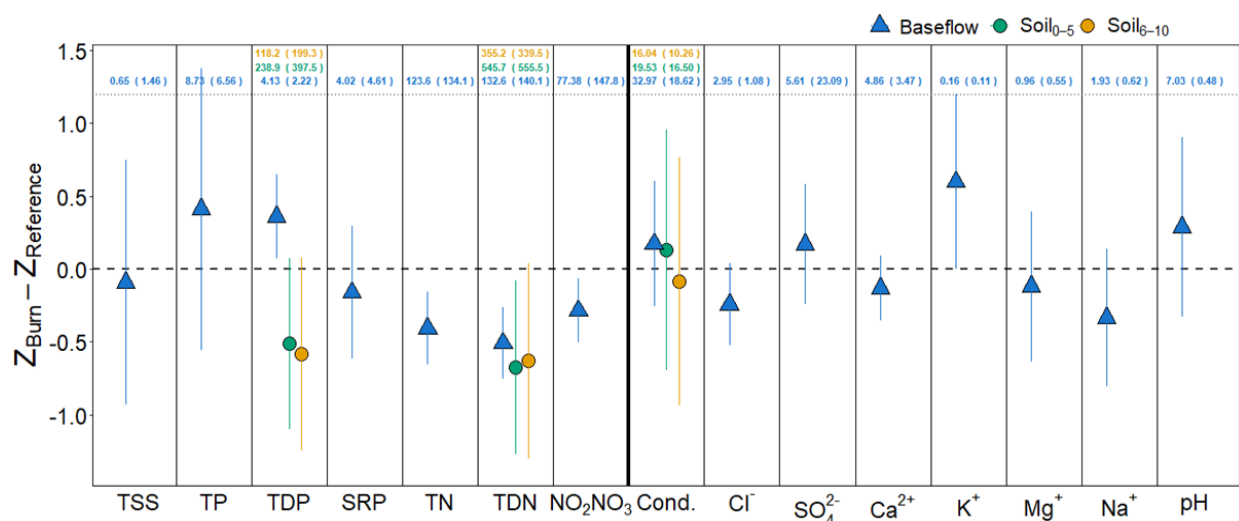


Figure 4. Z-score change of total suspended sediments (TSS, mg L⁻¹), nutrients (TP, µg L⁻¹; TDP, µg L⁻¹; SRP, µg L⁻¹; TN, µg L⁻¹; TDN, µg L⁻¹; NO₂+NO₃, µg L⁻¹) and specific conductance (µs cm⁻¹) and major ions (mg L⁻¹) for baseflow samples and soil leachates, when available. All data are centered and scaled by source (blue = baseflow, green = soil 0-5cm, yellow = soil 6-10cm). The y-axis shows the normalized (Z-score) difference between burn and reference sites expressed in standard deviations. The numbers show the mean and standard deviation (mean (SD)) of each metric, colour-coded according to data source and calculated using non-normalized data. Error bars represent 95% confidence intervals. Raw data can be found in Figures A5-A7; associated t-test outputs can be found in Table A2.

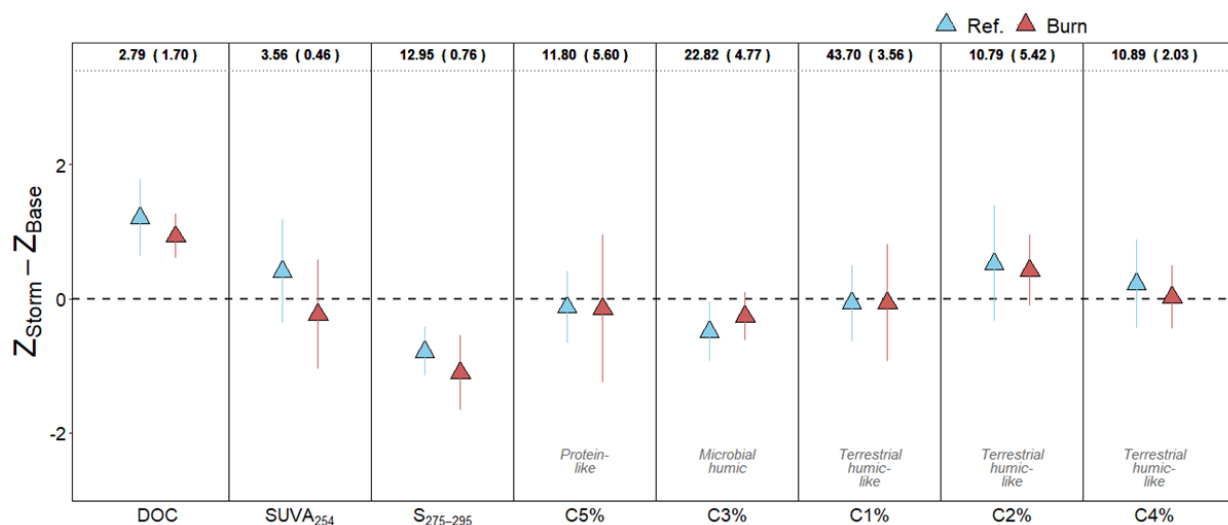


Figure 5. Z-score change of DOC (mg L^{-1}), DOM composition (SUVA_{254} : nm cm^{-1} ; $S_{275-295}$, nm^{-1}), and EEM components (C1-C5) for reference and burn samples. The y-axis shows the normalized (Z-score) difference between stormflow and baseflow samples expressed in standard deviations. Data are from the four sites with stormflow data (HC, NL, HO, and CT), centered and scaled. The numbers show the overall (combined baseflow and stormflow) mean and standard deviation (mean (SD)) of each metric calculated using the pre-normalized dataset. Error bars represent 95% confidence intervals. Raw data can be found in Figure A9; associated t-test outputs can be found in Table A2 & A4.

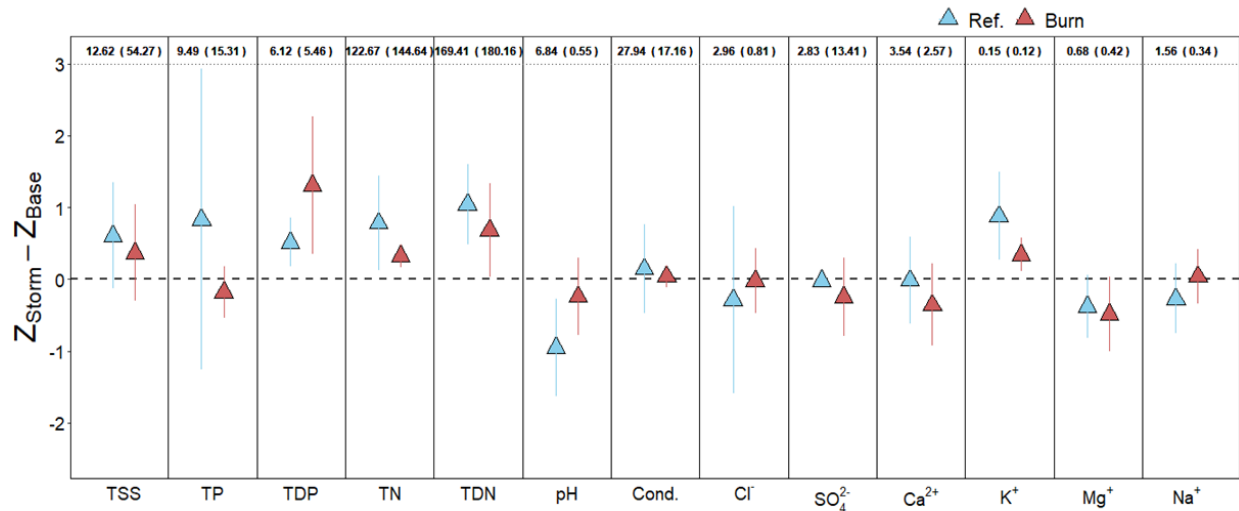


Figure 6. Z-score change of total suspended sediments (TSS, mg L^{-1}), nutrients (TP, $\mu\text{g L}^{-1}$; TDP, $\mu\text{g L}^{-1}$; TN, $\mu\text{g L}^{-1}$; TDN, $\mu\text{g L}^{-1}$) and pH, specific conductance ($\mu\text{S cm}^{-1}$), and major ions (mg L^{-1}) for reference and burn samples. The y-axis shows the normalized (Z-score) difference between stormflow and baseflow samples expressed in standard deviations. Data are from the four sites with stormflow data (HC, NL, HO, and CT), centered and scaled. The numbers show the overall (combined baseflow and stormflow) mean and standard deviation (mean (SD)) of each metric calculated using the pre-normalized dataset. Error bars represent 95% confidence intervals. Raw data can be found in Figure A9; associated t-test outputs can be found in Table A2 & A4.

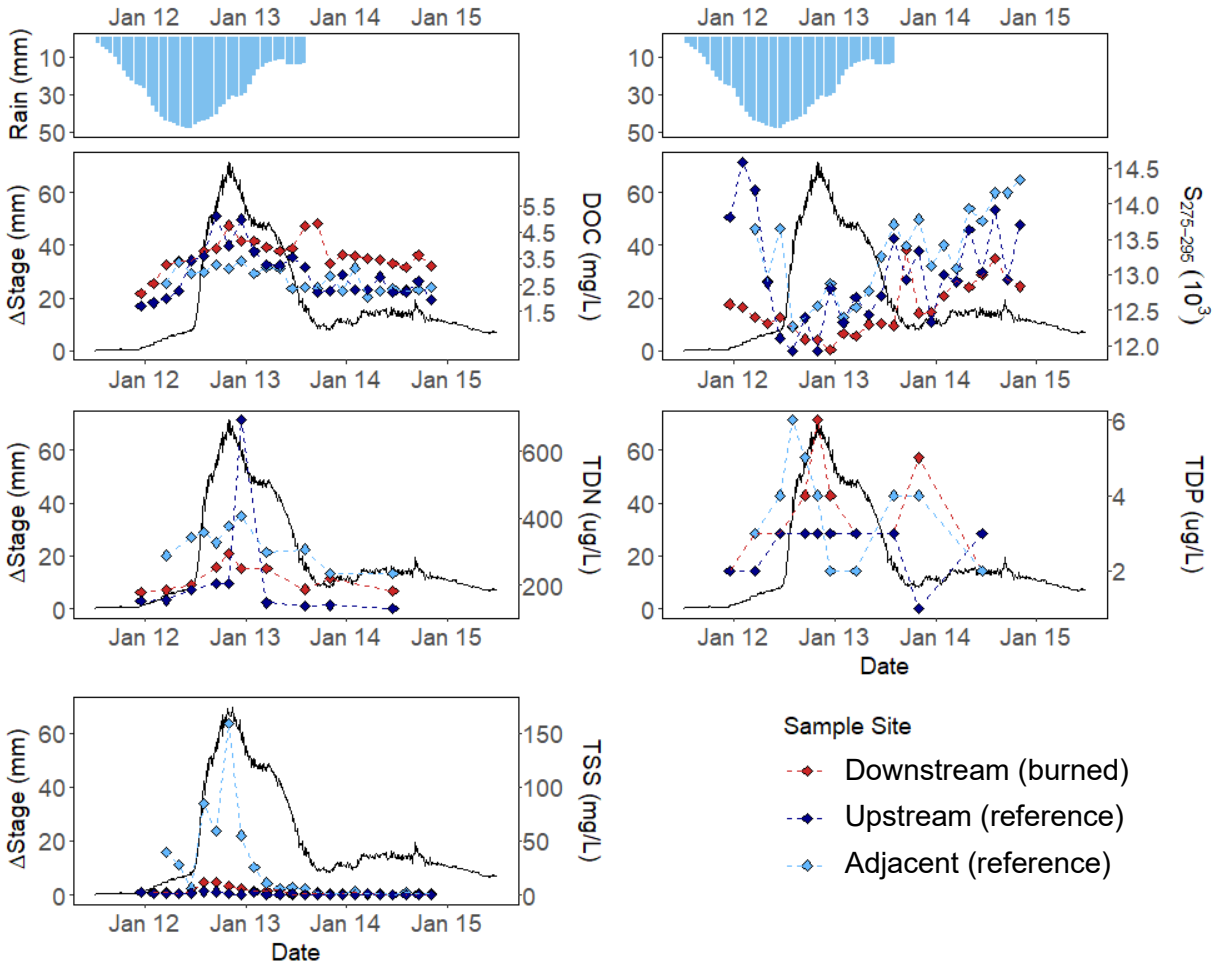


Figure 7. Rainfall (mm), stage (mm, normalized to zero), and water quality (DOC (mg L^{-1}), $S_{275-295}$ (10^3 nm^{-1}), TDN ($\mu\text{g L}^{-1}$), and TDP ($\mu\text{g L}^{-1}$), TSS (mg L^{-1})) responses during a storm event (January 11-14, 2023). Samples were collected every 3h using ISCO autosamplers. The hyetographs show the 24-hour rolling sum of precipitation from the Salt Spring weather station – data were unavailable for January 14-15. All other plots show the change in stage on the left axis and concentration on the right axis. Figure 2 shows site locations: Downstream (burned) and upstream (reference) are paired upstream/downstream sites on the same stream. The upstream site catchment (0.36km^2) represents 72% of the downstream catchment (0.5km^2). A tributary (0.06km^2) joins the stream between the upstream and downstream sites. Adjacent (reference) is a nearby small (0.06km^2) reference stream

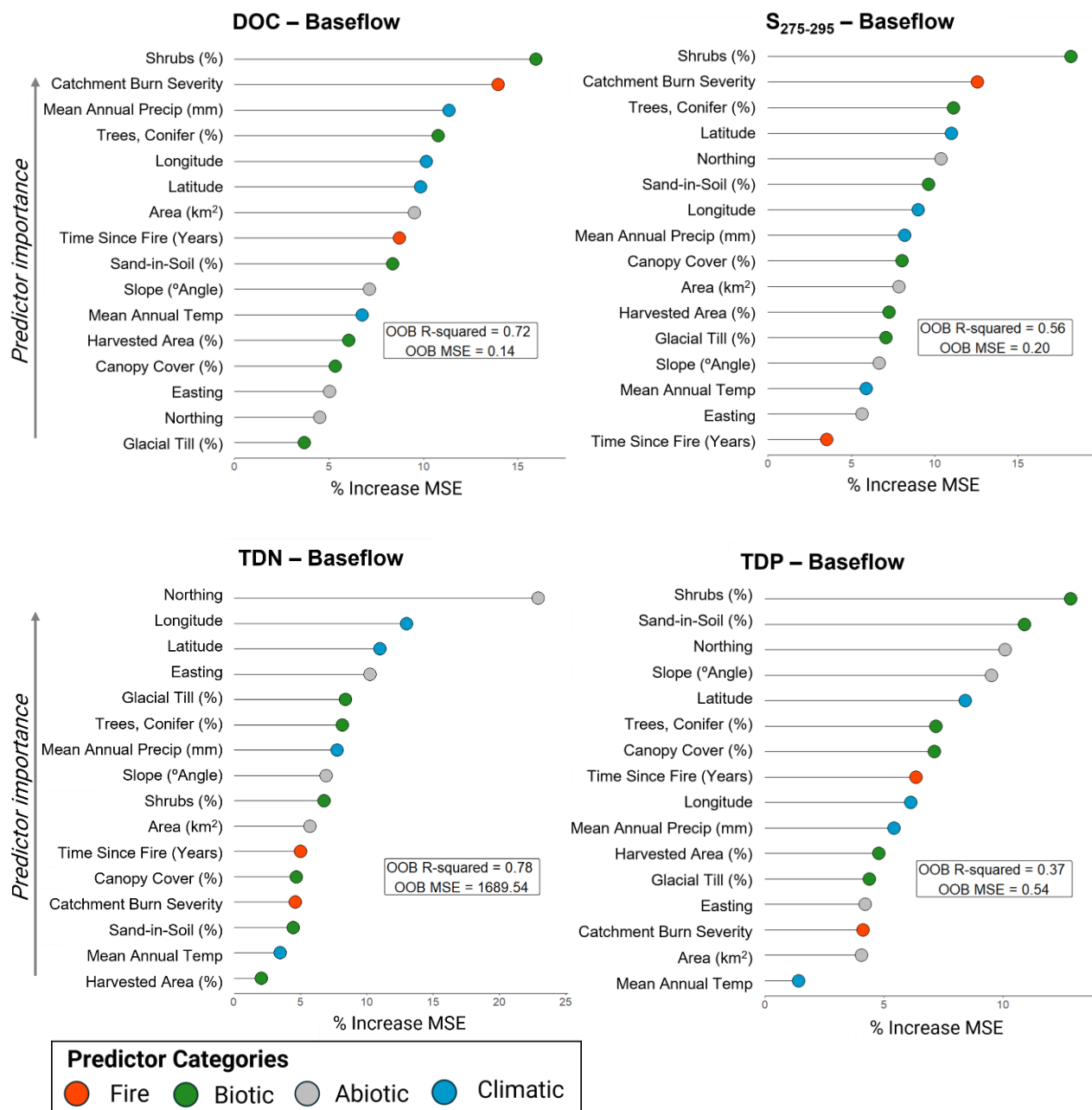


Figure 8. Surface water baseflow mixed-effect random forest outputs for DOC, S₂₇₅₋₂₉₅, TDN, and TDP. Plots show variable importance metrics (VIMs). The x-axis represents the percent increase in the mean squared error (MSE) of the model when that variable is removed; more important variables introduce more error when not considered. VIMs are coloured according to predictor characteristics: green = biotic, grey = abiotic, blue = climatic, red = fire. R^2 and mean squared error (MSE) calculated using out-of-bag (OOB) data. Associated partial dependence plots (PDPs) for the six most important predictors can be found in the appendix (Figure A10).

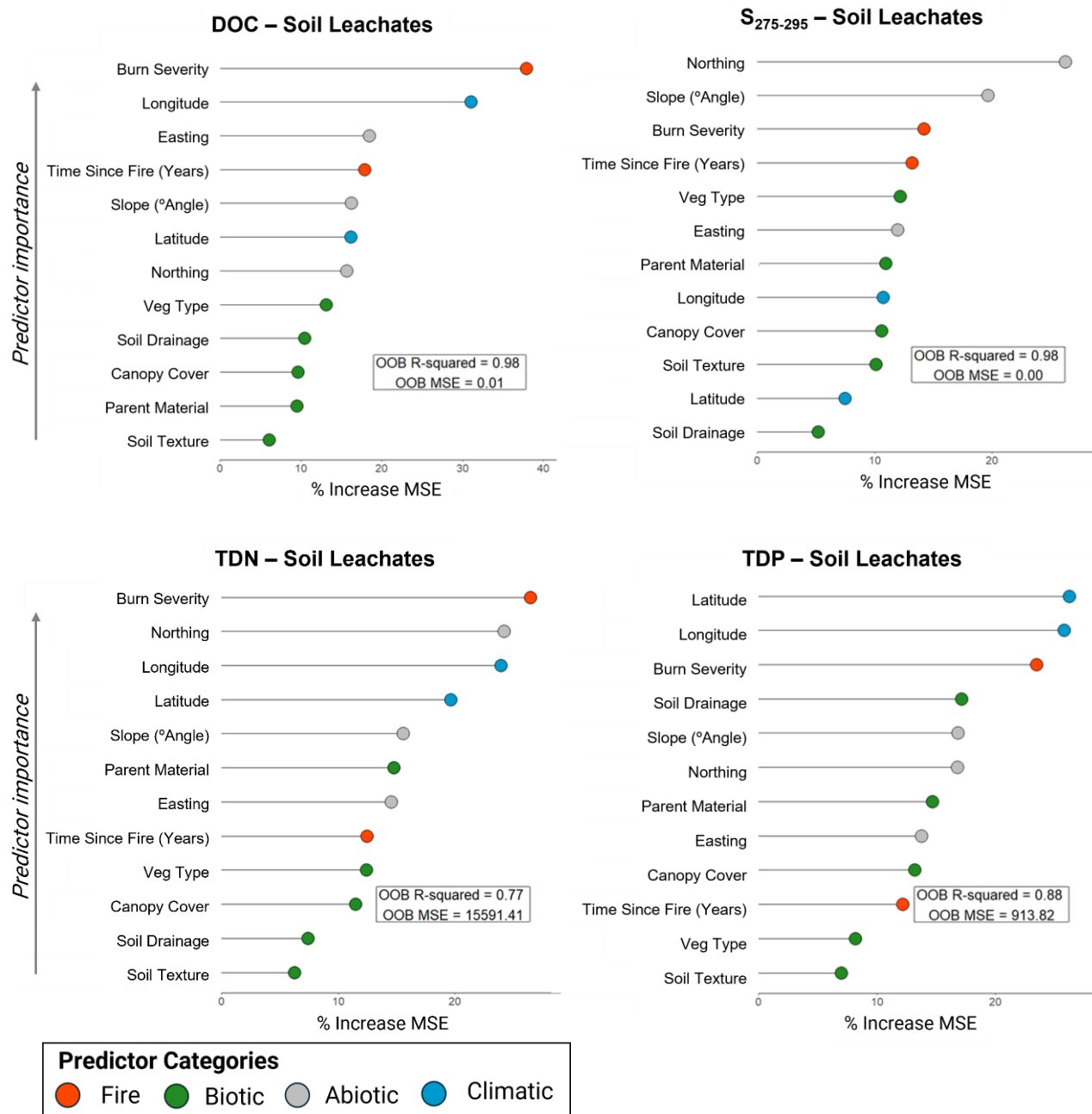


Figure 9. Soil leachate mixed-effect random forest outputs for DOC, S₂₇₅₋₂₉₅, TDN, and TDP. Plots show variable importance metrics (VIMs). The x-axis represents the percent increase in the mean squared error (MSE) of the model when that variable is removed; more important variables introduce more error when not considered. VIMs are coloured according to predictor characteristics: green = biotic, grey = abiotic, blue = climatic, red = fire. R² and mean squared error (MSE) were calculated using out-of-bag (OOB) data. Associated partial dependence plots (PDPs) for the six most important predictors can be found in the appendix (Figure A11).

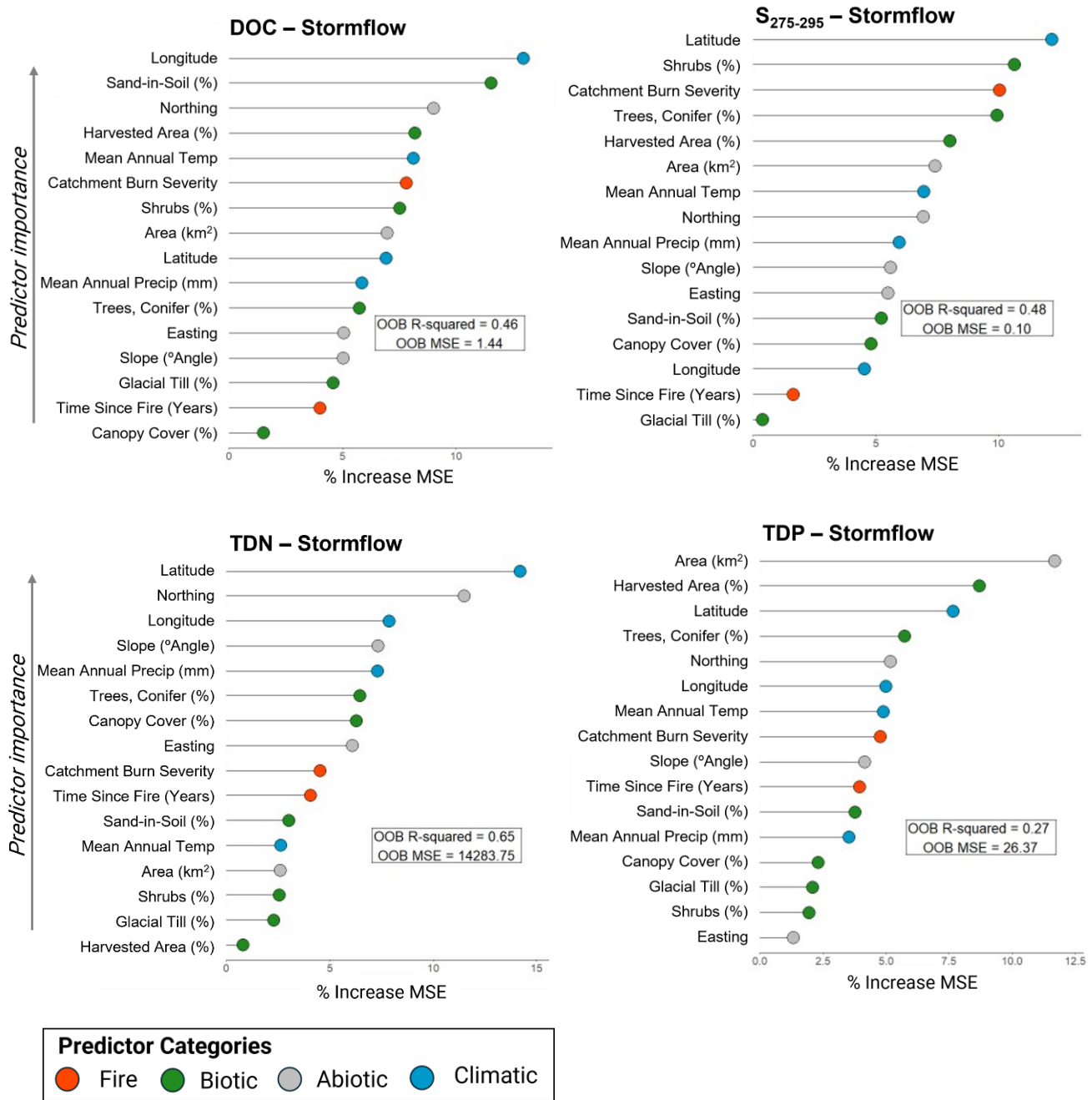


Figure 10. Surface water stormflow data mixed-effect random forest outputs for DOC, S₂₇₅₋₂₉₅, TDN, and TDP. Plots show variable importance metrics (VIMs). The x-axis represents the percent increase in the mean squared error (MSE) of the model when that variable is removed; more important variables introduce more error when not considered. VIMs are coloured according to predictor characteristics: green = biotic, grey = abiotic, blue = climatic, red = fire. R² and mean squared error (MSE) were calculated using out-of-bag (OOB) data. Associated partial dependence plots (PDPs) for the six most important predictors can be found in the appendix (Figure A12).

Chapter 3. General Conclusion

3.1 Summary of findings

Wildfire-affected streams in the PCTR had less DOC and N but higher in P as compared to reference streams. These changes can be expected to affect stream ecosystem function and possibly have drinking water quality implications. C:N:P stoichiometry has a controlling influence on primary producer communities (Frost et al., 2002). Since streams in the PCTR tend to be P-limited (Perrin et al., 1987), burn-affected streams may experience a shift in ecological communities, including increased algal biomass due to P-fertilization and more N-fixing cyanobacteria. In addition to modifying food web dynamics, shifting algal and bacterial communities could lead to objectionable taste and odour or produce toxins and may pose a challenge for drinking water.

The effect of burn status was most pronounced in soils and was dampened in streams. Streams at baseflow are generally sustained by groundwater inputs (Singh, 1969) and are therefore poorly connected to surficial soils, which may explain some of the differences observed. Further, nearly all the burn-affected streams I sampled had only partially burned catchments so there may also have been some dilution of effects. The overall magnitude of change in constituent concentration during storm events was not statistically different between burned and unburned catchments. This was surprising because I had expected to see a stronger response in burned areas due to fire-induced landscape changes that have been reported in studies in other regions, including soil hydrophobicity (Beatty and Smith, 2013; Doerr et al., 2006; Doerr and Cerdà, 2005) and reduced vegetation interception (Niemeyer et al., 2020) that could increase terrestrial subsidies to streams (Doerr et al., 2006). However, we were data limited, and responses may have been obscured by natural conditions (i.e., drought) or inter-site variability during the storms I sampled. In contrast to the low-resolution storm samples, higher resolution sampling (every 3h) of a recent (October 2022) fire throughout one of the first post-fire storm events (January 2023) showed a pattern of amplified storm response for DOC, MW, TDN, and TSS in burned catchments. Overall storm responses may have been dampened by a lack of hydrologic connectivity between catchments and streams, as the soils likely had very high infiltration and storage capacity following an unseasonably dry fall. Wildfire prevalence is predicted to increase and lead to larger and more severe fires in the traditionally wet PCTR

(Abatzoglou and Williams, 2016; Littell et al., 2018; Rupp et al., 2017). Higher severity fires are more likely to cause long-term landscape changes including higher vegetation mortality and soil hydrophobicity, which in turn can translate to more pronounced in-stream impacts. Larger fires may also burn larger proportions of catchment areas and leave less intact landscape to dilute impacts. Therefore, the results that are presented here may be modest compared to possible future effects but indicate that wildfire can influence water quality in the PCTR.

3.2 Limitations and improvements

Despite the valuable insights gained from this research, there are several opportunities for future improvements. Seasonal variation in water quality is natural in the PCTR (Oliver et al., 2017) and may influence wildfire response (Writer et al., 2012). While I attempted to capture a degree of seasonality by sampling in both spring and fall, logistical constraints prevented me from conducting a comprehensive spring campaign. Furthermore, fall 2022 on Vancouver Island constituted a historic drought (Government of British Columbia, 2024b) so the fall samples may not have been representative of the conditions that may be expected in a more “normal” year. Extending the sampling campaign to include more of the winter wet season may have revealed further changes in both the baseflow and stormflow samples as hydrologic connectivity between the landscape and streams was re-established. A multi-year study would have strengthened several components of this work by adding a degree of robustness to extraordinary weather conditions and capturing different seasonality. Further, repeated sampling at the same sites for more than one year would have contributed to a stronger understanding of the effects of time since fire, which may have been confounded by inter-site variability in the current study design.

Sample timing at a finer time scales is also important for capturing changes because constituents can have pulse responses and move quickly through stream systems (Paul et al., 2022). While this is unlikely to have impacted the baseflow samples, storm responses may have been underestimated by the low-resolution “rack” samples which only captured one to two samples on the rising limb. Even the site instrumented with ISCO autosamplers set to capture samples every three hours may have missed pulses as water moved quickly through the system. Although not feasible for this study, continuous monitoring via in-stream instrumentation would have been the most accurate approach (Olivares et al., 2019).

Antecedent moisture conditions play an important role in storm response and inform the level of connection between landscape and streams (Ali et al., 2010; Dunne and Black, 1970). While I used a threshold of 24-hour maximum rainfall prior to sample collection to determine whether a sample should be considered baseflow or stormflow (baseflow <20mm in 24h), a detailed approach to quantifying soil moisture and measuring water table depth would have helped gain a stronger understanding of the state of hydrologic connectivity. Likewise, a more detailed description of the soils in our catchments would have been helpful to elucidate infiltration rates and, importantly, determine whether a hydrophobic layer was in fact present in the burn-affected catchments. The precipitation values I used were drawn from weather stations with publicly available data covering the period of interest and were assumed to be representative of the conditions at the nearest fire sites (5-28km). This assumption may be problematic on Vancouver Island because steep topographies can result in the formation of micro-climates that create high spatial heterogeneity in precipitation patterns (Coops et al., 2007; Pojar et al., 1991).

Provincial GIS products were used to describe several key environmental characteristics, including soil composition, parent material, and vegetation. While this was an effective approach, it may not have captured smaller-scale variation within the study catchments. The vegetation classifications were broadly defined for composition (e.g., broadleaf, coniferous, shrub) and density (e.g., open, sparse, dense); on-the-ground assessments would have provided a more accurate and detailed picture. Information regarding the seral stage of forest stands prior to burning was not incorporated but would have contributed important details about the type and scale of changes wrought on the landscape by fire, beyond what can be inferred from the satellite imagery I used to derive burn severities. Additionally, a 32x32m resolution DEM was used to define stream drainage paths and catchment boundaries. Given the small size of the studied streams, this could have led to some inaccuracies that a higher resolution model would have eliminated. More detailed definitions of these site characteristics may have improved the random forest models and perhaps permitted a more detailed description of the most important factors controlling post-fire water quality.

3.3 Future directions

This study contributes to a baseline understanding of wildfire impacts on stream water quality but recommends several avenues for future research. First, a longer-term study with well-instrumented sites may help address many of the concerns listed above and help build causal relationships between fire behaviour, environmental characteristics, and water quality response. Furthermore, the changes in nutrient stoichiometry that were observed permitted the inference of an increase in primary producer biomass and a possible shift in basal food web dynamics, but further study is required to confirm which, if any, of these changes are occurring in the primarily oligotrophic streams of the PCTR. After severe fires, changes in community composition have been shown to lower taxonomic richness and increase abundance in favour of disturbance adapted r-strategists (short generation times, high fecundity, high dispersal) (Bixby et al., 2015), with a similar response noted across three fire-prone biomes (Verkaik et al., 2015) though no studies have yet considered this in the PCTR. Investigating ecological community changes would provide a complementary element to this study and solidify the broader implications that are suggested here. It would also better define how fire impacts in coastal temperate rainforests fit into the global context of fire research.

Wildfire management is a priority for water managers, especially with wildfire projected to increase in the PCTR (Capital Regional District, 2022; Robichaud and Padowski, 2024). Prescribed burning has been utilized in other parts of the world to reduce fuel buildups and reduce the likelihood of a severe wildfire, with relatively minor impacts on water quality compared to wildfire (Majidzadeh et al., 2019). Like wildfires however, outcomes may vary based on landscape characteristics (Klimas et al., 2020). A localized study investigating the water quality outcomes of a prescribed fire in the PCTR would help determine if they are a viable wildfire risk management tool. This study only considered small (first or second order) streams. Although the effects detected here were modest, it would be worthwhile to investigate how effects might transmit downstream, especially during periods of heightened hydrologic connectivity. Fire-altered DOM and nutrients could lead to complications if they are transported to water supply reservoirs or intakes, but it is also possible that in-stream processing and dilution almost fully mitigate potentially negative impacts like altered disinfection efficacy and increased algal biomass. A clearer understanding of which constituents are likely to be impacted and how changes might propagate downstream would help water managers know where to focus

mitigation efforts. The multiple catchments considered in this study also introduced a measure of landscape variability that may be underrepresenting the impacts a wildfire could have on a single drinking water supply watershed.

Finally, water quantity, as well as water quality, may be affected by wildfire and increase the risk of flash floods or alter the timing of high flows. Given the high annual precipitation of Pacific Coastal Temperate Rainforests and the influence of hydrology on water quality responses, it is important to bridge these two research domains. Developing an explicit connection between post-fire landscapes and hydrologic response in the PCTR will help ensure the delivery of stable, predictable, and clean water supplies as climate continues to change in the future.

References

- Abatzoglou, J.T., Rupp, D.E., O'Neill, L.W., Sadegh, M., 2021. Compound Extremes Drive the Western Oregon Wildfires of September 2020. *Geophysical Research Letters* 48, e2021GL092520. <https://doi.org/10.1029/2021GL092520>
- Abatzoglou, J.T., Williams, A.P., 2016. Impact of anthropogenic climate change on wildfire across western US forests. *Proceedings of the National Academy of Sciences* 113, 11770–11775. <https://doi.org/10.1073/pnas.1607171113>
- Abatzoglou, J.T., Williams, A.P., Boschetti, L., Zubkova, M., Kolden, C.A., 2018. Global patterns of interannual climate–fire relationships. *Global Change Biology* 24, 5164–5175. <https://doi.org/10.1111/gcb.14405>
- Adams, M.A., 2013. Mega-fires, tipping points and ecosystem services: Managing forests and woodlands in an uncertain future. *Forest Ecology and Management* 294, 250–261. <https://doi.org/10.1016/j.foreco.2012.11.039>
- Agbeshie, A.A., Abugre, S., Atta-Darkwa, T., Awuah, R., 2022. A review of the effects of forest fire on soil properties. *J. For. Res.* 33, 1419–1441. <https://doi.org/10.1007/s11676-022-01475-4>
- Aguilar, F.X., Obeng, E.A., Cai, Z., 2018. Water quality improvements elicit consistent willingness-to-pay for the enhancement of forested watershed ecosystem services. *Ecosystem Services* 30, 158–171. <https://doi.org/10.1016/j.ecoser.2018.02.012>
- Aiken, G.R., 2014. Dissolved Organic Matter in Aquatic Systems, in: *Comprehensive Water Quality and Purification*. Elsevier, pp. 205–220. <https://doi.org/10.1016/B978-0-12-382182-9.00014-1>
- Aitkenhead-Peterson, J., McDowell, W., Neff, J., 2003. Sources, Production, and Regulation of Allochthonous Dissolved Organic Matter Inputs to Surface Waters, in: *Aquatic Ecosystems: Interactivity of Dissolved Organic Matter*. pp. 71–91. <https://doi.org/10.1016/B978-012256371-3/50003-2>
- Alaback, P.B., 1991. Comparative ecology of temperate rainforests of the Americas along analogous climatic gradients. *Revista Chilena de Historia Natural* 64, 399–412.
- Ali, S., Ghosh, N.C., Singh, R., 2010. Rainfall–runoff simulation using a normalized antecedent precipitation index. *Hydrological Sciences Journal* 55, 266–274. <https://doi.org/10.1080/02626660903546175>
- Alizadeh, M.R., Adamowski, J., Nikoo, M.R., AghaKouchak, A., Dennison, P., Sadegh, M., 2020. A century of observations reveals increasing likelihood of continental-scale compound dry-hot extremes. *Science Advances* 6, eaaz4571. <https://doi.org/10.1126/sciadv.aaz4571>
- Anderson, A.E., Weiler, M., Alila, Y., Hudson, R.O., 2009. Dye staining and excavation of a lateral preferential flow network. *Hydrology and Earth System Sciences* 13, 935–944. <https://doi.org/10.5194/hess-13-935-2009>
- Antweiler, R.C., 2015. Evaluation of Statistical Treatments of Left-Censored Environmental Data Using Coincident Uncensored Data Sets. II. Group Comparisons. *Environ. Sci. Technol.* 49, 13439–13446. <https://doi.org/10.1021/acs.est.5b02385>
- Atchley, A.L., Kinoshita, A.M., Lopez, S.R., Trader, L., Middleton, R., 2018. Simulating Surface and Subsurface Water Balance Changes Due to Burn Severity. *Vadose Zone Journal* 17, undefined-undefined. <https://doi.org/10.2136/vzj2018.05.0099>
- Audry, S., Akerman, A., Riotte, J., Oliva, P., Maréchal, J.-C., Fraysse, F., Pokrovsky, O.S., Braun, J.-J., 2014. Contribution of forest fire ash and plant litter decay on stream dissolved composition in a sub-humid tropical watershed (Mule Hole, Southern India). *Chemical Geology* 372, 144–161. <https://doi.org/10.1016/j.chemgeo.2014.02.016>
- Baillie, B.R., Neary, D.G., 2015. Water quality in New Zealand's planted forests: a review. *N.Z. j. of For. Sci.* 45, 7. <https://doi.org/10.1186/s40490-015-0040-0>
- Barrett, T., Dowle, M., Srinivasan, A., 2023. data.table: Extension of “data.frame.”
- Barten, P.K., Ernst, C.E., 2004. Land Conservation and Watershed Management for Source Protection. *Journal AWWA* 96, 121–135. <https://doi.org/10.1002/j.1551-8833.2004.tb10603.x>

- Battin, T.J., Kaplan, L.A., Findlay, S., Hopkinson, C.S., Marti, E., Packman, A.I., Newbold, J.D., Sabater, F., 2008. Biophysical controls on organic carbon fluxes in fluvial networks. *Nature Geosci* 1, 95–100. <https://doi.org/10.1038/ngeo101>
- BC Flood and Wildfire Review Team, 2018. Addressing the new normal: 21st century disaster management in British Columbia, Report and findings of the BC flood and wildfire review.
- Beatty, S.M., Smith, J.E., 2013. Dynamic soil water repellency and infiltration in post-wildfire soils. *Geoderma* 192, 160–172. <https://doi.org/10.1016/j.geoderma.2012.08.012>
- Bedia, J., Herrera, S., Gutiérrez, J.M., Benali, A., Brands, S., Mota, B., Moreno, J.M., 2015. Global patterns in the sensitivity of burned area to fire-weather: Implications for climate change. *Agricultural and Forest Meteorology* 214–215, 369–379. <https://doi.org/10.1016/j.agrformet.2015.09.002>
- Beese, W.J., Blackwell, B.A., Green, R.N., Hawkes, B.C., 2006. Prescribed burning impacts on some coastal British Columbia ecosystems (Information Report No. 403), BC-X. Pacific Forestry Centre, Victoria, B.C.
- Belillas, C.M., Feller, M.C., 1998. Relationships Between Fire Severity and Atmospheric and Leaching Nutrient Losses in British Columbia's Coastal Western Hemlock Zone Forests. *Int. J. Wildland Fire* 8, 87–101. <https://doi.org/10.1071/wf9980087>
- Berglund, J., Müren, U., Båmstedt, U., Andersson, A., 2007. Efficiency of a phytoplankton-based and a bacterial-based food web in a pelagic marine system. *Limnology and Oceanography* 52, 121–131. <https://doi.org/10.4319/lo.2007.52.1.0121>
- Bergström, A.-K., 2010. The use of TN:TP and DIN:TP ratios as indicators for phytoplankton nutrient limitation in oligotrophic lakes affected by N deposition. *Aquat. Sci.* 72, 277–281. <https://doi.org/10.1007/s00027-010-0132-0>
- Biau, G., Scornet, E., 2016. A random forest guided tour. *TEST* 25, 197–227. <https://doi.org/10.1007/s11749-016-0481-7>
- Bidlack, A.L., Bisbing, S.M., Buma, B.J., Diefenderfer, H.L., Fellman, J.B., Floyd, W.C., Giesbrecht, I., Lally, A., Lertzman, K.P., Perakis, S.S., Butman, D.E., D'Amore, D.V., Fleming, S.W., Hood, E.W., Hunt, B.P.V., Kiffney, P.M., McNicol, G., Menounos, B., Tank, S.E., 2021. Climate-Mediated Changes to Linked Terrestrial and Marine Ecosystems across the Northeast Pacific Coastal Temperate Rainforest Margin. *BioScience* 71, 581–595. <https://doi.org/10.1093/biosci/biaa171>
- Bixby, R.J., Cooper, S.D., Gresswell, R.E., Brown, L.E., Dahm, C.N., Dwire, K.A., 2015. Fire effects on aquatic ecosystems: an assessment of the current state of the science. *Freshwater Science* 34, 1340–1350. <https://doi.org/10.1086/684073>
- Bladon, K.D., Emelko, M.B., Silins, U., Stone, M., 2014. Wildfire and the Future of Water Supply. *Environ. Sci. Technol.* 48, 8936–8943. <https://doi.org/10.1021/es500130g>
- Bladon, K.D., Silins, U., Wagner, M.J., Stone, M., Emelko, M.B., Mendoza, C.A., Devito, K.J., Boon, S., 2008. Wildfire impacts on nitrogen concentration and production from headwater streams in southern Alberta's Rocky Mountains. *Can. J. For. Res.* 38, 2359–2371. <https://doi.org/10.1139/X08-071>
- Bollen, G.J., 1969. The selective effect of heat treatment on the microflora of a greenhouse soil. *Netherlands Journal of Plant Pathology* 75, 157–163. <https://doi.org/10.1007/BF02137211>
- Breiman, L., 2001. Random Forests. *Machine Learning* 45, 5–32. <https://doi.org/10.1023/A:1010933404324>
- Brown, K.J., Hebda, N.J.R., Hebda, R.J., Fitton, R., Trofymow, J.A., Conder, N., 2022. Development and wildfire dynamics of dry coastal temperate forests, BC, Canada. *Can. J. For. Res.* 52, 1320–1333. <https://doi.org/10.1139/cjfr-2022-0020>
- Butler, O.M., Lewis, T., Rezaei Rashti, M., Maunsell, S.C., Elser, J.J., Chen, C., 2019. The stoichiometric legacy of fire regime regulates the roles of micro-organisms and invertebrates in decomposition. *Ecology* 100, e02732. <https://doi.org/10.1002/ecy.2732>

- Caldwell, P.V., Martin, K.L., Vose, J.M., Baker, J.S., Warziniack, T.W., Costanza, J.K., Frey, G.E., Nehra, A., Mihlar, C.M., 2023. Forested watersheds provide the highest water quality among all land cover types, but the benefit of this ecosystem service depends on landscape context. *Science of The Total Environment* 882, 163550. <https://doi.org/10.1016/j.scitotenv.2023.163550>
- Capitaine, L., 2020. LongituRF: Random Forests for Longitudinal Data.
- Capitaine, L., Genuer, R., Thiébaud, R., 2021. Random forests for high-dimensional longitudinal data. *Stat Methods Med Res* 30, 166–184. <https://doi.org/10.1177/0962280220946080>
- Capital Regional District, 2022. Regional Water Supply Master Plan (No. 1186), IWS. Regional Water Supply Service.
- Capital Regional District, 2016. Regional Water Supply Service [WWW Document]. URL <https://www.crd.bc.ca/service/drinking-water/systems/regional-water-supply-system> (accessed 2.10.22).
- Carvalho, F., Pradhan, A., Abrantes, N., Campos, I., Keizer, J.J., Cássio, F., Pascoal, C., 2019. Wildfire impacts on freshwater detrital food webs depend on runoff load, exposure time and burnt forest type. *Science of The Total Environment* 692, 691–700. <https://doi.org/10.1016/j.scitotenv.2019.07.265>
- Cawley, K.M., Hohner, A.K., McKee, G.A., Borch, T., Omur-Ozbek, P., Oropeza, J., Rosario-Ortiz, F.L., 2018. Characterization and spatial distribution of particulate and soluble carbon and nitrogen from wildfire-impacted sediments. *J Soils Sediments* 18, 1314–1326. <https://doi.org/10.1007/s11368-016-1604-1>
- Cawley, K.M., Hohner, A.K., Podgorski, D.C., Cooper, W.T., Korak, J.A., Rosario-Ortiz, F.L., 2017. Molecular and Spectroscopic Characterization of Water Extractable Organic Matter from Thermally Altered Soils Reveal Insight into Disinfection Byproduct Precursors. *Environ. Sci. Technol.* 51, 771–779. <https://doi.org/10.1021/acs.est.6b05126>
- Cawson, J.G., Sheridan, G.J., Smith, H.G., Lane, P.N.J., 2013. Effects of fire severity and burn patchiness on hillslope-scale surface runoff, erosion and hydrologic connectivity in a prescribed burn. *Forest Ecology and Management* 310, 219–233. <https://doi.org/10.1016/j.foreco.2013.08.016>
- Chen, H., Uzun, H., Chow, A.T., Karanfil, T., 2020. Low water treatability efficiency of wildfire-induced dissolved organic matter and disinfection by-product precursors. *Water Research* 184, 116111. <https://doi.org/10.1016/j.watres.2020.116111>
- Chhetri, B.K., Galanis, E., Sobie, S., Brubacher, J., Balshaw, R., Otterstatter, M., Mak, S., Lem, M., Lysyshyn, M., Murdock, T., Fleury, M., Zickfeld, K., Zubel, M., Clarkson, L., Takaro, T.K., 2019. Projected local rain events due to climate change and the impacts on waterborne diseases in Vancouver, British Columbia, Canada. *Environmental Health* 18, 116. <https://doi.org/10.1186/s12940-019-0550-y>
- Chow, A.T., Tsai, K.-P., Fegle, T.S., Pierson, D.N., Rhoades, C.C., 2019. Lasting effects of wildfire on disinfection by-product formation in forest catchments. *Journal of Environmental Quality*. 48: 1826-1834. 48, 1826–1834. <https://doi.org/10.2134/jeq2019.04.0172>
- Chowdhury, S., 2018. Water quality degradation in the sources of drinking water: an assessment based on 18 years of data from 441 water supply systems. *Environ Monit Assess* 190, 379. <https://doi.org/10.1007/s10661-018-6772-6>
- Coble, A.A., Penaluna, B.E., Six, L.J., Verschuyf, J., 2023. Fire severity influences large wood and stream ecosystem responses in western Oregon watersheds. *fire ecol* 19, 34. <https://doi.org/10.1186/s42408-023-00192-5>
- Coogan, S.C.P., Robinne, F.-N., Jain, P., Flannigan, M.D., 2019. Scientists' warning on wildfire — a Canadian perspective. *Can. J. For. Res.* 49, 1015–1023. <https://doi.org/10.1139/cjfr-2019-0094>
- Cool, G., Lebel, A., Sadiq, R., Rodriguez, M.J., 2014. Impact of catchment geophysical characteristics and climate on the regional variability of dissolved organic carbon (DOC) in surface water. *Science of The Total Environment* 490, 947–956. <https://doi.org/10.1016/j.scitotenv.2014.05.091>

- Coops, N.C., Coggins, S.B., Kurz, W.A., 2007. Mapping the environmental limitations to growth of coastal Douglas-fir stands on Vancouver Island, British Columbia. *Tree Physiology* 27, 805–815. <https://doi.org/10.1093/treephys/27.6.805>
- Cory, R.M., Boyer, E.W., McKnight, D.M., 2011. Spectral Methods to Advance Understanding of Dissolved Organic Carbon Dynamics in Forested Catchments, in: Levia, D.F., Carlyle-Moses, D., Tanaka, T. (Eds.), *Forest Hydrology and Biogeochemistry: Synthesis of Past Research and Future Directions*. Springer Netherlands, Dordrecht, pp. 117–135. https://doi.org/10.1007/978-94-007-1363-5_6
- Curran, M.P., 1994. Slashburning effects on tree growth and nutrients in the Coastal Western Hemlock zone, Southern British Columbia : longer term trends. University of British Columbia. <https://doi.org/10.14288/1.0099220>
- Dai, A., 2013. Increasing drought under global warming in observations and models. *Nature Clim Change* 3, 52–58. <https://doi.org/10.1038/nclimate1633>
- de la Cretaz, A.L., Barten, P.K., 2007. Forest Management and Natural Disturbances, in: *Land Use Effects on Streamflow and Water Quality in the Northeastern United States*. CRC Press, Boca Raton. <https://doi.org/10.1201/9781420008722>
- Degerman, R., Lefébure, R., Byström, P., Båmstedt, U., Larsson, S., Andersson, A., 2018. Food web interactions determine energy transfer efficiency and top consumer responses to inputs of dissolved organic carbon. *Hydrobiologia* 805, 131–146. <https://doi.org/10.1007/s10750-017-3298-9>
- Deka, H.K., Mishra, R.R., 1983. The effect of slash burning on soil microflora. *Plant Soil* 73, 167–175. <https://doi.org/10.1007/BF02197713>
- Delpla, I., Jung, A.-V., Baures, E., Clement, M., Thomas, O., 2009. Impacts of climate change on surface water quality in relation to drinking water production. *Environment International* 35, 1225–1233. <https://doi.org/10.1016/j.envint.2009.07.001>
- Delpla, I., Rodriguez, M.J., 2017. Variability of disinfection by-products at a full-scale treatment plant following rainfall events. *Chemosphere* 166, 453–462. <https://doi.org/10.1016/j.chemosphere.2016.09.096>
- Demars, B.O.L., Kemp, J.L., Marteau, B., Friberg, N., Thornton, B., 2021. Stream Macroinvertebrates and Carbon Cycling in Tangled Food Webs. *Ecosystems* 24, 1944–1961. <https://doi.org/10.1007/s10021-021-00626-8>
- Diemer, L.A., McDowell, W.H., Wymore, A.S., Prokushkin, A.S., 2015. Nutrient uptake along a fire gradient in boreal streams of Central Siberia. *Freshwater Science* 34, 1443–1456. <https://doi.org/10.1086/683481>
- Dingman, S.L., Dingman, S.L., 2015. *Physical hydrology*, Third edition. ed. Waveland Press, Inc, Long Grove, Illinois.
- Dodds, W., Smith, V., 2016. Nitrogen, phosphorus, and eutrophication in streams. *IW* 6, 155–164. <https://doi.org/10.5268/IW-6.2.909>
- Dodds, W.K., Jones, J.R., Welch, E.B., 1998. Suggested classification of stream trophic state: distributions of temperate stream types by chlorophyll, total nitrogen, and phosphorus. *Water Research* 32, 1455–1462. [https://doi.org/10.1016/S0043-1354\(97\)00370-9](https://doi.org/10.1016/S0043-1354(97)00370-9)
- Dodds, W.K., Martí, E., Tank, J.L., Pontius, J., Hamilton, S.K., Grimm, N.B., Bowden, W.B., McDowell, W.H., Peterson, B.J., Valett, H.M., Webster, J.R., Gregory, S., 2004. Carbon and nitrogen stoichiometry and nitrogen cycling rates in streams. *Oecologia* 140, 458–467. <https://doi.org/10.1007/s00442-004-1599-y>
- Doerr, S.H., Cerdà, A., 2005. Fire effects on soil system functioning: new insights and future challenges. *Int. J. Wildland Fire* 14, 339–342. <https://doi.org/10.1071/WF05094>
- Doerr, S.H., Shakesby, R.A., Blake, W.H., Chafer, C.J., Humphreys, G.S., Wallbrink, P.J., 2006. Effects of differing wildfire severities on soil wettability and implications for hydrological response. *Journal of Hydrology* 319, 295–311. <https://doi.org/10.1016/j.jhydrol.2005.06.038>

- Doerr, S.H., Shakesby, R.A., Walsh, R.P.D., 2000. Soil water repellency: its causes, characteristics and hydro-geomorphological significance. *Earth-Science Reviews* 51, 33–65. [https://doi.org/10.1016/S0012-8252\(00\)00011-8](https://doi.org/10.1016/S0012-8252(00)00011-8)
- Dunne, T., Black, R.D., 1970. An Experimental Investigation of Runoff Production in Permeable Soils. *Water Resources Research* 6, 478–490. <https://doi.org/10.1029/WR006i002p00478>
- Dye, A.W., Reilly, M.J., McEvoy, A., Lemons, R., Riley, K.L., Kim, J.B., Kerns, B.K., 2024. Simulated Future Shifts in Wildfire Regimes in Moist Forests of Pacific Northwest, USA. *Journal of Geophysical Research: Biogeosciences* 129, e2023JG007722. <https://doi.org/10.1029/2023JG007722>
- Eaton, B., Moore, R.D., 2010. Regional Hydrology, in: Pike, R.G., Redding, T.E., Moore, R.D., Winkler, R.D., Bladon, K.D. (Eds.), *Compendium of Forest Hydrology and Geomorphology in British Columbia*, Land Management Handbook.
- Elser, J.J., Goldman, C.R., 1991. Zooplankton effects on phytoplankton in lakes of contrasting trophic status. *Limnology and Oceanography* 36, 64–90. <https://doi.org/10.4319/lo.1991.36.1.0064>
- Emelko, M.B., Silins, U., Bladon, K.D., Stone, M., 2011. Implications of land disturbance on drinking water treatability in a changing climate: Demonstrating the need for “source water supply and protection” strategies. *Water Research* 45, 461–472. <https://doi.org/10.1016/j.watres.2010.08.051>
- Emelko, M.B., Stone, M., Silins, U., Allin, D., Collins, A.L., Williams, C.H.S., Martens, A.M., Bladon, K.D., 2016. Sediment-phosphorus dynamics can shift aquatic ecology and cause downstream legacy effects after wildfire in large river systems. *Global Change Biology* 22, 1168–1184. <https://doi.org/10.1111/gcb.13073>
- Emmerton, C.A., Cooke, C.A., Hustins, S., Silins, U., Emelko, M.B., Lewis, T., Kruk, M.K., Taube, N., Zhu, D., Jackson, B., Stone, M., Kerr, J.G., Orwin, J.F., 2020. Severe western Canadian wildfire affects water quality even at large basin scales. *Water Research* 183, 116071. <https://doi.org/10.1016/j.watres.2020.116071>
- Fellman, J.B., Hood, E., Behnke, M.I., Welker, J.M., Spencer, R.G.M., 2020. Stormflows Drive Stream Carbon Concentration, Speciation, and Dissolved Organic Matter Composition in Coastal Temperate Rainforest Watersheds. *Journal of Geophysical Research: Biogeosciences* 125, e2020JG005804. <https://doi.org/10.1029/2020JG005804>
- Fellman, J.B., Hood, E., Edwards, R.T., D’Amore, D.V., 2009. Changes in the concentration, biodegradability, and fluorescent properties of dissolved organic matter during stormflows in coastal temperate watersheds. *Journal of Geophysical Research: Biogeosciences* 114. <https://doi.org/10.1029/2008JG000790>
- Fernández, I., Cabaneiro, A., Carballas, T., 1997. Organic matter changes immediately after a wildfire in an atlantic forest soil and comparison with laboratory soil heating. *Soil Biology and Biochemistry* 29, 1–11. [https://doi.org/10.1016/S0038-0717\(96\)00289-1](https://doi.org/10.1016/S0038-0717(96)00289-1)
- Ferreira, V., Albariño, R., Larrañaga, A., LeRoy, C.J., Masese, F.O., Moretti, M.S., 2023. Ecosystem services provided by small streams: an overview. *Hydrobiologia* 850, 2501–2535. <https://doi.org/10.1007/s10750-022-05095-1>
- Flannigan, M., Cantin, A.S., de Groot, W.J., Wotton, M., Newbery, A., Gowman, L.M., 2013. Global wildland fire season severity in the 21st century. *Forest Ecology and Management, The Mega-fire reality* 294, 54–61. <https://doi.org/10.1016/j.foreco.2012.10.022>
- forWater, 2024. forWater: Research [WWW Document]. forWater. URL <https://www.forwater.ca/research.html> (accessed 5.13.24).
- Francos, M., Úbeda, X., Pereira, P., Alcañiz, M., 2018. Long-term impact of wildfire on soils exposed to different fire severities. A case study in Cadiretes Massif (NE Iberian Peninsula). *Science of the Total Environment* 615, 664–671. <https://doi.org/10.1016/j.scitotenv.2017.09.311>
- Frost, P.C., Stelzer, R.S., Lamberti, G.A., Elser, J., 2002. Ecological stoichiometry of trophic interactions in the benthos: Understanding the role of C:N:P ratios in lentic and lotic habitats. *Journal of the North American Benthological Society* 21, 515–528. <https://doi.org/10.2307/1468427>

- Gartner, T., Mehan III, G.T., Mulligan, J., Roberson, J.A., Stangel, P., Qin, Y., 2014. Protecting forested watersheds is smart economics for water utilities. *Journal AWWA* 106, 54–64. <https://doi.org/10.5942/jawwa.2014.106.0132>
- Gavin, D.G., Brubaker, L.B., Lertzman, K.P., 2003. An 1800-year record of the spatial and temporal distribution of fire from the west coast of Vancouver Island, Canada. *Can. J. For. Res.* 33, 573–586. <https://doi.org/10.1139/x02-196>
- Glibert, P.M., 2012. Ecological stoichiometry and its implications for aquatic ecosystem sustainability. *Current Opinion in Environmental Sustainability, Aquatic and marine systems* 4, 272–277. <https://doi.org/10.1016/j.cosust.2012.05.009>
- Goldman, C.R., 1968. Aquatic Primary Production. *American Zoologist* 8, 31–42. <https://doi.org/10.1093/icb/8.1.31>
- Gomez Isaza, D.F., Cramp, R.L., Franklin, C.E., 2022. Fire and rain: A systematic review of the impacts of wildfire and associated runoff on aquatic fauna. *Global Change Biology* 28, 2578–2595. <https://doi.org/10.1111/gcb.16088>
- Gomi, T., Sidle, R.C., Richardson, J.S., 2002. Understanding Processes and Downstream Linkages of Headwater Systems. *BioScience* 52, 905. [https://doi.org/10.1641/0006-3568\(2002\)052\[0905:UPADLO\]2.0.CO;2](https://doi.org/10.1641/0006-3568(2002)052[0905:UPADLO]2.0.CO;2)
- Goodridge, B.M., Hanan, E.J., Aguilera, R., Wetherley, E.B., Chen, Y.-J., D’Antonio, C.M., Melack, J.M., 2018. Retention of Nitrogen Following Wildfire in a Chaparral Ecosystem. *Ecosystems* 21, 1608–1622. <https://doi.org/10.1007/s10021-018-0243-3>
- Goss, C.W., Goebel, P.C., Sullivan, S.M.P., 2014. Shifts in attributes along agriculture-forest transitions of two streams in central Ohio, USA. *Agriculture, Ecosystems & Environment* 197, 106–117. <https://doi.org/10.1016/j.agee.2014.07.026>
- Government of British Columbia, 2024a. Vegetation Resource Inventory - 2022 [WWW Document]. URL <https://catalogue.data.gov.bc.ca/dataset/vri-2022-forest-vegetation-composite-polygons> (accessed 1.31.24).
- Government of British Columbia, 2024b. Historical Drought Levels Map [WWW Document]. BC Drought Information Portal - Historical Drought Levels. URL <https://droughtportal.gov.bc.ca/pages/historical-drought-levels> (accessed 5.24.24).
- Government of British Columbia, 2023a. Wildfire Averages - Province of British Columbia [WWW Document]. URL <https://www2.gov.bc.ca/gov/content/safety/wildfire-status/about-bcws/wildfire-statistics/wildfire-averages> (accessed 3.18.24).
- Government of British Columbia, 2023b. Wildfire Season Summary - Province of British Columbia [WWW Document]. URL <https://www2.gov.bc.ca/gov/content/safety/wildfire-status/about-bcws/wildfire-history/wildfire-season-summary#Provincial%20Statistics> (accessed 3.18.24).
- Government of British Columbia, 2023c. Fire Burn Severity - Same Year [WWW Document]. URL <https://catalogue.data.gov.bc.ca/dataset/fire-burn-severity-same-year> (accessed 4.30.24).
- Government of British Columbia, 2022. iMapBC [WWW Document]. URL <https://maps.gov.bc.ca/ess/hm/imap4m/> (accessed 2.16.24).
- Government of British Columbia, 2018. BC Soils Information Finder Tool [WWW Document]. URL <https://governmentofbc.maps.arcgis.com/apps/MapSeries/index.html?appid=cc25e43525c5471ca7b13d639bbcd7aa> (accessed 1.9.24).
- Government of British Columbia, 2000. Vancouver Island Summary Land Use Plan.
- Government of British Columbia, 1996. Community Watershed Guidebook [WWW Document]. Community Watershed Guidebook. URL <https://www.for.gov.bc.ca/ftp/hfp/external/!publish/FPC%20archive/old%20web%20site%20contents/fpc/fpcguide/WATRSLED/Watertoc.htm> (accessed 4.22.24).
- Government of Canada, 2023. Canadian Digital Elevation Model, 1945-2011.
- Government of Canada, 2015. Canadian Drinking Water Guidelines [WWW Document]. URL <https://www.canada.ca/en/services/health/publications/healthy-living.html> (accessed 2.9.22).

- Graczyk, D.J., Robertson, D.M., Rose, W.J., Steur, J.J., 2000. Comparison of water-quality samples collected by siphon samplers and automatic samplers in Wisconsin (No. 067–00), Fact Sheet. U.S. Geological Survey. <https://doi.org/10.3133/fs06700>
- Greenwell, B.M., 2017. pdp: An R Package for Constructing Partial Dependence Plots. *The R Journal* 9, 421–438.
- Gregory, S.V., Swanson, F.J., McKee, W.A., Cummins, K.W., 1991. An Ecosystem Perspective of Riparian Zones. *BioScience* 41, 540–551. <https://doi.org/10.2307/1311607>
- Grolemund, G., Wickham, H., 2011. Dates and Times Made Easy with lubridate. *Journal of Statistical Software* 40, 1–25.
- Grömping, U., 2009. Variable Importance Assessment in Regression: Linear Regression versus Random Forest. *The American Statistician* 63. <https://doi.org/10.1198/tast.2009.08199>
- Gustine, R.N., Hanan, E.J., Robichaud, P.R., Elliot, W.J., 2022. From burned slopes to streams: how wildfire affects nitrogen cycling and retention in forests and fire-prone watersheds. *Biogeochemistry* 157, 51–68. <https://doi.org/10.1007/s10533-021-00861-0>
- Hajjem, A., Bellavance, F., Larocque, D., 2014. Mixed-effects random forest for clustered data. *Journal of Statistical Computation and Simulation* 84, 1313–1328. <https://doi.org/10.1080/00949655.2012.741599>
- Hallema, D.W., Sun, G., Bladon, K.D., Norman, S.P., Caldwell, P.V., Liu, Y., McNulty, S.G., 2017. Regional patterns of postwildfire streamflow response in the Western United States: The importance of scale-specific connectivity. *Hydrol. Process.* 31, 2582–2598. <https://doi.org/10.1002/hyp.11208>
- Hallema, D.W., Sun, G., Caldwell, P.V., Norman, S.P., Cohen, E.C., Liu, Y., Bladon, K.D., McNulty, S.G., 2018. Burned forests impact water supplies. *Nat Commun* 9, 1307. <https://doi.org/10.1038/s41467-018-03735-6>
- Halofsky, J.E., Peterson, D.L., Harvey, B.J., 2020. Changing wildfire, changing forests: the effects of climate change on fire regimes and vegetation in the Pacific Northwest, USA. *fire ecol* 16, 4. <https://doi.org/10.1186/s42408-019-0062-8>
- Hansen, J., Ruedy, R., Sato, M., Lo, K., 2010. Global Surface Temperature Change. *Reviews of Geophysics* 48. <https://doi.org/10.1029/2010RG000345>
- Harris, R.M.B., Remenyi, T.A., Williamson, G.J., Bindoff, N.L., Bowman, D.M.J.S., 2016. Climate–vegetation–fire interactions and feedbacks: trivial detail or major barrier to projecting the future of the Earth system? *WIREs Climate Change* 7, 910–931. <https://doi.org/10.1002/wcc.428>
- Hauer, F.R., Spencer, C.N., 1998. Phosphorus and Nitrogen Dynamics in Streams Associated With Wildfire: a Study of Immediate and Longterm Effects. *Int. J. Wildland Fire* 8, 183–198. <https://doi.org/10.1071/wf9980183>
- Haugo, R.D., Kellogg, B.S., Cansler, C.A., Kolden, C.A., Kemp, K.B., Robertson, J.C., Metlen, K.L., Vaillant, N.M., Restaino, C.M., 2019. The missing fire: quantifying human exclusion of wildfire in Pacific Northwest forests, USA. *Ecosphere* 10, e02702. <https://doi.org/10.1002/ecs2.2702>
- Havel, A., Tasdighi, A., Arabi, M., 2018. Assessing the hydrologic response to wildfires in mountainous regions. *Hydrol. Earth Syst. Sci.* 22, 2527–2550. <https://doi.org/10.5194/hess-22-2527-2018>
- Health Canada, 2004. From Source To Tap - The Multi-Barrier Approach To Safe Drinking Water [WWW Document]. URL <https://www.canada.ca/en/health-canada/services/environmental-workplace-health/reports-publications/water-quality/source-multi-barrier-approach-safe-drinking-water-health-canada.html> (accessed 5.13.24).
- Heiri, O., Lotter, A.F., Lemcke, G., 2001. Loss on ignition as a method for estimating organic and carbonate content in sediments: reproducibility and comparability of results. *Journal of Paleolimnology* 25, 101–110. <https://doi.org/10.1023/A:1008119611481>
- Helms, J.R., Stubbins, A., Ritchie, J.D., Minor, E.C., Kieber, D.J., Mopper, K., 2008. Absorption spectral slopes and slope ratios as indicators of molecular weight, source, and photobleaching of chromophoric dissolved organic matter. *Limnology and Oceanography* 53, 955–969. <https://doi.org/10.4319/lo.2008.53.3.0955>

- Heyerdahl, E.K., Lertzman, K., Wong, C.M., 2012. Mixed-severity fire regimes in dry forests of southern interior British Columbia, Canada. *Can. J. For. Res.* 42, 88–98. <https://doi.org/10.1139/x11-160>
- Hoffman, K.M., Gavin, D.G., Starzomski, B.M., 2016. Seven hundred years of human-driven and climate-influenced fire activity in a British Columbia coastal temperate rainforest. *Royal Society Open Science* 3, 160608. <https://doi.org/10.1098/rsos.160608>
- Hohner, A.K., Cawley, K., Oropeza, J., Summers, R.S., Rosario-Ortiz, F.L., 2016. Drinking water treatment response following a Colorado wildfire. *Water Research* 105, 187–198. <https://doi.org/10.1016/j.watres.2016.08.034>
- Hohner, A.K., Rhoades, C.C., Wilkerson, P., Rosario-Ortiz, F.L., 2019. Wildfires Alter Forest Watersheds and Threaten Drinking Water Quality. *Acc. Chem. Res.* 52, 1234–1244. <https://doi.org/10.1021/acs.accounts.8b00670>
- Hohner, A.K., Terry, L.G., Townsend, E.B., Summers, R.S., Rosario-Ortiz, F.L., 2017. Water treatment process evaluation of wildfire-affected sediment leachates. *Environ. Sci.: Water Res. Technol.* 3, 352–365. <https://doi.org/10.1039/C6EW00247A>
- Holden, Z.A., Swanson, A., Luce, C.H., Jolly, W.M., Maneta, M., Oyler, J.W., Warren, D.A., Parsons, R., Affleck, D., 2018. Decreasing fire season precipitation increased recent western US forest wildfire activity. *Proceedings of the National Academy of Sciences* 115, E8349–E8357. <https://doi.org/10.1073/pnas.1802316115>
- Homann, P.S., Bormann, B.T., Darbyshire, R.L., Morrisette, B.A., 2011. Forest Soil Carbon and Nitrogen Losses Associated with Wildfire and Prescribed Fire. *Soil Science Society of America Journal* 75, 1926–1934. <https://doi.org/10.2136/sssaj2010-0429>
- Hope, G., Jordan, P., Winkler, R., Giles, T., Curran, M., Soneff, K., Chapman, B., 2015. Post-wildfire Natural Hazards Risk Analysis in British Columbia (Land Management Handbook No. 69). Province of British Columbia, Victoria, B.C.
- Hoskins, B., Ross, D., 2009. Soil Sample Preparation and Extraction. Recommended Soil Testing Procedures for the Northeastern United States, Northeastern Regional Publication 493, 3–10.
- House, W.A., Denison, F.H., Armitage, P.D., 1995. Comparison of the uptake of inorganic phosphorus to a suspended and stream bed-sediment. *Water Research* 29, 767–779. [https://doi.org/10.1016/0043-1354\(94\)00237-2](https://doi.org/10.1016/0043-1354(94)00237-2)
- Howarth, R.W., Marino, R., Cole, J.J., 1988. Nitrogen fixation in freshwater, estuarine, and marine ecosystems. 2. Biogeochemical controls. *Limnology and Oceanography* 33. <https://doi.org/10.4319/lo.1988.33.4part2.0688>
- Hu, J., Szymczak, S., 2023. A review on longitudinal data analysis with random forest. *Briefings in Bioinformatics* 24, bbad002. <https://doi.org/10.1093/bib/bbad002>
- Hua, L.-C., Chao, S.-J., Huang, K., Huang, C., 2020. Characteristics of low and high SUVA precursors: Relationships among molecular weight, fluorescence, and chemical composition with DBP formation. *Sci Total Environ* 727, 138638. <https://doi.org/10.1016/j.scitotenv.2020.138638>
- Huguet, A., Vacher, L., Relexans, S., Saubusse, S., Froidefond, J.M., Parlanti, E., 2009. Properties of fluorescent dissolved organic matter in the Gironde Estuary. *Organic Geochemistry* 40, 706–719. <https://doi.org/10.1016/j.orggeochem.2009.03.002>
- Hutchins, R.H.S., Tank, S.E., Olefeldt, D., Quinton, W.L., Spence, C., Dion, N., Mengistu, S.G., 2023. Influence of Wildfire on Downstream Transport of Dissolved Carbon, Nutrients, and Mercury in the Permafrost Zone of Boreal Western Canada. *J. Geophys. Res.-Biogeosci.* 128, e2023JG007602. <https://doi.org/10.1029/2023JG007602>
- IPCC, 2023. IPCC, 2023: Summary for Policymakers. In: *Climate Change 2023: Synthesis Report. Contribution of Working Groups I, II and III to the Sixth Assessment Report of the Intergovernmental Panel on Climate Change*, IPCC. Intergovernmental Panel on Climate Change (IPCC), Geneva, Switzerland. <https://doi.org/10.59327/IPCC/AR6-9789291691647>
- Island Health, 2014. Water, Water, Everywhere. Drinking Water in Island Health (Medical Health Officer's Report).

- Jablánczy, A., 1964. Influence of slash burning on the establishment and initial growth of seedlings of Douglas-fir, western hemlock and western redcedar : a study of the effect of simulated slash burn on soil blocks from some sites of the Coastal Western Hemlock Zone. University of British Columbia. <https://doi.org/10.14288/1.0105271>
- Jager, H.I., Long, J.W., Malison, R.L., Murphy, B.P., Rust, A., Silva, L.G.M., Sollmann, R., Steel, Z.L., Bowen, M.D., Dunham, J.B., Ebersole, J.L., Flitcroft, R.L., 2021. Resilience of terrestrial and aquatic fauna to historical and future wildfire regimes in western North America. *Ecology and Evolution* 11, 12259–12284. <https://doi.org/10.1002/ece3.8026>
- Jones, M.W., Abatzoglou, J.T., Veraverbeke, S., Andela, N., Lasslop, G., Forkel, M., Smith, A.J.P., Burton, C., Betts, R.A., van der Werf, G.R., Sitch, S., Canadell, J.G., Santín, C., Kolden, C., Doerr, S.H., Le Quéré, C., 2022. Global and Regional Trends and Drivers of Fire Under Climate Change. *Reviews of Geophysics* 60, e2020RG000726. <https://doi.org/10.1029/2020RG000726>
- Judd, K.E., Crump, B.C., Kling, G.W., 2006. Variation in Dissolved Organic Matter Controls Bacterial Production and Community Composition. *Ecology* 87, 2068–2079. [https://doi.org/10.1890/0012-9658\(2006\)87\[2068:VIDOMC\]2.0.CO;2](https://doi.org/10.1890/0012-9658(2006)87[2068:VIDOMC]2.0.CO;2)
- Jungen, J.R., 1985. Soils of Southern Vancouver Island (Technical No. 44), British Columbia Soil Survey. Ministry of Environment, British Columbia.
- Keck, F., Lepori, F., 2012. Can we predict nutrient limitation in streams and rivers? *Freshwater Biology* 57, 1410–1421. <https://doi.org/10.1111/j.1365-2427.2012.02802.x>
- Kellerman, A.M., Guillemette, F., Podgorski, D.C., Aiken, G.R., Butler, K.D., Spencer, R.G.M., 2018. Unifying Concepts Linking Dissolved Organic Matter Composition to Persistence in Aquatic Ecosystems. *Environ. Sci. Technol.* 52, 2538–2548. <https://doi.org/10.1021/acs.est.7b05513>
- Kelly, L.T., Giljohann, K.M., Duane, A., Aquilué, N., Archibald, S., Batllori, E., Bennett, A.F., Buckland, S.T., Canelles, Q., Clarke, M.F., Fortin, M.-J., Hermoso, V., Herrando, S., Keane, R.E., Lake, F.K., McCarthy, M.A., Morán-Ordóñez, A., Parr, C.L., Pausas, J.G., Penman, T.D., Regos, A., Rumpff, L., Santos, J.L., Smith, A.L., Syphard, A.D., Tingley, M.W., Brotons, L., 2020. Fire and biodiversity in the Anthropocene. *Science* 370, eabb0355. <https://doi.org/10.1126/science.abb0355>
- Keser, N., St. Pierre, D., 1973. Soils of Vancouver Island - A compendium (Research Note No. 56). British Columbia Forest Service Research Division.
- Kirkwood, R.S.M., Lawton, J.H., 1981. Efficiency of biomass transfer and the stability of model food-webs. *Journal of Theoretical Biology* 93, 225–237. [https://doi.org/10.1016/0022-5193\(81\)90067-9](https://doi.org/10.1016/0022-5193(81)90067-9)
- Klimas, K., Hiesl, P., Hagan, D., Park, D., 2020. Prescribed fire effects on sediment and nutrient exports in forested environments: A review. *Journal of Environmental Quality* 49, 793–811. <https://doi.org/10.1002/jeq2.20108>
- Knighton, D., 1998. *Fluvial Forms and Processes: A New Perspective*, 2nd ed. Routledge, London. <https://doi.org/10.4324/9780203784662>
- Koetsier, P., Tuckett, Q., White, J., 2007. Present effects of past wildfires on the diets of stream fish. *Western North American Naturalist* 67, 429–438. [https://doi.org/10.3398/1527-0904\(2007\)67\[429:PEOPWO\]2.0.CO;2](https://doi.org/10.3398/1527-0904(2007)67[429:PEOPWO]2.0.CO;2)
- Kothawala, D.N., Ji, X., Laudon, H., Ågren, A.M., Futter, M.N., Köhler, S.J., Tranvik, L.J., 2015. The relative influence of land cover, hydrology, and in-stream processing on the composition of dissolved organic matter in boreal streams. *Journal of Geophysical Research: Biogeosciences* 120, 1491–1505. <https://doi.org/10.1002/2015JG002946>
- Larocque, I.M.S., 2014. The Hydrogeology of Salt Spring Island, British Columbia [WWW Document]. URL <https://summit.sfu.ca/item/14464> (accessed 2.17.23).
- Leonard, J.M., Magaña, H.A., Bangert, R.K., Neary, D.G., Montgomery, W.L., 2017. Fire and Floods: The Recovery of Headwater Stream Systems Following High-Severity Wildfire. *fire ecol* 13, 62–84. <https://doi.org/10.4996/fireecology.130306284>

- Leopold, L.B., Wolman, M.G., Miller, J.P., Wohl, E.E., 2020. *Fluvial Processes in Geomorphology*. Courier Dover Publications.
- Levine, A.D., Yang, Y.J., Goodrich, J.A., 2016. Enhancing climate adaptation capacity for drinking water treatment facilities. *Journal of Water and Climate Change* 7, 485–497. <https://doi.org/10.2166/wcc.2016.011>
- Littell, J.S., McKenzie, D., Wan, H.Y., Cushman, S.A., 2018. Climate Change and Future Wildfire in the Western United States: An Ecological Approach to Nonstationarity. *Earth's Future* 6, 1097–1111. <https://doi.org/10.1029/2018EF000878>
- Liu, H., Xu, H., Wu, Y., Ai, Z., Zhang, J., Liu, G., Xue, S., 2021. Effects of natural vegetation restoration on dissolved organic matter (DOM) biodegradability and its temperature sensitivity. *Water Research* 191, 116792. <https://doi.org/10.1016/j.watres.2020.116792>
- Long, C.J., Whitlock, C., 2002. Fire and Vegetation History from the Coastal Rain Forest of the Western Oregon Coast Range. *Quaternary Research* 58, 215–225. <https://doi.org/10.1006/qres.2002.2378>
- Lowe, W.H., Likens, G.E., 2005. Moving Headwater Streams to the Head of the Class. *BioScience* 55, 196–197. [https://doi.org/10.1641/0006-3568\(2005\)055\[0196:MHSTTH\]2.0.CO;2](https://doi.org/10.1641/0006-3568(2005)055[0196:MHSTTH]2.0.CO;2)
- Luke, S.H., Luckai, N.J., Burke, J.M., Prepas, E.E., 2007. Riparian areas in the Canadian boreal forest and linkages with water quality in streams. *Environ. Rev.* 15, 79–97. <https://doi.org/10.1139/A07-001>
- MacKenzie, W., Meidinger, D., 2017. The Biogeoclimatic Ecosystem Classification Approach: an ecological framework for vegetation classification. *Phytocoenologia* 48. <https://doi.org/10.1127/phyto/2017/0160>
- Majidzadeh, H., Chen, H., Coates, T.A., Tsai, K.-P., Olivares, C.I., Trettin, C., Uzun, H., Karanfil, T., Chow, A.T., 2019. Long-term watershed management is an effective strategy to reduce organic matter export and disinfection by-product precursors in source water. *Int. J. Wildland Fire* 28, 804. <https://doi.org/10.1071/WF18174>
- Malmon, D.V., Reneau, S.L., Katzman, D., Lavine, A., Lyman, J., 2007. Suspended sediment transport in an ephemeral stream following wildfire. *Journal of Geophysical Research: Earth Surface* 112. <https://doi.org/10.1029/2005JF000459>
- Matveev, V., Robson, B.J., 2014. Aquatic Food Web Structure and the Flow of Carbon. *frer* 7, 1–24. <https://doi.org/10.1608/FRJ-7.1.720>
- McGlynn, B.L., McDonnell, J.J., Seibert, J., Kendall, C., 2004. Scale effects on headwater catchment runoff timing, flow sources, and groundwater-streamflow relations. *Water Resources Research* 40. <https://doi.org/10.1029/2003WR002494>
- McKay, G., K. Hohner, A., L. Rosario-Ortiz, F., 2020. Use of optical properties for evaluating the presence of pyrogenic organic matter in thermally altered soil leachates. *Environmental Science: Processes & Impacts* 22, 981–992. <https://doi.org/10.1039/C9EM00413K>
- McLauchlan, K.K., Higuera, P.E., Miesel, J., Rogers, B.M., Schweitzer, J., Shuman, J.K., Tepley, A.J., Varner, J.M., Veblen, T.T., Adalsteinsson, S.A., Balch, J.K., Baker, P., Batllori, E., Bigio, E., Brando, P., Cattau, M., Chipman, M.L., Coen, J., Crandall, R., Daniels, L., Enright, N., Gross, W.S., Harvey, B.J., Hatten, J.A., Hermann, S., Hewitt, R.E., Kobziar, L.N., Landesmann, J.B., Loranty, M.M., Maezumi, S.Y., Mearns, L., Moritz, M., Myers, J.A., Pausas, J.G., Pellegrini, A.F.A., Platt, W.J., Roozeboom, J., Safford, H., Santos, F., Scheller, R.M., Sherriff, R.L., Smith, K.G., Smith, M.D., Watts, A.C., 2020. Fire as a fundamental ecological process: Research advances and frontiers. *Journal of Ecology* 108, 2047–2069. <https://doi.org/10.1111/1365-2745.13403>
- McSorley, H.J., 2020. Spatial and temporal variation in natural organic matter quantity and quality across a second growth forested drinking water supply area on Vancouver Island, BC. University of British Columbia. <https://doi.org/10.14288/1.0395411>
- Meidinger, D., Pojar, J. (Eds.), 1991. *Ecosystems of British Columbia*, Special report series; 6. British Columbia Ministry of Forests, Victoria.

- Meyer, J.L., Kaplan, L.A., Newbold, D., Strayer, D.L., Woltemade, C.J., Zedler, J.B., Beilfuss, R., Carpenter, Q., 2007. The Scientific Imperative for Defending Small Streams and Wetlands. American Rivers and Sierra Club.
- Minshall, G.W., 2003. Responses of stream benthic macroinvertebrates to fire. *Forest Ecology and Management, The Effect of Wildland Fire on Aquatic Ecosystems in the Western USA*. 178, 155–161. [https://doi.org/10.1016/S0378-1127\(03\)00059-8](https://doi.org/10.1016/S0378-1127(03)00059-8)
- Minshall, G.W., Brock, J.T., Andrews, D.A., Robinson, C.T., 2001. Water quality, substratum and biotic responses of five central Idaho (USA) streams during the first year following the Mortar Creek fire. *Int. J. Wildland Fire* 10, 185–199. <https://doi.org/10.1071/wf01017>
- Modified Copernicus Sentinel data, 2023. Sentinel Hub.
- Moghaddam-Ghadimi, S., Tam, A., Khan, U.T., Gora, S.L., 2023. How might climate change impact water safety and boil water advisories in Canada? *FACETS* 8, 1–21. <https://doi.org/10.1139/facets-2022-0223>
- Moody, C.S., Worrall, F., 2017. Modeling rates of DOC degradation using DOM composition and hydroclimatic variables. *Journal of Geophysical Research: Biogeosciences* 122, 1175–1191. <https://doi.org/10.1002/2016JG003493>
- Moody, J.A., Shakesby, R.A., Robichaud, P.R., Cannon, S.H., Martin, D.A., 2013. Current research issues related to post-wildfire runoff and erosion processes. *Earth-Science Reviews* 122, 10–37. <https://doi.org/10.1016/j.earscirev.2013.03.004>
- Morales Parrado, J., Paes, N., Moreschi, A., Teixido, A., 2023. Fire and water: fire impacts on physicochemical properties of freshwater ecosystems. *Fundamental and Applied Limnology / Archiv für Hydrobiologie* 196, 137–153. <https://doi.org/10.1127/fal/2023/1488>
- Moustaka-Gouni, M., Sommer, U., 2020. Effects of Harmful Blooms of Large-Sized and Colonial Cyanobacteria on Aquatic Food Webs. *Water* 12, 1587. <https://doi.org/10.3390/w12061587>
- Mulholland, P.J., 2004. The importance of in-stream uptake for regulating stream concentrations and outputs of N and P from a forested watershed: evidence from long-term chemistry records for Walker Branch Watershed. *Biogeochemistry* 70, 403–426. <https://doi.org/10.1007/s10533-004-0364-y>
- Murphy, K.R., Stedmon, C.A., Graeber, D., Bro, R., 2013. Fluorescence spectroscopy and multi-way techniques. *PARAFAC. Analytical Methods* 5, 6557–6566. <https://doi.org/10.1039/C3AY41160E>
- Murphy, K.R., Stedmon, C.A., Wenig, P., Bro, R., 2014. OpenFluor– an online spectral library of auto-fluorescence by organic compounds in the environment. *Anal. Methods* 6, 658–661. <https://doi.org/10.1039/C3AY41935E>
- Murphy, S.F., Writer, J.H., McCleskey, R.B., Martin, D.A., 2015. The role of precipitation type, intensity, and spatial distribution in source water quality after wildfire. *Environ. Res. Lett.* 10, 084007. <https://doi.org/10.1088/1748-9326/10/8/084007>
- MWH, 2012. *MWH's Water Treatment: Principles and Design*, Third Edition. John Wiley & Sons, Ltd. <https://doi.org/10.1002/9781118131473>
- Myers-Pigg, A.N., Louchouart, P., Amon, R.M.W., Prokushkin, A., Pierce, K., Rubtsov, A., 2015. Labile pyrogenic dissolved organic carbon in major Siberian Arctic rivers: Implications for wildfire-stream metabolic linkages. *Geophysical Research Letters* 42, 377–385. <https://doi.org/10.1002/2014GL062762>
- Nadeau, T.-L., Rains, M.C., 2007. Hydrological Connectivity Between Headwater Streams and Downstream Waters: How Science Can Inform Policy. *JAWRA Journal of the American Water Resources Association* 43, 118–133. <https://doi.org/10.1111/j.1752-1688.2007.00010.x>
- Neary, D.G., Ice, G.G., Jackson, C.R., 2009. Linkages between forest soils and water quality and quantity. *Forest Ecology and Management, Forest Soil Science: Celebrating 50 Years of Research on Properties, Processes and Management of Forest Soils* Forest Soil Science: Celebrating 50 Years of Research on Properties, Processes and Management of Forest Soils Forest Soil Science: Celebrating 50 Years of Research on Properties, Processes and Management of Forest Soils

- Forest Soil Science: Celebrating 50 Years of Research on Properties, Processes and Management of Forest Soils 258, 2269–2281. <https://doi.org/10.1016/j.foreco.2009.05.027>
- Neary, D.G., Ryan, K.C., DeBano, L.F., 2005. Wildland fire in ecosystems: effects of fire on soils and water. Gen. Tech. Rep. RMRS-GTR-42-vol.4. Ogden, UT: U.S. Department of Agriculture, Forest Service, Rocky Mountain Research Station. 250 p. 042. <https://doi.org/10.2737/RMRS-GTR-42-V4>
- Neris, J., Santin, C., Lew, R., Robichaud, P.R., Elliot, W.J., Lewis, S.A., Sheridan, G., Rohlf, A.-M., Ollivier, Q., Oliveira, L., Doerr, S.H., 2021. Designing tools to predict and mitigate impacts on water quality following the Australian 2019/2020 wildfires: Insights from Sydney’s largest water supply catchment. *Integrated Environmental Assessment and Management* 17, 1151–1161. <https://doi.org/10.1002/ieam.4406>
- Niemeyer, R.J., Bladon, K.D., Woodsmith, R.D., 2020. Long-term hydrologic recovery after wildfire and post-fire forest management in the interior Pacific Northwest. *Hydrological Processes* 34, 1182–1197. <https://doi.org/10.1002/hyp.13665>
- Norwood, M.J., Louchouart, P., Kuo, L.-J., Harvey, O.R., 2013. Characterization and biodegradation of water-soluble biomarkers and organic carbon extracted from low temperature chars. *Organic Geochemistry* 56, 111–119. <https://doi.org/10.1016/j.orggeochem.2012.12.008>
- Nunes, J.P., Doerr, S.H., Sheridan, G., Neris, J., Santin, C., Emelko, M.B., Silins, U., Robichaud, P.R., Elliot, W.J., Keizer, J., 2018. Assessing water contamination risk from vegetation fires: Challenges, opportunities and a framework for progress. *Hydrological Processes* 32, 687–694. <https://doi.org/10.1002/hyp.11434>
- Ohno, T., 2002. Fluorescence Inner-Filtering Correction for Determining the Humification Index of Dissolved Organic Matter. *Environ. Sci. Technol.* 36, 742–746. <https://doi.org/10.1021/es0155276>
- Olivares, C.I., Zhang, W., Uzun, H., Erdem, C.U., Majidzadeh, H., Trettin, C., Karanfil, T., Chow, A., Olivares, C.I., Zhang, W., Uzun, H., Erdem, C.U., Majidzadeh, H., Trettin, C., Karanfil, T., Chow, A., 2019. Optical in-situ sensors capture dissolved organic carbon (DOC) dynamics after prescribed fire in high-DOC forest watersheds. *Int. J. Wildland Fire* 28, 761–768. <https://doi.org/10.1071/WF18175>
- Oliver, A.A., Reuter, J.E., Heyvaert, A.C., Dahlgren, R.A., 2012. Water quality response to the Angora Fire, Lake Tahoe, California. *Biogeochemistry* 111, 361–376. <https://doi.org/10.1007/s10533-011-9657-0>
- Oliver, A.A., Tank, S.E., Giesbrecht, I., Korver, M.C., Floyd, W.C., Sanborn, P., Bulmer, C., Lertzman, K.P., 2017. A global hotspot for dissolved organic carbon in hypermaritime watersheds of coastal British Columbia. *Biogeosciences* 14, 3743–3762. <https://doi.org/10.5194/bg-14-3743-2017>
- Pacific Climate Impacts Consortium, 2024. BC Station Data [WWW Document]. URL <https://www.pacificclimate.org/data/bc-station-data> (accessed 1.11.24).
- Parr, T.B., Inamdar, S.P., Miller, M.J., 2019. Overlapping anthropogenic effects on hydrologic and seasonal trends in DOC in a surface water dependent water utility. *Water Research* 148, 407–415. <https://doi.org/10.1016/j.watres.2018.10.065>
- Paul, M.J., LeDuc, S.D., Lassiter, M.G., Moorhead, L.C., Noyes, P.D., Leibowitz, S.G., 2022. Wildfire Induces Changes in Receiving Waters: A Review With Considerations for Water Quality Management. *Water Resources Research* 58, e2021WR030699. <https://doi.org/10.1029/2021WR030699>
- Perrin, C.J., Bothwell, M.L., Slaney, P.A., 1987. Experimental Enrichment of a Coastal Stream in British Columbia: Effects of Organic and Inorganic Additions on Autotrophic Periphyton Production. *Can. J. Fish. Aquat. Sci.* 44, 1247–1256. <https://doi.org/10.1139/f87-147>
- Pike, R., Feller, M., Stednick, J.D., Rieberger, K.J., Carver, M., 2010. Water Quality and Forest Management., in: *Compendium of Forest Hydrology and Geomorphology in British Columbia, Land Management Handbook*. BC Ministry of Forests and Range, Forest Science Program, Victoria, B.C.

- Pinto, P., Vaz, P., Robinson, C., Morais, M., 2009. Wildfire impacts on aquatic ecosystems. *Sustainable Development*.
- Pojar, J., Klinka, D.A., Demarchi, D.A., 1991. Coastal Western Hemlock Ecozone, in: *Ecosystems of British Columbia*.
- Poulin, B.A., Ryan, J.N., Aiken, G.R., 2014. Effects of Iron on Optical Properties of Dissolved Organic Matter. *Environ. Sci. Technol.* 48, 10098–10106. <https://doi.org/10.1021/es502670r>
- Pradhan, A., Carvalho, F., Abrantes, N., Campos, I., Keizer, J.J., Cássio, F., Pascoal, C., 2020. Biochemical and functional responses of stream invertebrate shredders to post-wildfire contamination. *Environmental Pollution* 267, 115433. <https://doi.org/10.1016/j.envpol.2020.115433>
- Price, J.I., Heberling, M.T., 2018. The Effects of Source Water Quality on Drinking Water Treatment Costs: A Review and Synthesis of Empirical Literature. *Ecological Economics* 151, 195–209. <https://doi.org/10.1016/j.ecolecon.2018.04.014>
- R Core Team, 2023. R: A Language and Environment for Statistical Computing.
- Reilly, M.J., Dunn, C.J., Meigs, G.W., Spies, T.A., Kennedy, R.E., Bailey, J.D., Briggs, K., 2017. Contemporary patterns of fire extent and severity in forests of the Pacific Northwest, USA (1985–2010). *Ecosphere* 8, e01695. <https://doi.org/10.1002/ecs2.1695>
- Reilly, M.J., Zupan, A., Halofsky, J.S., Raymond, C., McEvoy, A., Dye, A.W., Donato, D.C., Kim, J.B., Potter, B.E., Walker, N., Davis, R.J., Dunn, C.J., Bell, D.M., Gregory, M.J., Johnston, J.D., Harvey, B.J., Halofsky, J.E., Kerns, B.K., 2022. Cascadia Burning: The historic, but not historically unprecedented, 2020 wildfires in the Pacific Northwest, USA. *Ecosphere* 13, e4070. <https://doi.org/10.1002/ecs2.4070>
- Revchuk, A.D., Suffet, I.H. (Mel), 2014. Effect of Wildfires on Physicochemical Changes of Watershed Dissolved Organic Matter. *Water Environment Research* 86, 372–381. <https://doi.org/10.2175/106143013X13736496909671>
- Rhoades, C.C., Chow, A.T., Covino, T.P., Fegle, T.S., Pierson, D.N., Rhea, A.E., 2019a. The Legacy of a Severe Wildfire on Stream Nitrogen and Carbon in Headwater Catchments. *Ecosystems* 22, 643–657. <https://doi.org/10.1007/s10021-018-0293-6>
- Rhoades, C.C., Nunes, J.P., Silins, U., Doerr, S.H., Rhoades, C.C., Nunes, J.P., Silins, U., Doerr, S.H., 2019b. The influence of wildfire on water quality and watershed processes: new insights and remaining challenges. *Int. J. Wildland Fire* 28, 721–725. https://doi.org/10.1071/WFv28n10_FO
- Richardson, C., Montalvo, M., Wagner, S., Barton, R., Paytan, A., Redmond, M., Zimmer, M., 2024. Exploring the Complex Effects of Wildfire on Stream Water Chemistry: Insights From Concentration-Discharge Relationships. *Water Resources Research* 60, e2023WR034940. <https://doi.org/10.1029/2023WR034940>
- Richardson, J., 2019. Biological Diversity in Headwater Streams. *Water* 11, 366. <https://doi.org/10.3390/w11020366>
- Richardson, S.D., Postigo, C., 2012. Drinking Water Disinfection By-products, in: Barceló, D. (Ed.), *Emerging Organic Contaminants and Human Health, The Handbook of Environmental Chemistry*. Springer, Berlin, Heidelberg, pp. 93–137. https://doi.org/10.1007/698_2011_125
- Rizhinashvili, A.L., 2022. An Outline of the Theory of the Functioning of Aquatic Ecosystems: Nutrient Limitation. *Biol Bull Rev* 12, 596–608. <https://doi.org/10.1134/S2079086422060068>
- Robichaud, P.J.L., Padowski, J.C., 2024. Drinking water under fire: Water utilities' vulnerability to wildfires in the Pacific Northwest. *JAWRA Journal of the American Water Resources Association* 60, 590–602. <https://doi.org/10.1111/1752-1688.13174>
- Robinne, F.-N., Bladon, K.D., Miller, C., Parisien, M.-A., Mathieu, J., Flannigan, M.D., 2018. A spatial evaluation of global wildfire-water risks to human and natural systems. *Science of The Total Environment* 610–611, 1193–1206. <https://doi.org/10.1016/j.scitotenv.2017.08.112>
- Robinne, F.N., Bladon, K.D., Silins, U., Emelko, M.B., Flannigan, M.D., Parisien, M.A., Wang, X., Kienzie, S.W., Dupont, D.P., 2019. A regional-scale index for assessing the exposure of drinking-water sources to wildfires. *Forests* 10, undefined-undefined. <https://doi.org/10.3390/f10050384>

- Robbinne, F.-N., Hallema, D.W., Bladon, K.D., Buttle, J.M., 2020. Wildfire impacts on hydrologic ecosystem services in North American high-latitude forests: A scoping review. *Journal of Hydrology* 581, 124360. <https://doi.org/10.1016/j.jhydrol.2019.124360>
- Robbinne, F.-N., Hallema, D.W., Bladon, K.D., Flannigan, M.D., Boisramé, G., Bréthaut, C.M., Doerr, S.H., Di Baldassarre, G., Gallagher, L.A., Hohner, A.K., Khan, S.J., Kinoshita, A.M., Mordecai, R., Nunes, J.P., Nyman, P., Santín, C., Sheridan, G., Stoof, C.R., Thompson, M.P., Waddington, J.M., Wei, Y., 2021. Scientists' warning on extreme wildfire risks to water supply. *Hydrological Processes* 35, e14086. <https://doi.org/10.1002/hyp.14086>
- Robson, B.J., Chester, E.T., Matthews, T.G., Johnston, K., 2018. Post-wildfire recovery of invertebrate diversity in drought-affected headwater streams. *Aquat Sci* 80, 21. <https://doi.org/10.1007/s00027-018-0570-7>
- Roces-Díaz, J.V., Santín, C., Martínez-Vilalta, J., Doerr, S.H., 2022. A global synthesis of fire effects on ecosystem services of forests and woodlands. *Frontiers in Ecology and the Environment* 20, 170–178. <https://doi.org/10.1002/fee.2349>
- Rogers, B.M., Neilson, R.P., Drapek, R., Lenihan, J.M., Wells, J.R., Bachelet, D., Law, B.E., 2011. Impacts of climate change on fire regimes and carbon stocks of the U.S. Pacific Northwest. *Journal of Geophysical Research: Biogeosciences* 116. <https://doi.org/10.1029/2011JG001695>
- Ruhala, S.S., Zarnetske, J.P., 2017. Using in-situ optical sensors to study dissolved organic carbon dynamics of streams and watersheds: A review. *Science of The Total Environment* 575, 713–723. <https://doi.org/10.1016/j.scitotenv.2016.09.113>
- Rupp, D.E., Li, S., Mote, P.W., Shell, K.M., Massey, N., Sparrow, S.N., Wallom, D.C.H., Allen, M.R., 2017. Seasonal spatial patterns of projected anthropogenic warming in complex terrain: a modeling study of the western US. *Clim Dyn* 48, 2191–2213. <https://doi.org/10.1007/s00382-016-3200-x>
- Rust, A.J., Hogue, T.S., Saxe, S., McCray, J., Rust, A.J., Hogue, T.S., Saxe, S., McCray, J., 2018. Post-fire water-quality response in the western United States. *Int. J. Wildland Fire* 27, 203–216. <https://doi.org/10.1071/WF17115>
- Rust, A.J., Saxe, S., McCray, J., Rhoades, C.C., Hogue, T.S., 2019. Evaluating the factors responsible for post-fire water quality response in forests of the western USA. *International Journal of Wildland Fire* 28, 769–784. <https://doi.org/10.1071/WF18191>
- Santín, C., Doerr, S.H., Otero, X.L., Chafer, C.J., 2015. Quantity, composition and water contamination potential of ash produced under different wildfire severities. *Environmental Research* 142, 297–308. <https://doi.org/10.1016/j.envres.2015.06.041>
- Santos, F., Russell, D., Berhe, A.A., 2016. Thermal alteration of water extractable organic matter in climosequence soils from the Sierra Nevada, California. *Journal of Geophysical Research: Biogeosciences* 121, 2877–2885. <https://doi.org/10.1002/2016JG003597>
- Santos, F., Wymore, A.S., Jackson, B.K., Sullivan, S.M.P., McDowell, W.H., Berhe, A.A., 2019. Fire severity, time since fire, and site-level characteristics influence streamwater chemistry at baseflow conditions in catchments of the Sierra Nevada, California, USA. *Fire Ecology* 15, 3. <https://doi.org/10.1186/s42408-018-0022-8>
- Sayed, S.S., Abbott, B.W., Vannière, B., Leys, B., Colombaroli, D., Romera, G.G., Słowiński, M., Aleman, J.C., Blarquez, O., Feurdean, A., Brown, K., Aakala, T., Alenius, T., Allen, K., Andric, M., Bergeron, Y., Biagioni, S., Bradshaw, R., Bremond, L., Brisset, E., Brooks, J., Brugger, S.O., Brussel, T., Cadd, H., Cagliero, E., Carcaillet, C., Carter, V., Catry, F.X., Champreux, A., Chaste, E., Chavardès, R.D., Chipman, M., Conedera, M., Connor, S., Constantine, M., Courtney Mustaphi, C., Dabengwa, A.N., Daniels, W., De Boer, E., Dietze, E., Estrany, J., Fernandes, P., Finsinger, W., Flantua, S.G.A., Fox-Hughes, P., Gaboriau, D.M., M.Gayo, E., Girardin, Martin.P., Glenn, J., Glückler, R., González-Arango, C., Groves, M., Hamilton, D.S., Hamilton, R.J., Hantson, S., Hapsari, K.A., Hardiman, M., Hawthorne, D., Hoffman, K., Inoue, J., Karp, A.T., Krebs, P., Kulkarni, C., Kuosmanen, N., Lacourse, T., Ledru, M.-P., Lestienne, M., Long, C., López-Sáez, J.A., Loughlin, N., Niklasson, M., Madrigal, J., Maezum, S.Y., Marcisz, K.,

- Mariani, M., McWethy, D., Meyer, G., Molinari, C., Montoya, E., Mooney, S., Morales-Molino, C., Morris, J., Moss, P., Oliveras, I., Pereira, J.M., Pezzatti, G.B., Pickarski, N., Pini, R., Rehn, E., Remy, C.C., Revelles, J., Rius, D., Robin, V., Ruan, Y., Rudaya, N., Russell-Smith, J., Seppä, H., Shumilovskikh, L., T.Sommers, W., Tavşanoğlu, Ç., Umbanhowar, C., Urquiaga, E., Urrego, D., Vachula, R.S., Wallenius, T., You, C., Daniau, A.-L., 2024. Assessing changes in global fire regimes. *fire ecol* 20, 18. <https://doi.org/10.1186/s42408-023-00237-9>
- Schinck, M.-P., L'Ecuyer-Sauvageau, C., Leroux, J., Kermagoret, C., Dupras, J., 2020. Risk, Drinking Water and Harmful Algal Blooms: A Contingent Valuation of Water Bans. *Water Resour Manage* 34, 3933–3947. <https://doi.org/10.1007/s11269-020-02653-x>
- Serpa, D., Ferreira, R.V., Machado, A.I., Cerqueira, M.A., Keizer, J.J., 2020. Mid-term post-fire losses of nitrogen and phosphorus by overland flow in two contrasting eucalypt stands in north-central Portugal. *Science of The Total Environment* 705, 135843. <https://doi.org/10.1016/j.scitotenv.2019.135843>
- Shakesby, R.A., Doerr, S.H., 2006. Wildfire as a hydrological and geomorphological agent. *Earth-Science Reviews* 74, 269–307. <https://doi.org/10.1016/j.earscirev.2005.10.006>
- Sharma, A.R., Déry, S.J., 2020. Variability and trends of landfalling atmospheric rivers along the Pacific Coast of northwestern North America. *International Journal of Climatology* 40, 544–558. <https://doi.org/10.1002/joc.6227>
- Sharma, U., Garima, Sharma, J.C., Devi, M., 2017. Effect of Forest fire on soil nitrogen mineralization and microbial biomass: A review. *J Pharmacogn Phytochem* 6, 682–685.
- Silins, U., Bladon, K.D., Kelly, E.N., Esch, E., Spence, J.R., Stone, M., Emelko, M.B., Boon, S., Wagner, M.J., Williams, C.H.S., Tichkowsky, I., 2014. Five-year legacy of wildfire and salvage logging impacts on nutrient runoff and aquatic plant, invertebrate, and fish productivity. *Ecohydrology* 7, 1508–1523. <https://doi.org/10.1002/eco.1474>
- Singh, K.P., 1969. Theoretical Baseflow Curves. *Journal of the Hydraulics Division* 95, 2029–2048. <https://doi.org/10.1061/JYCEAJ.0002203>
- Smith, H.G., Sheridan, G.J., Lane, P.N.J., Nyman, P., Haydon, S., 2011. Wildfire effects on water quality in forest catchments: A review with implications for water supply. *Journal of Hydrology* 396, 170–192. <https://doi.org/10.1016/j.jhydrol.2010.10.043>
- Son, J.-H., Kim, S., Carlson, K.H., 2015. Effects of Wildfire on River Water Quality and Riverbed Sediment Phosphorus. *Water Air Soil Pollut* 226, 26. <https://doi.org/10.1007/s11270-014-2269-2>
- Spencer, C.N., Gabel, K.O., Hauer, F.R., 2003. Wildfire effects on stream food webs and nutrient dynamics in Glacier National Park, USA. *Forest Ecology and Management, The Effect of Wildland Fire on Aquatic Ecosystems in the Western USA*. 178, 141–153. [https://doi.org/10.1016/S0378-1127\(03\)00058-6](https://doi.org/10.1016/S0378-1127(03)00058-6)
- Statistics Canada, 2023. Potable water volumes processed by drinking water plants, by source water type [WWW Document]. URL <https://www150.statcan.gc.ca/t1/tbl1/en/tv.action?pid=3810009201> (accessed 5.15.24).
- Statistics Canada, 2011. Survey of Drinking Water Plants (Catalogue No. 16-403– X).
- Stedmon, C.A., Bro, R., 2008. Characterizing dissolved organic matter fluorescence with parallel factor analysis: a tutorial. *Limnology and Oceanography: Methods* 6, 572–579. <https://doi.org/10.4319/lom.2008.6.572>
- Stednick, J.D., 2010. Effects of fuel management practices on water quality. In: Elliot, William J.; Miller, Ina Sue; Audin, Lisa, eds. *Cumulative watershed effects of fuel management in the western United States*. Gen. Tech. Rep. RMRS-GTR-231. Fort Collins, CO: U.S. Department of Agriculture, Forest Service, Rocky Mountain Research Station. p. 149-163. 231, 149–163.
- Stockner, J.G., Shortreed, K.R.S., 1978. Enhancement of Autotrophic Production by Nutrient Addition in a Coastal Rainforest Stream on Vancouver Island. *J. Fish. Res. Bd. Can.* 35, 28–34. <https://doi.org/10.1139/f78-004>

- Stubbins, A., Lapierre, J.-F., Berggren, M., Prairie, Y.T., Dittmar, T., del Giorgio, P.A., 2014. What's in an EEM? Molecular Signatures Associated with Dissolved Organic Fluorescence in Boreal Canada. *Environ. Sci. Technol.* 48, 10598–10606. <https://doi.org/10.1021/es502086e>
- Teele, A., Neary, D., 2015. Water Quality Impacts of Forest Fires. *J Pollut Eff Cont* 03. <https://doi.org/10.4172/2375-4397.1000140>
- Thuile Bistarelli, L., Poyntner, C., Santin, C., Doerr, S.H., Talluto, M.V., Singer, G., Sigmund, G., 2021. Wildfire-Derived Pyrogenic Carbon Modulates Riverine Organic Matter and Biofilm Enzyme Activities in an In Situ Flume Experiment. *ACS EST Water* 1, 1648–1656. <https://doi.org/10.1021/acsestwater.1c00185>
- Trenberth, K.E., 2011. Changes in precipitation with climate change. *Climate Research* 47, 123–138. <https://doi.org/10.3354/cr00953>
- Tyralis, H., Papacharalampous, G., Langousis, A., 2019. A Brief Review of Random Forests for Water Scientists and Practitioners and Their Recent History in Water Resources. *Water* 11, 910. <https://doi.org/10.3390/w11050910>
- Uzun, H., Dahlgren, R.A., Olivares, C., Erdem, C.U., Karanfil, T., Chow, A.T., 2020. Two years of post-wildfire impacts on dissolved organic matter, nitrogen, and precursors of disinfection by-products in California stream waters. *Water Research* 181, 115891. <https://doi.org/10.1016/j.watres.2020.115891>
- Valentine, K.W., Sprout, P.N., Baker, T.E., Lavkulich, L.M. (Eds.), 1978. The soil landscapes of British Columbia, 4. print. ed. Reserve Analysis Branch, Ministry of the Environment, Victoria, B.C.
- Valipour, M., Bateni, S.M., Jun, C., 2021. Global Surface Temperature: A New Insight. *Climate* 9, 81. <https://doi.org/10.3390/cli9050081>
- Verkaik, I., Vila-Escalé, M., Rieradevall, M., Baxter, C.V., Lake, P.S., Minshall, G.W., Reich, P., Prat, N., 2015. Stream macroinvertebrate community responses to fire: are they the same in different fire-prone biogeographic regions? *Freshwater Science* 34, 1527–1541. <https://doi.org/10.1086/683370>
- Vonk, J.E., Tank, S.E., Mann, P.J., Spencer, R.G.M., Treat, C.C., Striegl, R.G., Abbott, B.W., Wickland, K.P., 2015. Biodegradability of dissolved organic carbon in permafrost soils and aquatic systems: a meta-analysis. *Biogeosciences* 12, 6915–6930. <https://doi.org/10.5194/bg-12-6915-2015>
- Wagenbrenner, J.W., Ebel, B.A., Bladon, K.D., Kinoshita, A.M., 2021. Post-wildfire hydrologic recovery in Mediterranean climates: A systematic review and case study to identify current knowledge and opportunities. *Journal of Hydrology* 602, 126772. <https://doi.org/10.1016/j.jhydrol.2021.126772>
- Walker, X.J., Rogers, B.M., Baltzer, J.L., Cumming, S.G., Day, N.J., Goetz, S.J., Johnstone, J.F., Schuur, E.A.G., Turetsky, M.R., Mack, M.C., 2018. Cross-scale controls on carbon emissions from boreal forest megafires. *Global Change Biology* 24, 4251–4265. <https://doi.org/10.1111/gcb.14287>
- Wall, C.B., Spiegel, C.J., Diaz, E.M., Tran, C.H., Fabiani, A., Broe, T.Y., Perez-Coronel, E., Jackrel, S.L., Mladenov, N., Symons, C.C., Shurin, J.B., 2024. Fire transforms effects of terrestrial subsidies on aquatic ecosystem structure and function. *Global Change Biology* 30, e17058. <https://doi.org/10.1111/gcb.17058>
- Wampler, K.A., Bladon, K.D., Myers-Pigg, A.N., 2024. The influence of burn severity on dissolved organic carbon concentrations across a stream network differs based on seasonal wetness conditions post-fire. *EGUsphere* [preprint]. <https://doi.org/10.5194/egusphere-2024-273>
- Wan, H., Zhang, X., Zwiers, F., 2019. Human influence on Canadian temperatures. *Clim Dyn* 52, 479–494. <https://doi.org/10.1007/s00382-018-4145-z>
- Wang, J.-J., Dahlgren, R.A., Chow, A.T., 2015a. Controlled Burning of Forest Detritus Altering Spectroscopic Characteristics and Chlorine Reactivity of Dissolved Organic Matter: Effects of Temperature and Oxygen Availability. *Environ. Sci. Technol.* 49, 14019–14027. <https://doi.org/10.1021/acs.est.5b03961>
- Wang, J.-J., Dahlgren, R.A., Erşan, M.S., Karanfil, T., Chow, A.T., 2016. Temporal variations of disinfection byproduct precursors in wildfire detritus. *Water Research* 99, 66–73. <https://doi.org/10.1016/j.watres.2016.04.030>

- Wang, J.-J., Dahlgren, R.A., Erşan, M.S., Karanfil, T., Chow, A.T., 2015b. Wildfire Altering Terrestrial Precursors of Disinfection Byproducts in Forest Detritus. *Environ. Sci. Technol.* 49, 5921–5929. <https://doi.org/10.1021/es505836m>
- Wang, T., Hamann, A., Spittlehouse, D., Carroll, C., 2016. Locally Downscaled and Spatially Customizable Climate Data for Historical and Future Periods for North America. *PLoS ONE* 11, e0156720. <https://doi.org/10.1371/journal.pone.0156720>
- Wang, T., Mahoney, C., Spittlehouse, D., Hamann, A., 2023. ClimateBC.
- Wang, X., Parisien, M.-A., Taylor, S.W., Candau, J.-N., Stralberg, D., Marshall, G.A., Little, J.M., Flannigan, M.D., 2017. Projected changes in daily fire spread across Canada over the next century. *Environ. Res. Lett.* 12, 025005. <https://doi.org/10.1088/1748-9326/aa5835>
- Webb, A., 2021. forWater: Managing Canada's drinking water from catchment to tap. *wspg*. <https://doi.org/10.53014/HXNK9240>
- Weishaar, J.L., Aiken, G.R., Bergamaschi, B.A., Fram, M.S., Fujii, R., Mopper, K., 2003. Evaluation of Specific Ultraviolet Absorbance as an Indicator of the Chemical Composition and Reactivity of Dissolved Organic Carbon. *Environ. Sci. Technol.* 37, 4702–4708. <https://doi.org/10.1021/es030360x>
- Wickham, H., 2016. *ggplot2: Elegant Graphics for Data Analysis*.
- Wickham, H., François, R., Henry, L., Müller, K., Vaughan, D., 2023. *dplyr: A Grammar of Data Manipulation*.
- Wilson, C., Kampf, S.K., Wagenbrenner, J.W., MacDonald, L.H., 2018. Rainfall thresholds for post-fire runoff and sediment delivery from plot to watershed scales. *Forest Ecology and Management* 430, 346–356. <https://doi.org/10.1016/j.foreco.2018.08.025>
- Wimberly, M.C., Liu, Z., 2014. Interactions of climate, fire, and management in future forests of the Pacific Northwest. *Forest Ecology and Management* 327, 270–279. <https://doi.org/10.1016/j.foreco.2013.09.043>
- Wohl, E., 2017. The significance of small streams. *Front. Earth Sci.* 11, 447–456. <https://doi.org/10.1007/s11707-017-0647-y>
- Wotton, B.M., Flannigan, M.D., Marshall, G.A., 2017. Potential climate change impacts on fire intensity and key wildfire suppression thresholds in Canada. *Environ. Res. Lett.* 12, 095003. <https://doi.org/10.1088/1748-9326/aa7e6e>
- Writer, J.H., McCleskey, B.R., Murphy, S.F., 2012. Effects of wildfire on source-water quality and aquatic ecosystems, Colorado Front Range, in: *Wildfire and Water Quality: Processes, Impacts and Challenges*. Presented at the International Association of Hydrological Sciences, Banff.
- Yang, L., Hur, J., Lee, S., Chang, S.-W., Shin, H.-S., 2015. Dynamics of dissolved organic matter during four storm events in two forest streams: source, export, and implications for harmful disinfection byproduct formation. *Environ Sci Pollut Res* 22, 9173–9183. <https://doi.org/10.1007/s11356-015-4078-6>
- Yu, M., Bishop, T.F.A., Van Ogtrop, F.F., 2019. Assessment of the Decadal Impact of Wildfire on Water Quality in Forested Catchments. *Water* 11, 533. <https://doi.org/10.3390/w11030533>
- Zhang, Y., Biswas, A., 2017. The Effects of Forest Fire on Soil Organic Matter and Nutrients in Boreal Forests of North America: A Review, in: Rakshit, A., Abhilash, P.C., Singh, H.B., Ghosh, S. (Eds.), *Adaptive Soil Management : From Theory to Practices*. Springer, Singapore, pp. 465–476. https://doi.org/10.1007/978-981-10-3638-5_21

Appendix 1 – Supporting Information for Chapter 2

Sample Collection

Prior to stream water sample collection, all glassware and plastic were pre-rinsed with 18.2 M Ω (Milli-Q) water, acid-washed with 10% hydrochloric acid, and rinsed thoroughly again with Milli-Q. After acid-washing, glassware was muffled at 500°C for 4h and all clean supplies were carefully stored until transportation to stream sites. Grab samples were collected immediately below the stream surface, above the deepest part of the channel, and were subset and processed as follows. Samples for DOC, DOM, SRP, NO₂⁻+NO₃⁻, NH₄⁺, TDN, TDP, cations, and anions, were filtered streamside using a 60mL syringe with a 0.45 μ m luer-lock polyethersulfone (PES) filter (Fisherbrand Basix), after pre-rinsing the filter, and rinsing the sample bottle with filtered water. Samples for DOC were filtered into a pre-combusted glass EPA vial and those for DOM composition were filtered into a polycarbonate (PC) bottle. All other filtered samples were collected into sterile Corning centrifuge tubes. TSS was collected in a PC bottle and TN and TP were collected in sterile Corning centrifuge tubes, all pre-rinsed three times and filled with raw water. After collection, samples were stored in cool (4°C) and dark conditions and transported to the laboratory. At the end of each sampling day, water collected for TSS analysis was filtered through a 0.7 μ m nominal pore size pre-weighed and pre-combusted 47mm Whatman GF/F filter using a vacuum pump. Samples collected for SRP, NO₂⁻+NO₃⁻, NH₄⁺, and DOM compositional analysis were frozen upright. Samples for dissolved cations were preserved with trace-metal grade nitric acid, to a pH of ≤ 2 . Samples for DOC were acidified to pH ≤ 2 using trace-metal grade hydrochloric acid (Vonk et al., 2015). All acidified and otherwise untreated samples (anions, TN, TP, TDN, TDP) were kept in the dark and refrigerated (4°C) until analysis.

Water Quality Analyses

Nutrient, cation, and anion samples were analyzed at the University of Alberta's ISO-certified Biogeochemical Analytical Service Laboratory. Cations were analyzed using inductively coupled mass spectrometry (Agilent 7900 ICP-MS), anions using ion chromatography (Dionex DX-600), and nutrients (TDN, TDP, TN, TP, SRP, NO₂⁻+NO₃⁻, NH₄⁺) were analyzed by flow injection analysis (Lachat QuickChem QC8500 FIA). Analyses for DOC and DOM composition were also completed at the University of Alberta. DOC was quantified by combustion of non-purgeable

organic carbon (NPOC) using a Shimadzu TOC-V 5000A. MilliQ blanks and reference waters were analyzed every 10 samples to measure instrument drift. References were made using caffeine (Sigma-Aldrich, CAS# 58-08-2) and KHP standards (AccuSPEC, SCP Science). A standard curve was made for each run based on projected concentration. DOC was calculated as the mean of the best three of five sample injections that had a coefficient of variance < 2%.

DOM composition was evaluated by measuring absorbance and fluorescence on an Aqualog Spectrofluorometer (Horiba Scientific). Absorbance samples were scanned from 240–800 nm at 1-nm increments, then used to derive the spectral slope coefficient from 275–295 nm ($S_{275-295}$; inversely related to molecular weight) and specific ultraviolet absorbance at 254 nm ($SUVA_{254}$; positively related to aromaticity) following common protocols (Helms et al., 2008; Weishaar et al., 2003). Concentrations of dFe, which can increase specific absorbances (Poulin et al., 2014), were often below detection (0.02 mg L^{-1}), and always less than 0.10 mg L^{-1} . Fluorescence excitation-emission matrices (EEMs) were constructed over a 230–500 nm excitation wavelength range at 5-nm increments and a 230–500 nm emission wavelength range at 2.33-nm increments. Raw EEMs were corrected for inner filter effects, blank corrected (Milli-Q blank subtraction), and normalized to Raman units (Murphy et al., 2013) before further analyses (see below).

Soil Leachates

In the laboratory, all subsamples were dried in an oven at 50°C overnight (Audry et al., 2014), combined to form a representative sample, and ground in three short (~3-5 second) bursts using a clean coffee grinder to break up aggregates and ensure adequate homogenization. Samples were then passed through a 2mm screen to remove any remaining large debris and conform to the standard definition of soil particle size (Hoskins and Ross, 2009; Wang et al., 2015b).

To measure water-extractable organic matter and nutrients, a solution of MilliQ, NaCl and NaHCO_3 was created to mimic the ionic strength and composition of rainwater on Vancouver Island (Larocque, 2014; Revchuk and Suffet, 2014). The soil and rainwater solution were combined at a 1:10 ratio (2.5g:250mL) in an acid-washed, pre-combusted glass bottle (Cawley et al., 2017) and agitated at 100 rpm at 10°C in the dark to mimic average ambient air temperature on Vancouver Island. After 24h of contact time (Hohner et al., 2017), the leachate was measured for specific conductance and pH using a YSI probe then passed through a $0.45\mu\text{m}$ PES filter

(Sterlitech) and analyzed for DOC concentration, DOM composition (within 24h), TDN, and TDP as described above. All soils were leached in triplicates; reported values for DOC concentration and DOM composition of the soil leachates represent the mean of each sample triplicate. Samples analyzed for TDN and TDP were composited using equal volume from each replicate prior to analysis. DOC/DOM triplicates were checked for consistency among replicates before combining extracts for nutrient analyses.

Loss-On-Ignition (LOI) was measured to estimate the relative amount of organic matter in the soil samples (Heiri et al., 2001). Approximately 1g of each sample was placed in a drying oven at 100°C overnight (~16h), weighed, and then combusted at 550°C for four hours. After combustion, samples were cooled at 50°C for 1h and then re-weighed. The percent organic matter was calculated by subtraction.

Statistical Analyses

Data were explored for normality using the Shapiro-Wilks test and visual inspection of Q-Q plots. Several variables of interest exhibited some departure from normality when considered as a whole but were acceptable when considered by their individual sources (baseflow, soils, stormflow). Below detect data were treated using the generalized Wilcoxon technique ($\sqrt{2}/2$ times the detection limit) if less than 25% of the total data were below the detection limit (BDL) (Antweiler, 2015). Data with more than 40% BDL were omitted from analyses (NH_4^+ ; 72% BDL; used only to calculate DIN with BDL values input as $\sqrt{2}/2$ DL). Two paired samples, HOBrl1 (DS; 2022-11-10) and HOREfl (US; 2022-11-10), were removed from further analysis because SO_4^{2-} and Ca^{2+} were one to two orders of magnitude larger than any observed in this study. Four samples were collected from each of HOBrl1 and HOREfl, two during baseflow and two during stormflow. The removed data therefore represents half of the available baseflow data at this site.

EEMs were analyzed using a parallel factor (PARAFAC) analysis, which separates the complex EEM signal into its individual underlying fluorescent components and calculates the relative contribution of each component to the total fluorescence for each sample (Stedmon and Bro, 2008). This analysis was performed in MATLAB (9.14.0) with the drEEM toolbox (0.6.5) following the procedure of Murphy et al. (2013). The final PARAFAC model identified five components and was validated using random split-half analysis. All components successfully matched published fluorescence components with similarity scores > 0.95 in the OpenFluor

database (Murphy et al., 2013); matched studies were used to help identify the characteristics associated with each of our fluorescent components.

MERF is an extension of the random forest (RF) algorithm (Breiman, 2001), which gained popularity for its ability to handle non-parametric and high dimensional data, and the calculation of variable importance metrics (VIMs) for each parameter, which allows for explicit interpretation of the model outputs (Biau and Scornet, 2016; Tyralis et al., 2019). The RF algorithm calculates VIMs by systematically removing predictor variables and quantifying the change in an accuracy metric like mean squared error (MSE). MSE was selected as the most appropriate prediction accuracy measure because it directly quantifies how much each variable contributes to reducing the overall prediction error (Grömping, 2009). MSE and other model assessment techniques are based on out-of-bag (OOB) data, which is the approximately one-third of the data left over from the original bagging (i.e., bootstrap aggregation) procedure. Since the OOB data represent real data from the original training dataset, they are a good measure of the performance of the constructed model.

While the standard RF algorithm is fairly robust to multicollinearity, there is evidence that highly correlated observations (as occurs in repeated measures) can serve to inflate the importance of recurring static variables (Hajjem et al., 2014), and the mixed-effect approach has been shown to have marked improvements in accuracy when dealing with clustered or repeat data (Capitaine et al., 2021; Hu and Szymczak, 2023). Input variables were assessed using the package *VSURF* (Variable Selection Using Random Forests), which ranks predictors based on their variable importance, removes those with a low importance score, and reintroduces those that are left one by one until the model with the minimal OOB error is selected. Pearson's correlation coefficient was also employed to identify highly correlated variables, some of which (with low importance scores) were removed for ease of interpretation. We also constructed partial dependence plots (PDPs) (R package *pdp*; Greenwell, 2017), which modulate a variable of interest while holding all others constant to evaluate the relationship between the variable of interest and the response, for the six most important variables in each MERF.

Tables

Table A1. Weather stations used for precipitation data and associated fire sites. Maximum 24h rolling sum precipitation (mm) values are reported for each station for the three storm events captured in this study. Storm 1 occurred between October 27-November 01, 2022, storm 2 occurred between December 24-27, 2022, and storm 3 occurred between January 11-14, 2023. San Juan, Salt Spring, and Nanaimo stations collect hourly data and are operated by the Ministry of Forests, Lands and Natural Resource Operations - Wildfire Management Branch (FNLRO-WMB), Sheringham Point station collects daily data and is operated by Environment Canada (EC). All data were retrieved from the Pacific Climate Impacts Consortium (PCIC) (Pacific Climate Impacts Consortium, 2024). Storms 1 and 2 were captured by passive siphon “rack” samplers sites HC, NL, HO, or CT; storm 3 was captured by ISCO autosamplers at the CT fire site.

Station Name	PCIC Database ID	Latitude	Longitude	Associated fire sites	Storm 1 (mm) *HC	Storm 2 (mm) *HC, NL, HO, CT	Storm 3 (mm) *CT
San Juan	2321	48° 34' 15.96"	124° 12' 2.16"	HC	102	137	82.4
Sheringham Point	6650	48° 22' 36.48"	123° 55' 15.6"	JC, TC	24.8	39.4	24.2
Salt Spring	1637	48° 46' 26.4"	123° 28' 26.4"	ML, MM, HO, CT	31.6	54.6	48
Nanaimo	1648	49° 2' 53.88"	123° 52' 30"	NL, MH	20.6	43.6	45.6

* Sites where at least one sample was captured

Table A2. Outputs from one-sample ($\mu = 0$), two-tailed t-tests comparing whether reference and burn samples are different from each other. $P < 0.05$ indicates that the mean Z-score difference ($Z_{\text{burn}} - Z_{\text{ref}}$) is significantly different from zero and the reference and burn sites are statistically different. These t-tests were conducted for each water quality metric and sample type using the same input data that was used to calculate Z-scores (one average value for each combination of site and burn status) for baseflow, soil 0-5cm, and soil 6-10cm which are associated with Figures 3 & 4, and storm burn and storm reference, which are associated with Figures 5 & 6. $P < 0.05$ shown in bold.

Metric	Baseflow			Soil 0-5cm			Soil 6-10cm			Storm Burn			Storm Ref		
	statistic	p-value	df	statistic	p-value	df	statistic	p-value	df	statistic	p-value	df	statistic	p-value	df
Sp. Cond.	0.931	0.383	7	0.358	0.729	8	-0.227	0.826	8	0.516	0.625	6	0.461	0.668	4
LOI				-2.885	0.020	8	-2.819	0.023	8						
pH	1.075	0.318	7							-0.885	0.41	6	-2.800	0.049	4
TSS	-0.252	0.808	7							1.236	0.251	8	1.939	0.101	6
DOC	-2.009	0.085	7	-3.062	0.016	8	-2.693	0.027	8	6.416	<0.001	8	5.016	0.002	6
SUVA ₂₅₄	0.294	0.777	7	1.494	0.174	8	0.321	0.757	8	-0.653	0.532	8	1.240	0.261	6
A ₂₅₄	-1.678	0.137	7												
C1 (%)	-1.313	0.231	7	0.862	0.414	8	0.250	0.809	8	-0.172	0.868	8	-0.278	0.79	6
C2 (%)	-0.815	0.442	7	0.176	0.865	8	-2.259	0.054	8	1.824	0.106	8	1.445	0.199	6
C3 (%)	1.715	0.13	7	3.378	0.010	8	4.626	0.002	8	-1.645	0.139	8	-2.674	0.037	6
C4 (%)	-0.436	0.676	7	2.048	0.075	8	0.006	0.995	8	0.099	0.924	8	0.806	0.451	6
C5 (%)	0.502	0.631	7	-4.128	0.003	8	-1.913	0.092	8	-0.310	0.765	8	-0.569	0.59	6
HIX	0.012	0.99	7	3.475	0.008	8	0.591	0.571	8	-0.031	0.976	8	-0.661	0.533	6
BIX	2.515	0.04	7	4.446	0.002	8	4.031	0.004	8	-0.597	0.567	8	-0.016	0.988	6
S ₂₇₅₋₂₉₅	1.846	0.107	7	-4.163	0.003	8	-0.405	0.696	8	-4.517	0.002	8	-5.136	0.002	6
TDP	2.857	0.024	7	-2.016	0.079	8	-2.040	0.076	8	3.099	0.015	8	3.547	0.012	6
TDN	-4.731	0.002	7	-2.619	0.031	8	-2.172	0.062	8	2.379	0.045	8	4.406	0.005	6
TN	-3.786	0.007	7							4.106	0.006	6	2.372	0.077	4
TP	0.980	0.36	7							-0.995	0.358	6	0.797	0.470	4
SRP	-0.804	0.448	7												
NO ₂ NO ₃	-2.965	0.021	7												
Cl	-1.989	0.087	7							-0.112	0.913	8	-0.518	0.623	6
SO ₄	0.946	0.376	7							-1.039	0.329	8	-1.521	0.179	6
Ca	-1.288	0.245	6							-1.056	0.35	4	-0.051	0.962	4
K	2.160	0.074	6							2.451	0.07	4	2.865	0.046	4
Mg	-0.501	0.634	6							-1.601	0.185	4	-1.715	0.162	4
Na	-1.533	0.176	6							0.176	0.869	4	-1.117	0.326	4

Table A3. Properties of the five fluorescent DOM components identified using PARAFAC analysis, including excitation (Ex.) and emission (Em.) peak values, mean percent composition, similarity scores, potential component characteristics, and related references for similar components. The OpenFluor database was used to obtain information on similarity scores and component characteristics (Murphy et al., 2014).

Component	Ex. (nm)	Em. (nm)	% composition*	Similarity score	Potential characteristics	References [†] (matching component)
C1	340	458	37.7 ± 6.3	0.99	Terrestrial humic-like; fulvic acid, ubiquitous in aquatic environments	Logozzo et al., 2023 (C1)
				0.99	Peak A and C, humic-like, terrestrial, ubiquitous	Shutova et al., 2014 (C1)
				0.99	Humic-like, DOM Fe & Al associated	Kothawala et al., 2014 (C1 & C4)
C2	305	414	23.9 ± 10.6	0.99	Diverse, relatively HMW terrigenous molecules; carbon-rich and nitrogen poor	Shakil et al., 2020 (C1)
				0.99	Humic-like organic matter, ubiquitous	Cawley et al. 2012 (C1)
				0.99	Terrestrial humic-like, peak M	Vines & Terry, 2020 (B-C1)
C3	240	391	13.6 ± 8.5	0.99	Microbially-transformed humic-like, Peak M	Du et al., 2021 (C2)
				0.99	Microbial-humic	Osburn et al., 2016 (C2)
				0.99	HMW organic-matter, terrestrial	Gonçalves-Araujo et al., 2016 (C2)
				0.99	Peak AM, recent photochemical or microbial origin	Moona et al., 2021 (C4)
C4	270/ 405	499	9.1 ± 2	0.96	Terrestrial, humic-like, Peaks A and C	Vines & Terry, 2020 (C-C3)
				0.97	Terrestrial, humic-like, HMW, aromatic, more hydrophobic, relatively fast in-stream processing	Kothawala et al., 2014 (C3)
				0.96	Terrestrial, humic-like, surface processes	Guéguen et al., 2014 (C3)
C5	280	327	15.6 ± 7.7	0.99	Amino acids or proteins, algal production	Wauthy et al., 2018 (C5)
				0.99	Protein, tryptophan-like, biological production	Gao & Guéguen, 2018 (C4)
				0.99	Protein-like, recent biological production, common in aquatic environments	Dainard et al., 2015 (C4)

*Mean ± standard deviation calculated from all samples.

[†] 131 studies were identified with at least one component similarity score >0.95. Studies with the highest similarity score were chosen for comparison.

Table A4. Outputs for stormflow two sample, two-tailed t-tests. The “Storm & Base” group compare all stormflow data to all associated baseflow data regardless of burn status to investigate the presence of an overall storm response. The “Storm Ref & Storm Burn” group compare the stormflow reference and burn samples to investigate if burn status impacts storm response. The data are associated with Figures 5 & 6. $P < 0.05$ shown in bold.

Metric	Storm & Base - All data			Storm Ref & Storm Burn		
	statistic	p-value	df	statistic	p-value	df
Sp. Cond.	-1.354	0.182	51.224	-1.009	0.349	6.553
pH	-4.171	<0.001	59.975	-0.686	0.509	9.560
TSS	2.027	0.049	43.008	-0.545	0.595	13.509
DOC	6.319	<0.001	68.934	-1.170	0.262	13.860
SUVA ₂₅₄	0.249	0.805	59.399	0.517	0.613	13.746
C1 (%)	-0.846	0.400	77.013	-0.975	0.349	11.641
C2 (%)	2.924	0.005	77.976	-0.028	0.978	13.406
C3 (%)	-1.796	0.076	77.004	0.037	0.971	9.793
C4 (%)	-0.495	0.622	76.380	-0.831	0.421	13.335
C5 (%)	-0.484	0.630	74.517	0.871	0.401	11.817
S ₂₇₅₋₂₉₅	-4.735	<0.001	52.483	0.239	0.815	10.961
HIX	-0.293	0.770	68.359	-0.840	0.419	10.923
BIX	-0.304	0.762	60.872	0.643	0.531	13.652
TDP	4.927	<0.001	49.993	2.129	0.056	11.245
TDN	3.114	0.003	64.137	-1.206	0.250	12.440
TN	1.471	0.148	44.256	-1.479	0.209	4.272
TP	0.736	0.467	31.591	-1.010	0.370	4.002
Cl	0.129	0.898	68.405	-1.744	0.116	8.695
SO ₄	-1.045	0.303	35.017	0.585	0.570	11.176
Ca	-1.629	0.115	27.646	-1.564	0.157	7.916
K	1.312	0.195	48.973	-0.509	0.629	5.785
Mg	-2.476	0.020	27.486	-2.705	0.041	5.155
Na	-1.187	0.244	32.943	-1.547	0.176	5.680

Figures

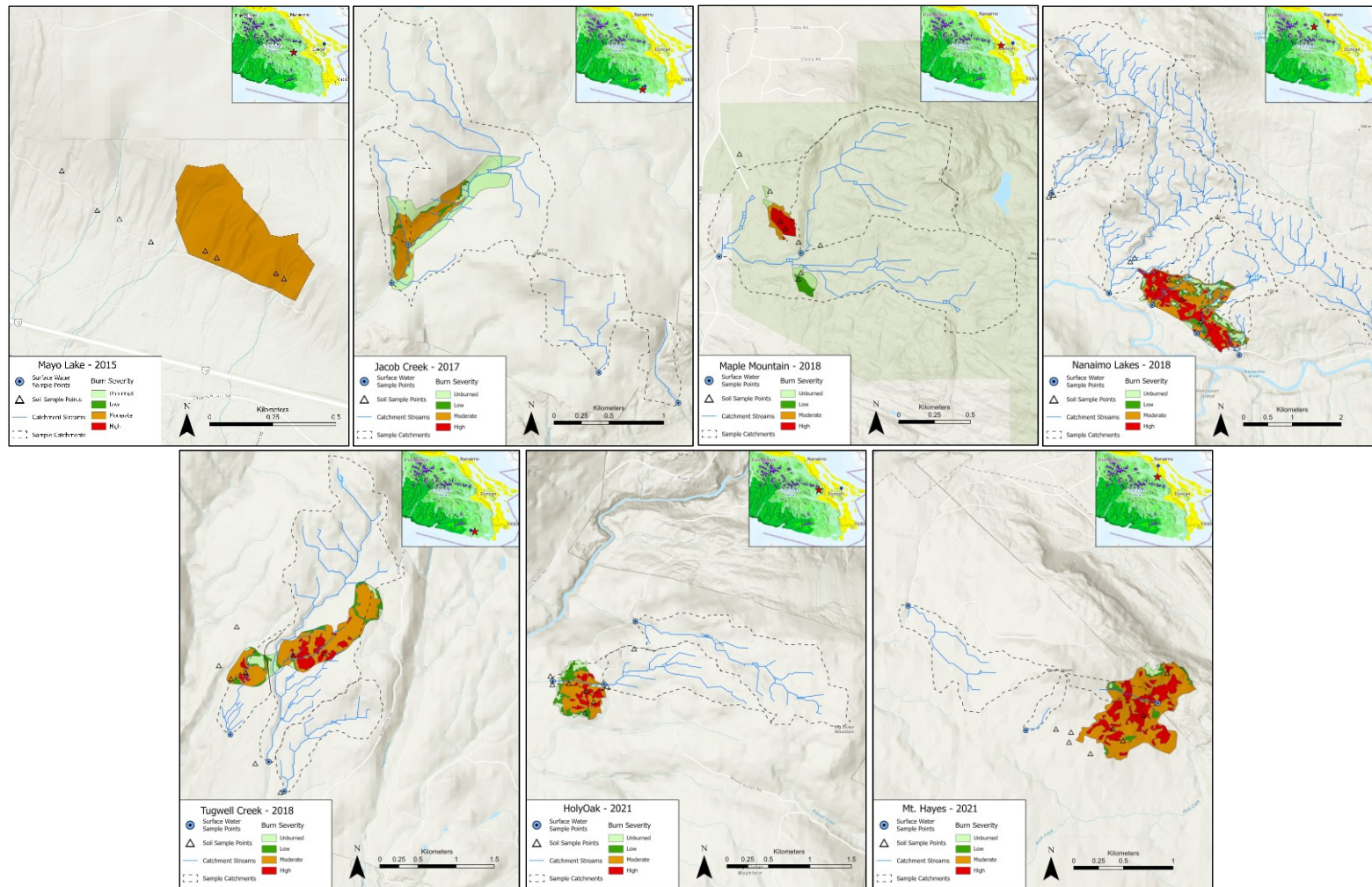


Figure A1. Detailed maps of historic fire sites and sampled catchments. The year next to the site name represents the burn year. The inset maps show southern Vancouver Island – the red star represents the location of the fire site, and the pin shows the associated weather station. Maps of the other the fire sites are shown in Figure 2.



Figure A2. Field pictures of passive siphon “rack” samplers set up at the Harris Creek (HC, 2015) fire site in a burn-affected (HCBn1 - left) and reference stream (HCRef1 - right). Rack samplers were typically installed during periods of low flow.

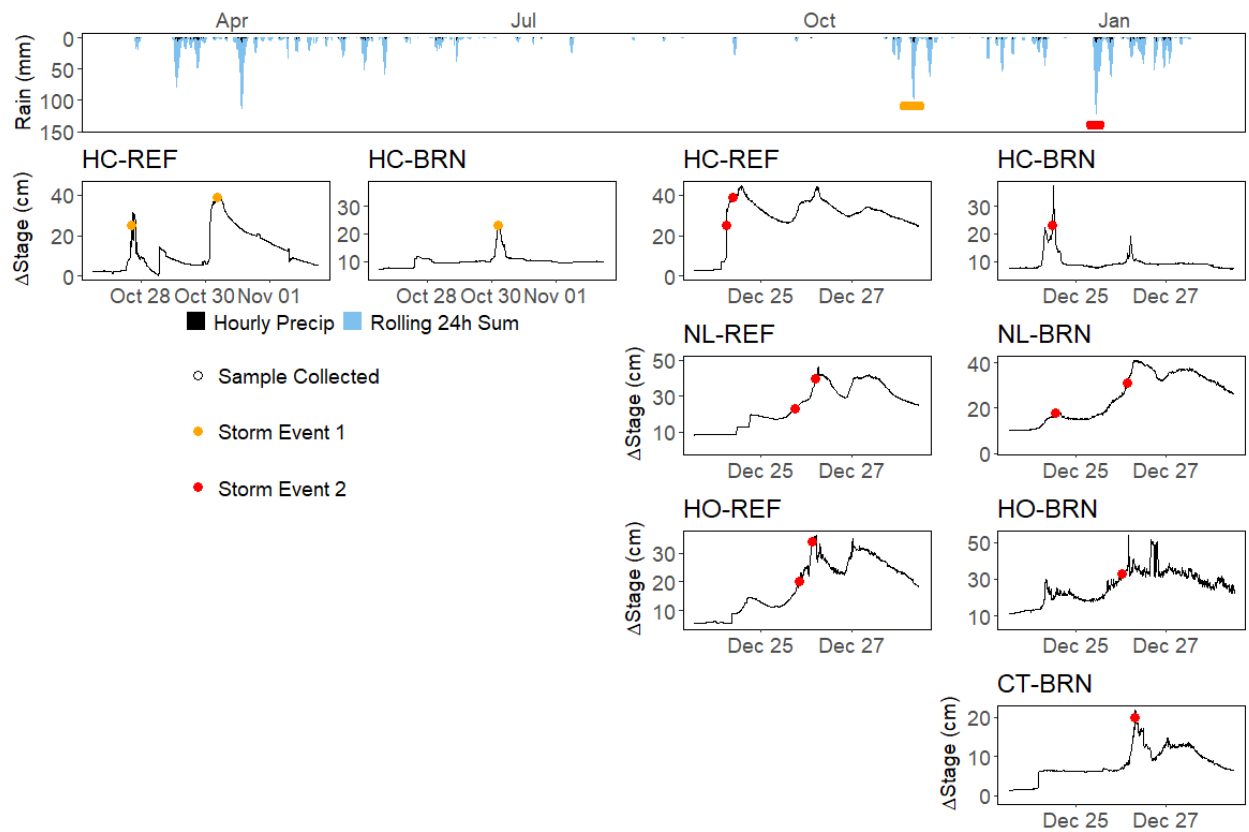


Figure A3. Hyetograph spanning March 2022 to January 2023 and stage hydrographs for two storm events captured by at least one rack sampler (Figure A2). Points on the hydrographs show where a sample was collected. Orange represents a storm event from October 27 – November 01, 2022, red represents a storm event from December 24 – 28, 2022. Precipitation data was acquired from the San Juan weather station.

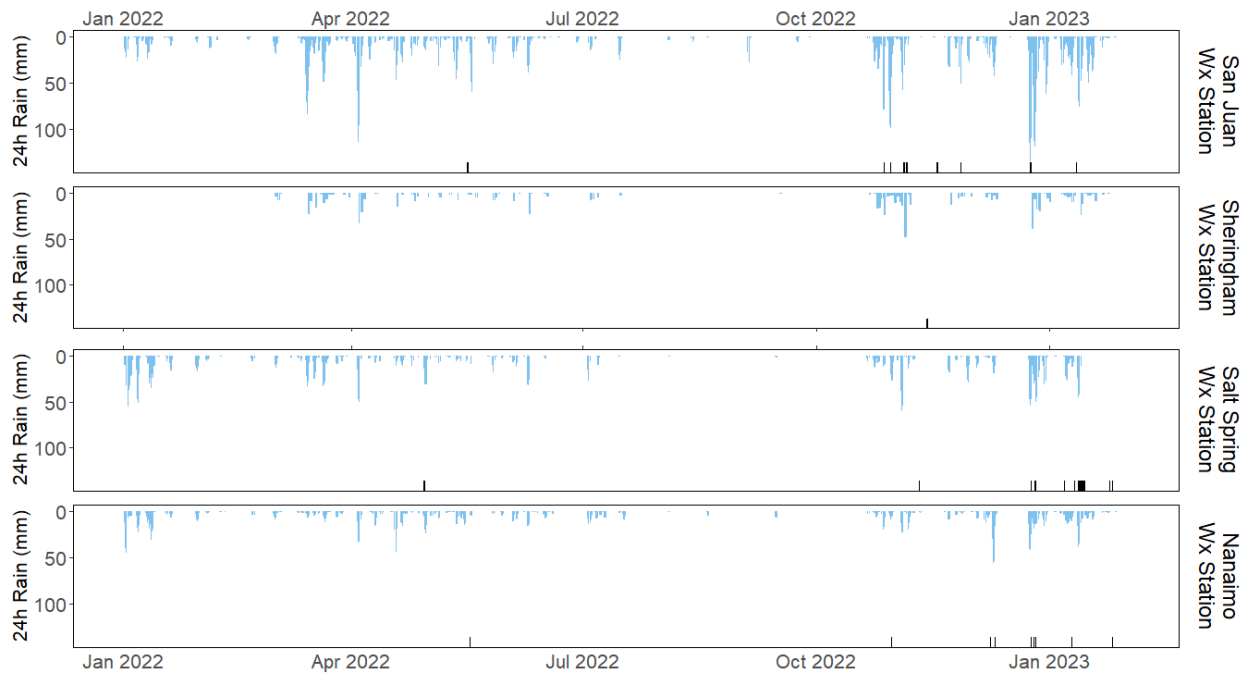


Figure A4. Precipitation data from the four weather stations used in associated with wildfire sites. All data were retrieved from the Pacific Climate Impacts Consortium (PCIC) (Pacific Climate Impacts Consortium, 2024). The San Juan, Salt Spring, and Nanaimo weather stations collect hourly data which are shown here as a 24-hour rolling sum and are operated by the Ministry of Forests, Lands and Natural Resource Operations - Wildfire Management Branch (FNLRO-WMB). Sheringham Point station collects daily data which is shown here a 24-hour total precipitation and is operated by Environment Canada. San Juan was associated with site HC, Salt Spring was associated with sites ML, MM, HO, and CT, Nanaimo was associated with sites NL and MH, and Sheringham Point was associated with sites JC and TC. The rug ticks show when a sample was collected at one of the associated sites.

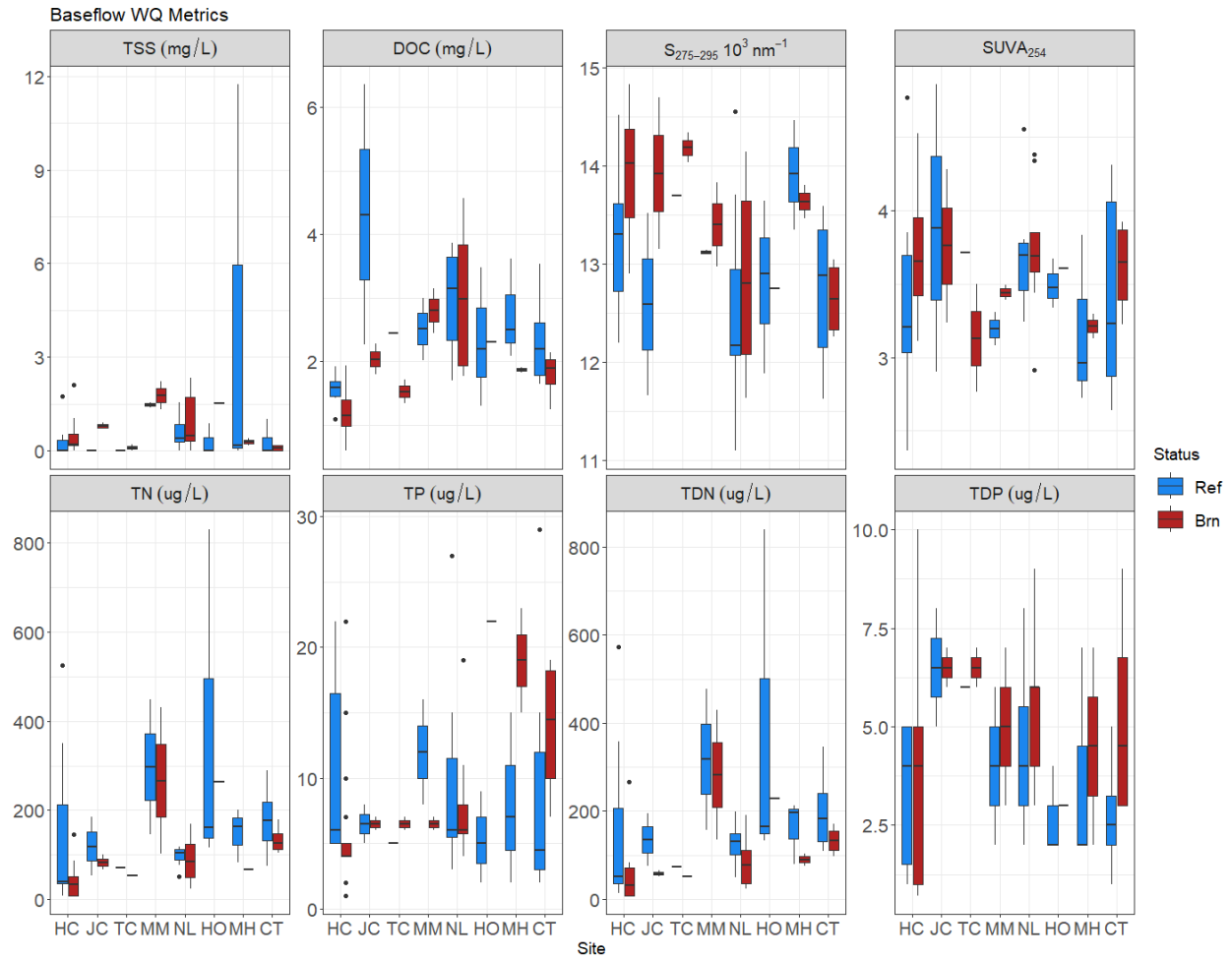


Figure A5. Boxplots comparing water quality metrics (TSS, DOC, $S_{275-295}$, SUVA₂₅₄, TDN, TDP, TN, TP) from reference and burn-affected streams at eight sites (HC, JC, TC, MM, NL, HO, MH, CT) during baseflow. Sites are ordered chronologically by date of wildfire, from oldest to newest (2015 – 2022).

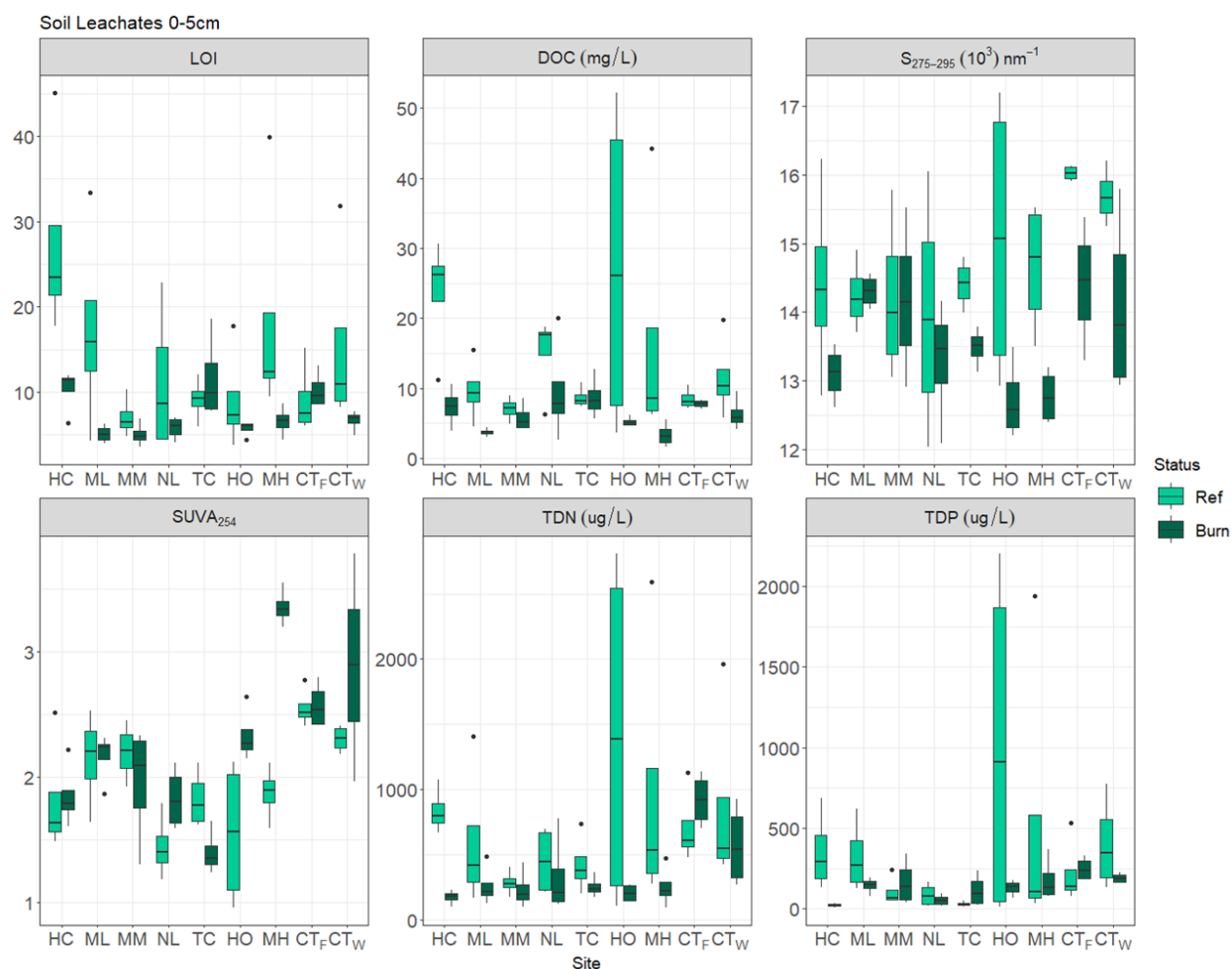


Figure A6. Boxplots showing loss-on-ignition (LOI) and water quality metrics (DOC, $S_{275-295}$, SUVA₂₅₄, TDN, TDP) for 0-5cm soil leachates. Sites are ordered chronologically, by date of wildfire, from oldest to newest (2015 – 2022) and colour coded according to burn status (reference or burn). CT_F and CT_W represent samples from the Cowichan Trail (2022) fire site, collected prior to wet-up in the fall (CT_F) or during the winter wet season (CT_W).

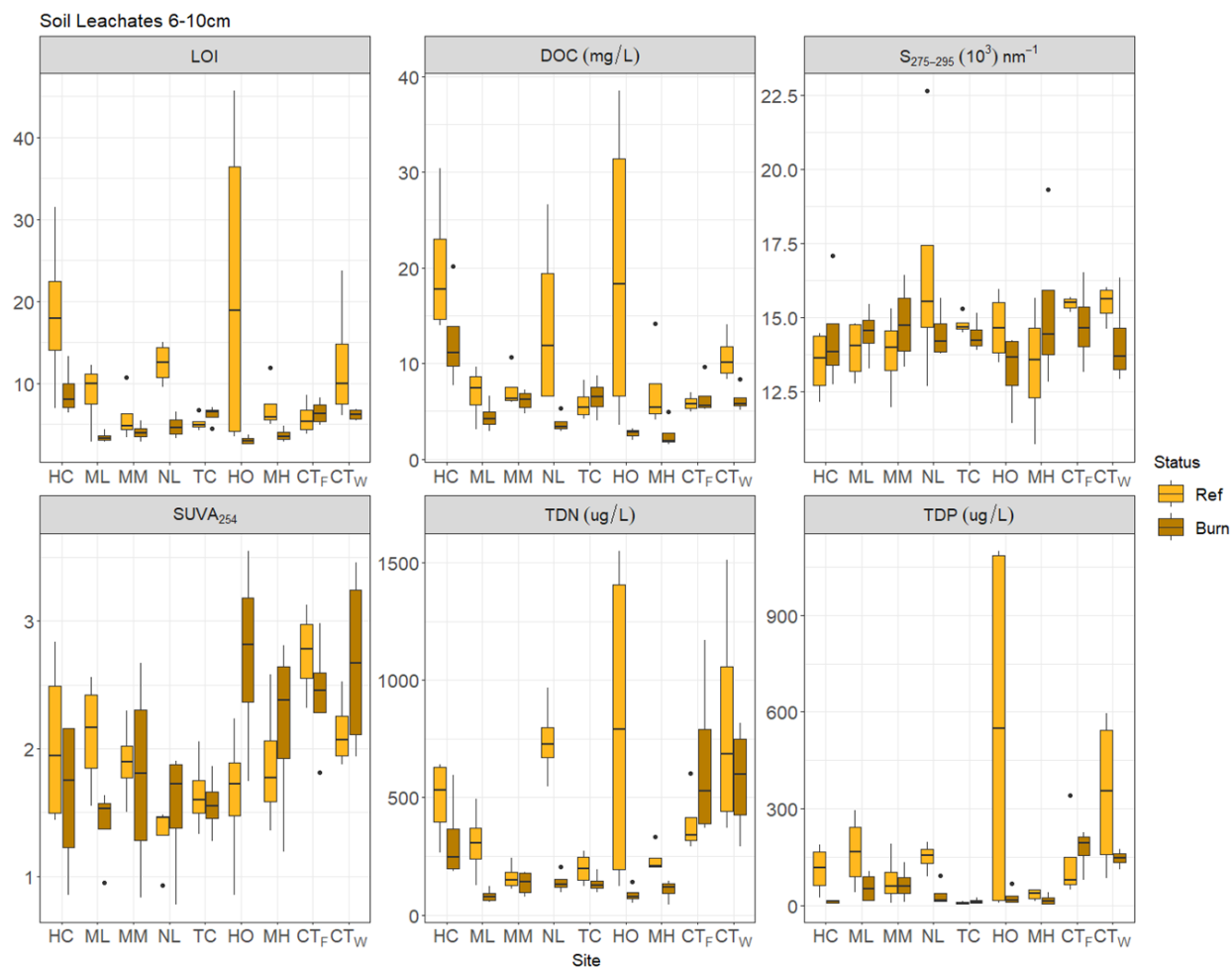


Figure A7. Boxplots showing loss-on-ignition (LOI) and water quality metrics (DOC, $S_{275-295}$, $SUVA_{254}$, TDN, TDP) for 6-10cm soil leachates. Sites are ordered chronologically, by date of wildfire, from oldest to newest (2015 – 2022) and colour coded according to burn status (reference or burn). CT_F and CT_W represent samples from the Cowichan Trail (2022) fire site, collected prior to wet-up in the fall (CT_F) or during the winter wet season (CT_W).

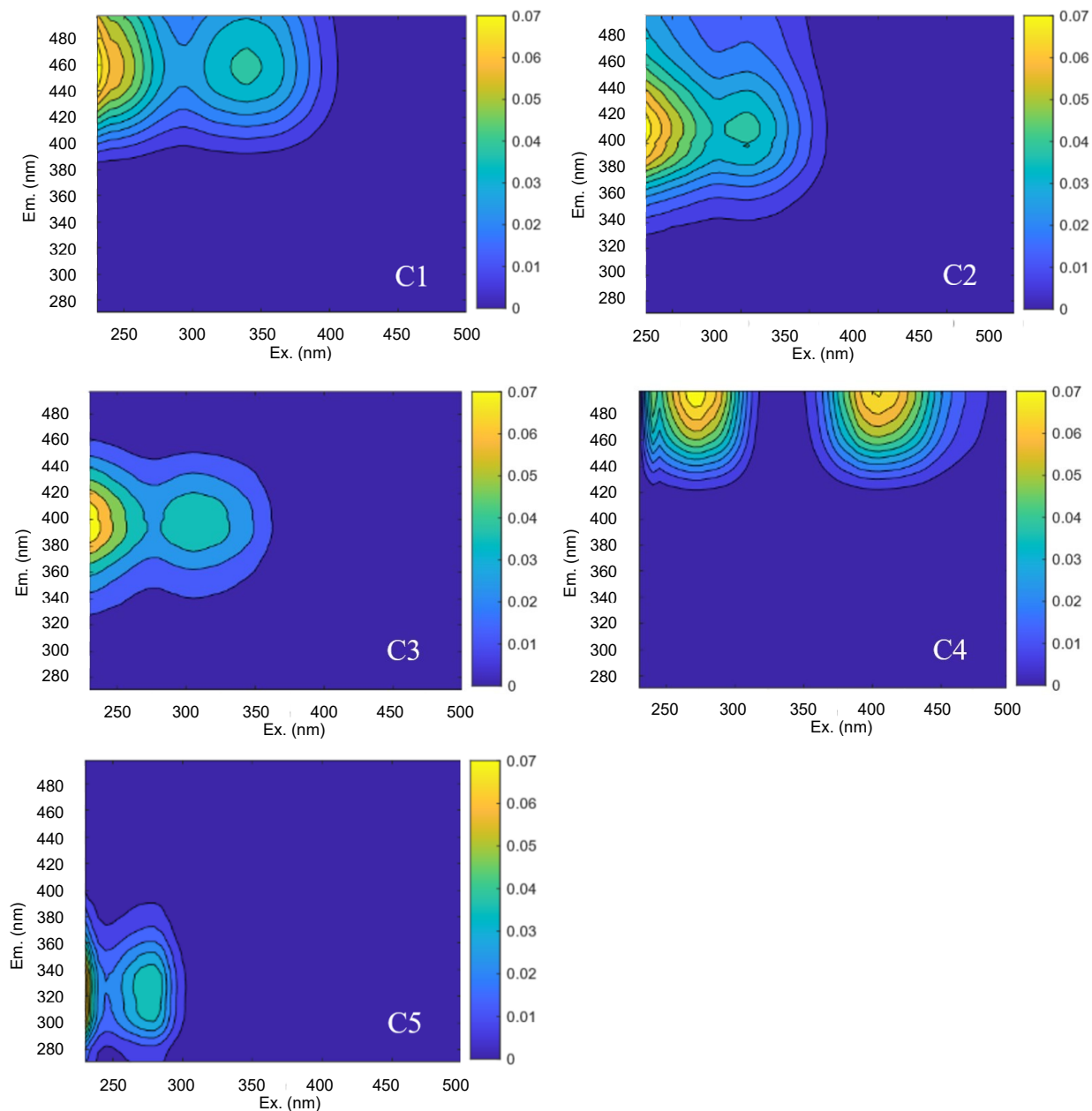


Figure A8. PARAFAC components of excitation-emission matrices (EEMs) measured in samples collected across southern Vancouver Island. Five fluorescence peaks (C1-C5) were identified and displayed in optical space. The colour gradient indicates fluorescence intensity in Raman units.

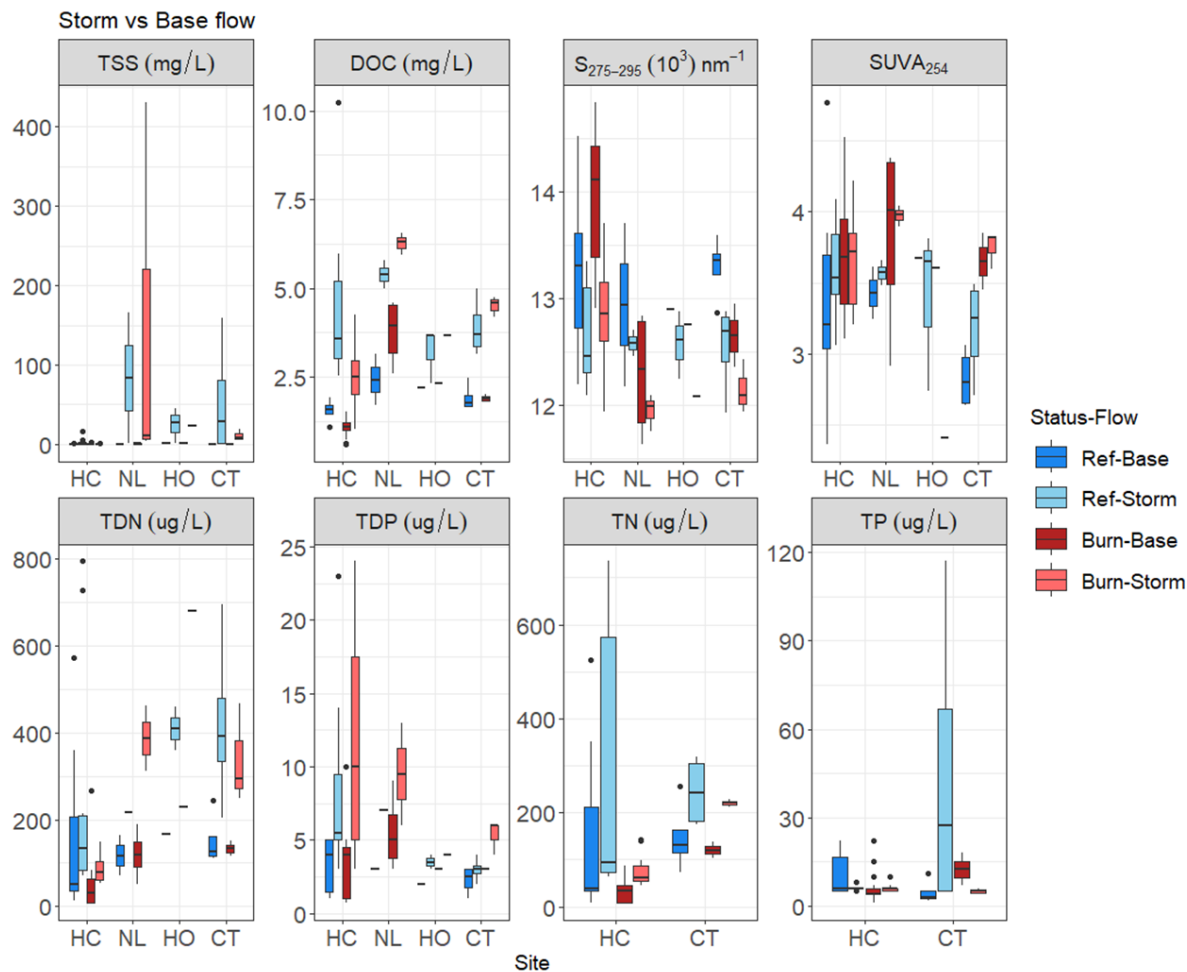


Figure A9. Boxplots comparing water quality metrics (TSS, DOC, $S_{275-295}$, SUVA₂₅₄, TDN, TDP, TN, TP) from reference and burn-affected stream samples at four sites (HC, NL, HO, CT) during baseflow and stormflow. Sites are ordered chronologically, by date of wildfire, from oldest to newest (2015 – 2022). No samples were available at NL and HO for TN and TP because the passive siphon collection method did not capture enough volume for all analyses.

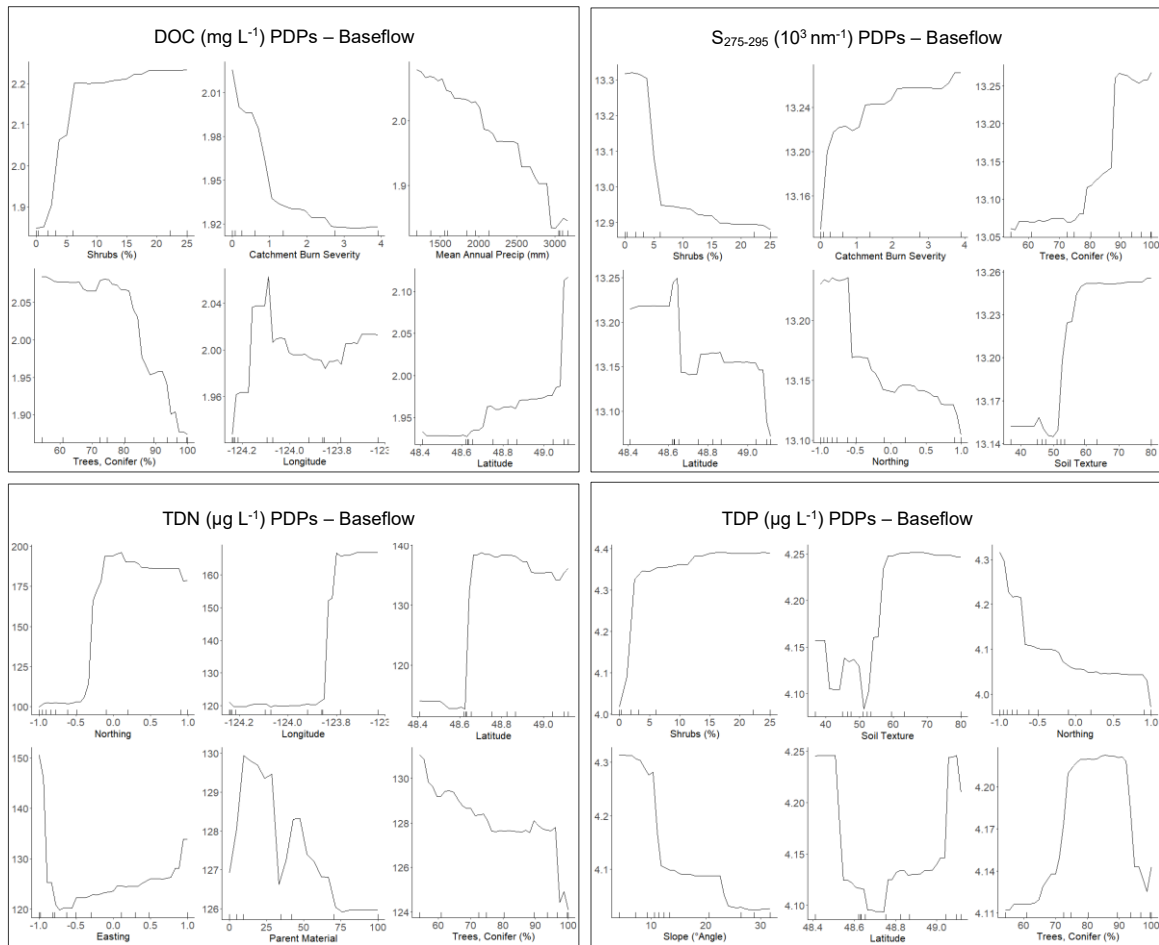


Figure A10. Partial dependence plots (PDPs) for the six most important predictors in the baseflow MERFs. PDPs show the interaction between a subset of variables while accounting for the average effect of the other predictors in the model. Here, each subset of six shows the predicted response of one of variables of interest (DOC, S₂₇₅₋₂₉₅, TDN, TDP) across different values of each predictor. The y-axis represents the change in concentration (DOC mg L⁻¹, TDN μg L⁻¹, TDP μg L⁻¹) or slope (S₂₇₅₋₂₉₅ 10³ nm⁻¹).

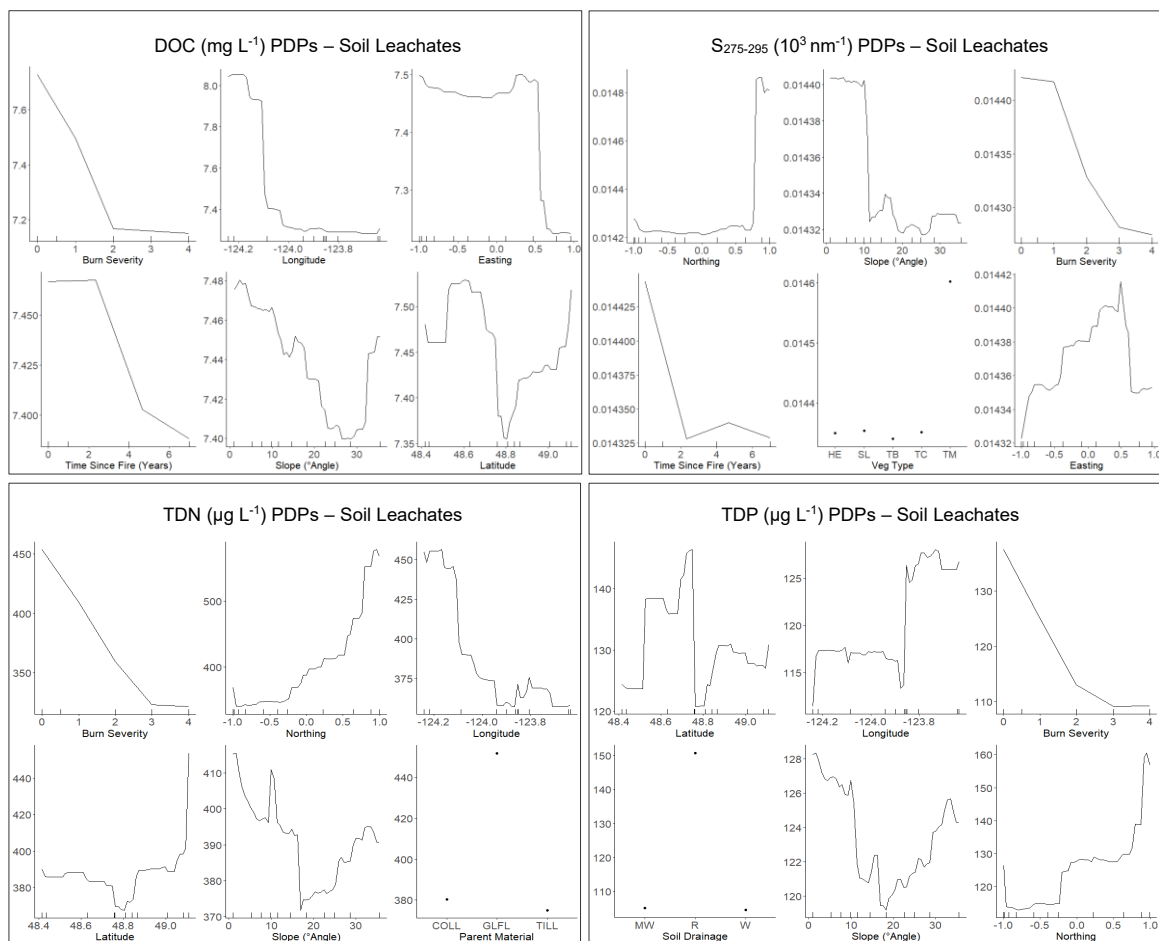


Figure A11. Partial dependence plots (PDPs) for the six most important predictors in the soil leachate MERFs. PDPs show the interaction between a subset of variables while accounting for the average effect of the other predictors in the model. Here, each subset of six shows the predicted response of one of variables of interest (DOC, S₂₇₅₋₂₉₅, TDN, TDP) across different values of each predictor. The y-axis represents the change in concentration (DOC mg L⁻¹, TDN μg L⁻¹, TDP μg L⁻¹) or slope (S₂₇₅₋₂₉₅ 10³ nm⁻¹).

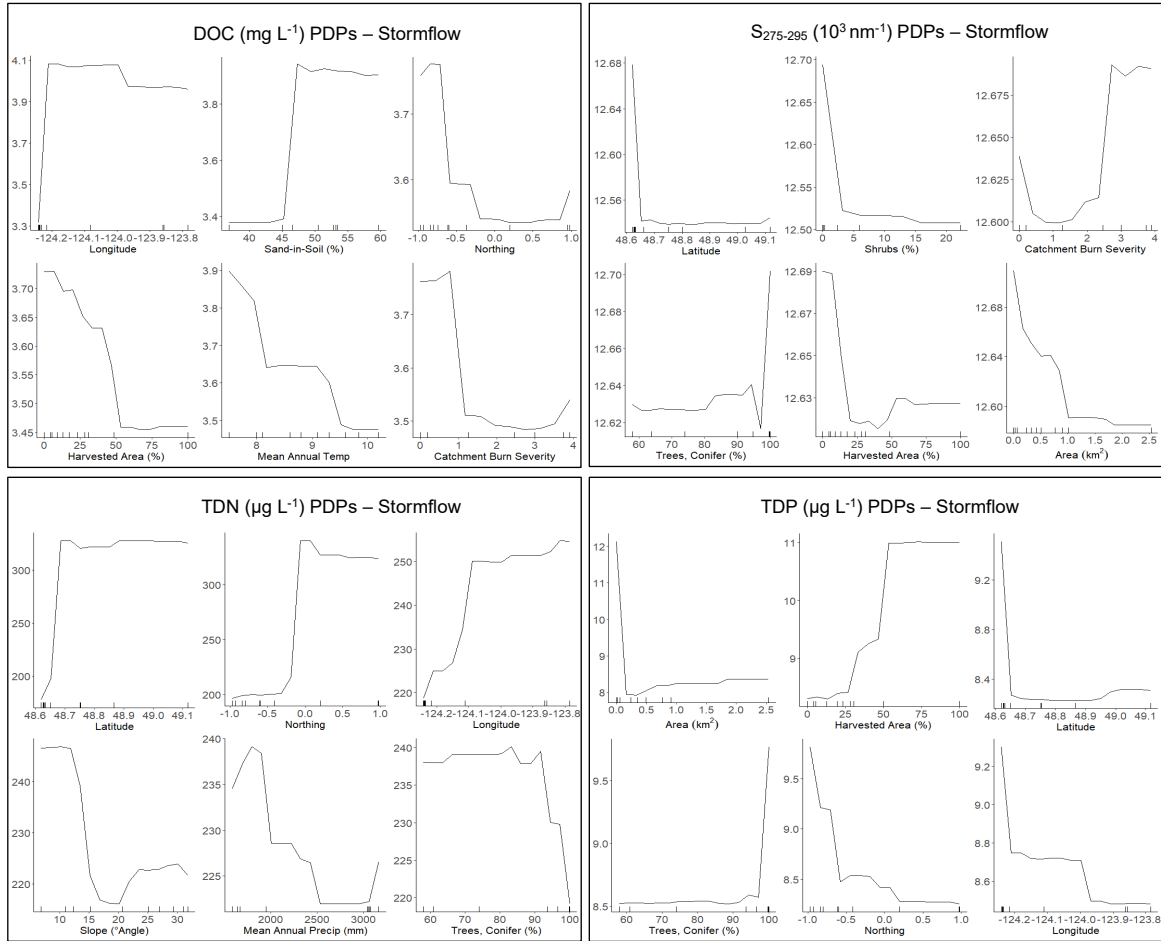


Figure A12. Partial dependence plots (PDPs) for the six most important predictors in the for stormflow MERFs. PDPs show the interaction between a subset of variables while accounting for the average effect of the other predictors in the model. Here, each subset of six shows the predicted response of one of variables of interest (DOC, $S_{275-295}$, TDN, TDP) across different values of each predictor. The y-axis represents the change in concentration (DOC mg L^{-1} , TDN $\mu\text{g L}^{-1}$, TDP $\mu\text{g L}^{-1}$) or slope ($S_{275-295}$ 10^3 nm^{-1}).

Hysteresis, Jan 11-14 Storm

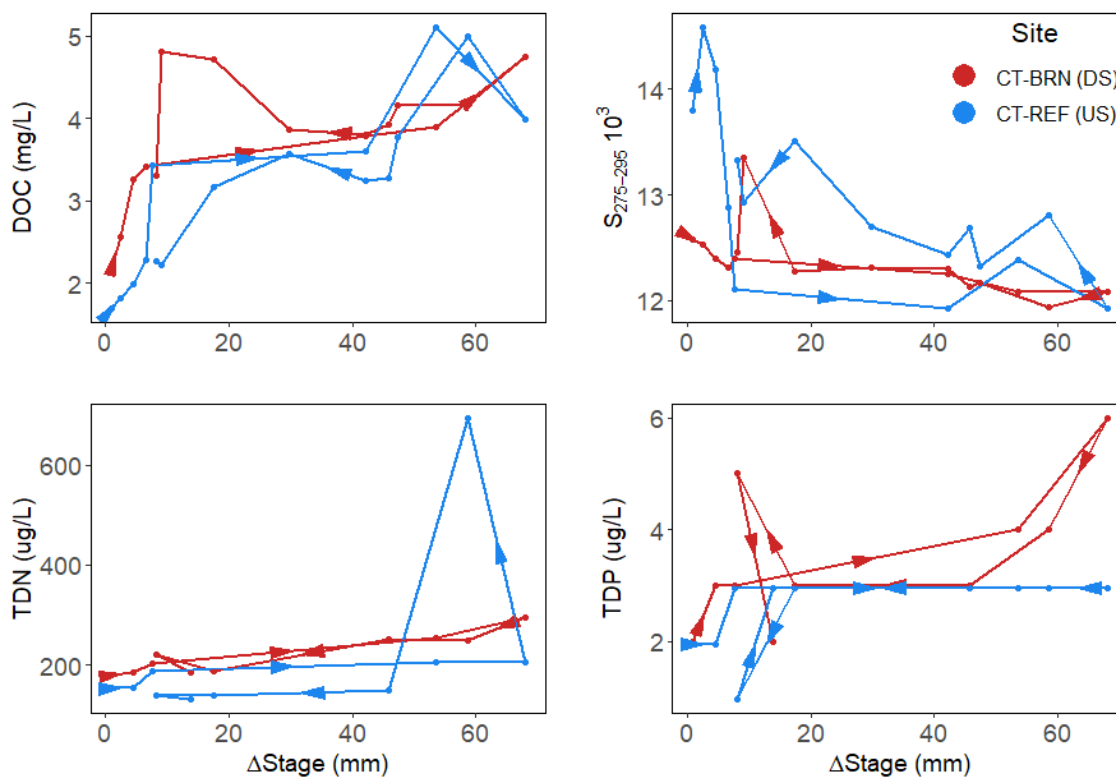


Figure A13. DOC (mg L^{-1}), $S_{275-295}$ (10^3 nm^{-1}), TDN ($\mu\text{g L}^{-1}$), and TDP ($\mu\text{g L}^{-1}$) versus change in stream water level (mm) at the upstream and downstream sampling sites of the Cowichan Trail fire (CT, 2022) during the Jan. 11–14, 2023 storm event. The arrows represent the temporal direction of the storm from the rising to the falling limb. Stream water level data were normalized to zero.